olivine phenocrysts embedded in epoxy resin were doubly polished to a chip with the thickness of about 50-100 μm. Spectra in the near-infrared and infrared regions were collected on the FTIR-300E (JASCO) spectrometer of Earthquake Research Institute, University of Tokyo. H_2O and OH contents of the glass were determined from the IR spectra which were calibrated from manometric and spectroscopic measurements of natural and synthetic basaltic samples (Yasuda, unpublished data). The values for the fundamental OH stretch band at 3550 cm^{-1} of basaltic glass were calibrated.

H_2O contents of glass inclusions are presented in Table 4.5. Each inclusion contains a small shrinkage bubble that accounts for less than 5 vol.% of total volume. Results of analyses show that H_2O contents are about 0.5-0.7 wt.%. H_2O content in the pristine magma of Deccan Trap would have been lower than 0.5 wt.%, because NY-02-51 sample (MgO = 5.6 wt.%) was estimated to be suffered fractional crystallization more than 20 wt.% (see chapter IV-5).

7. Petrological investigations of the pristine magma

A. Constrains from compositions of partial melts of mantle lherzolites

a. Definition of typical mantle lherzolites

It has been proposed that there are primitive and MORB-source mantles in the earth (*e.g.*, McDonough and Sun, 1995). Before we discuss the composition of the partial melt of mantle material, we have to define the major and trace element composition of mantle lherzolite.

First, I selected major element compositions of primitive and MORB-source mantles. KLB-1 (Takahashi, 1986a) and MM3 (Baker and Stolper, 1994) can be regard as MORB-source mantle (Table 4.6). The major element compositions of these mantle lherzolites are close to the various estimates of MORB-source mantle (*e.g.*, Hart and

Table 4.5 H_2O content of glass inclusions in olivine phenocrysts in the uncontaminated basalts (NY-02-51) collected from Deccan Traps.

Sample	Run No.	peak-hight (3550/cm)	thickness (micron)	H2O (wt.%)	constructions
NY-02-51	IC15	0.0385	80	0.6	gl
	IC17	0.0430	80	0.7	gl
	IC21	0.0345	82	0.5	gl,bubble

gl: glass

Table 4.6 Concentrations and partition coefficients used for calculations. Data are from Baker and Stolper (1994), McKenzie and O'Nions (1991, 1995), Takahashi (1986a) and Takahashi and Kushiro (1983).

Major element (wt.%)	SiO2	TiO2	Al2O3	FeO*	MgO
H&K HK-66	48.51	0.22	4.93	9.99	32.68
H&K KLB-1	44.80	0.16	3.62	8.16	39.50
B&S MM3	45.98	0.11	4.02	7.26	38.71

Major element (wt.%)	CaO	Na2O	Mg#
H&K HK-66	3.00	0.67	85.4
H&K KLB-1	3.46	0.30	89.6
B&S MM3	3.61	0.31	90.5

Trace element (ppm)	Rb	K	Ba	Th	Nb
Primitive mantle	0.62±10%	200±20%	6.5±50%	0.07±15%	0.54±15%
Depleated mantle	0.062±10%	20±50%	0.65±50%	0.007±50%	0.39±15%
Dol	0.00018	0.00018	0.0003	0.0001	0.005
Dopx	0.0006	0.001	0.0001	0.0001	0.005
Dcpx	0.001	0.002	0.0005	0.00026	0.02
Dplag	0.03	0.18	0.33	0.05	0.01
Dsp	0.0001	0.0001	0.0001		
Dgar	0.0007	0.001	0.0005	0.0001	0.07

Trace element (ppm)	Sr	P	Zr	Y	V
Primitive mantle	20±15%	61±30%	8.51±15%	3.45±15%	103±15%
Depleated mantle	14.7±20%	51±30%	7.19±15%	3.18±15%	100±15%
Dol	0.00019		0.01	0.005	0.06
Dopx	0.007	0.03	0.03	0.005	0.9
Dcpx	0.13	0.03	0.1	0.2	1.31
Dplag	2		0.01	0.03	
Dsp	0.0011				
Dgar	0.12	0.1	0.32	2.11	1.57

Trace element (ppm)	Mn	Cr	Ni
Primitive mantle	1000±30%	3000±30%	2000±30%
Depleated mantle	1000±30%	3000±30%	2000±30%

REE (ppm)	La	Ce	Nd	Sm	Eu
Primitive mantle	0.55±10%	1.40±10%	1.08±10%	0.35±10%	0.13±10%
Depleated mantle	0.206±30%	0.722±25%	0.815±20%	0.299±20%	0.115±15%
Dol	0.0004	0.0005	0.001	0.0013	0.0016
Dopx	0.002	0.003	0.0068	0.01	0.013
Dcpx	0.054	0.098	0.21	0.26	0.31
Dplag	0.27	0.2	0.14	0.11	0.73
Dsp	0.01	0.01	0.01	0.01	0.01
Dgar	0.01	0.021	0.087	0.217	0.32

REE (ppm)	Tb	Yb	Lu
Primitive mantle	0.084±10%	0.372±10%	0.057±10%
Depleated mantle	0.077±10%	0.347±10%	0.054±10%
Dol	0.0015	0.0015	0.0015
Dopx	0.019	0.049	0.06
Dcpx	0.31	0.28	0.28
Dplag	0.06	0.031	0.025
Dsp	0.01	0.01	0.01
Dgar	0.75	4.03	5.5

Zindler, 1986). As a candidate of primitive mantle, HK-66 (Takahashi and Kushiro, 1983) can be selected (Table 4.6). Takahashi and Kushiro (1983) reported that Fo content of olivine in HK-66 is about 85 (mol.%). The whole rock and mineral compositions show that this lherzolites is one of the most fertile lherzolite in the earth (Maaløe and Aoki, 1977).

Introduction of H_2O into mantle lherzolite dramatically change melting temperature and composition of melt at a given pressure (*e.g.*, Mysen and Boettcher, 1975). As discussed in chapter IV-6, H_2O content of the pristine magma of Deccan Traps is estimated to be less than 0.5 wt.%. Consequently, H_2O content of the source is lower than this value, because basaltic melts must be formed by partial melting of the source. Therefore, the effect of H_2O should be negligibly small on magma genesis of the Deccan pristine magma. In the following discussions, therefore, it is assumed that the mantle lherzolites melt partially under dry condition.

Major element compositions of melts formed by partial melting of primitive and MORB-source mantle lherzolites have been determined at pressures among 1 to 3 GPa under dry conditions using the diamond aggregate method (Baker and Stolper, 1994; Hirose and Kushiro, 1993). Experimentally determined major element compositions of partial melts of the primitive and MORB-source mantle lherzolites at various pressures (1-3 GPa) are presented in Table 4.7.

Trace element concentrations of primitive and MORB-source mantles have been proposed by many workers (*e.g.*, Sun and McDonough, 1989). Because McKenzie and O'Nions (1991, 1995) have estimated the trace element concentrations of primitive and MORB-source mantles (Table 4.6), and simultaneously presented distribution coefficients of elements between main mineral phases and melts, the trace element concentrations of primitive and MORB-source mantle presented by McKenzie and O'Nions (1991, 1995) are used in this study (Table 4.6).

The trace element concentrations of partial melts are calculated for two melting models, batch melting and accumulated fractional melting models (Shaw, 1970). Before we calculate the trace element concentrations using these melting models, we have to

Table 4.7 Major element compositions of partial melts reported by Baker and Stolper (1994) and Hirose and Kushiro (1993).

Run No.	P(GPa)	T(°C)	SiO2	TiO2	Al2O3	FeO*	MgO	CaO	Na2O	X	residue	ref.
HK-66(1)	1	1250	51.14	1.13	18.68	8.03	7.82	9.50	3.71	0.179	ol,op,cpsp	H&K
HK-66(2)	1	1300	49.83	0.79	16.57	8.93	10.40	11.32	2.16	0.307	ol,op,cp	H&K
HK-66(3)	1	1350	50.63	0.54	14.60	9.49	13.53	9.60	1.61	0.412	ol,op	H&K
HK-66(4)	1.5	1275	50.17	1.08	18.93	8.08	8.32	7.98	5.45	0.122	ol,op,cp,sp	H&K
HK-66(5)	1.5	1350	48.62	0.85	16.67	9.46	11.30	10.73	2.37	0.279	ol,op	H&K
HK-66(6)	1.5	1400	48.71	0.78	13.12	10.84	14.33	10.55	1.67	0.398	ol,op	H&K
HK-66(7)	2	1350	47.81	1.45	16.05	10.47	10.94	9.34	3.94	0.169	ol,op,cp,sp	H&K
HK-66(8)	2	1375	47.79	1.19	15.69	10.63	12.07	10.01	2.62	0.253	ol,op,cp	H&K
HK-66(9)	2	1425	47.31	1.17	14.02	10.51	14.80	10.27	1.91	0.347	ol,op	H&K
HK-66(10)	2.5	1425	47.15	1.17	13.91	11.76	13.37	10.29	2.36	0.282	ol,op,cp	H&K
HK-66(11)	2.5	1450	47.65	0.82	12.35	11.75	15.62	10.22	1.59	0.418	ol,op	H&K
HK-66(12)	3	1475	46.20	1.41	12.51	13.00	14.40	9.96	2.53	0.263	ol,op	H&K
HK-66(13)	3	1500	45.89	1.19	12.43	12.64	16.08	9.73	2.03	0.327	ol,op	H&K
KLB-1(14)	1	1250	51.59	1.10	19.19	6.41	8.18	8.90	4.62	0.065	ol,op,cp,sp	H&K
KLB-1(15)	1	1300	50.65	0.65	18.00	6.71	10.11	11.41	2.48	0.121	ol,op,cp,sp	H&K
KLB-1(16)	1	1350	50.98	0.42	14.70	7.69	13.47	11.24	1.51	0.2	ol,op	H&K
KLB-1(17)	1	1400	51.95	0.44	12.67	8.01	16.53	9.49	0.92	0.331	ol,op	H&K
KLB-1(18)	1.5	1300	51.24	1.05	19.51	6.44	8.40	7.83	5.53	0.055	ol,op,cp,sp	H&K
KLB-1(19)	1.5	1350	49.42	0.60	15.27	7.58	13.19	12.35	1.59	0.189	ol,op,cp	H&K
KLB-1(20)	1.5	1400	50.13	0.45	13.85	7.96	15.82	10.74	1.05	0.289	ol,op	H&K
KLB-1(21)	2	1375	47.69	0.75	15.60	8.55	14.01	11.16	2.23	0.135	ol,op,cp	H&K
KLB-1(22)	2	1425	49.07	0.51	13.25	8.86	15.80	11.13	1.38	0.219	ol,op,cp	H&K
KLB-1(23)	2.5	1425	48.42	0.84	15.02	9.52	13.49	10.33	2.39	0.126	ol,op,cp	H&K
KLB-1(24)	2.5	1450	48.56	0.69	13.86	8.50	15.94	10.97	1.47	0.206	ol,op,cp	H&K
KLB-1(25)	3	1500	45.78	0.99	14.37	9.61	16.77	10.67	1.80	0.166	ol,op,cp	H&K
KLB-1(26)	3	1525	47.09	0.55	12.96	9.88	17.94	10.70	0.88	0.347	ol,op,cp	H&K
#55T	1	1270	50.32	0.67	18.14	6.11	10.52	11.43	2.81	0.084	ol,op,cp,sp	B&S
#15	1	1280	51.01	0.69	17.04	6.11	11.12	11.62	2.41	0.092	ol,op,cp,sp	B&S
#16	1	1300	50.18	0.54	16.16	6.52	12.14	12.55	1.91	0.134	ol,op,cp,sp	B&S
#24	1	1330	50.46	0.47	14.75	6.72	13.14	12.84	1.63	0.176	ol,op,cp,sp	B&S
#21	1	1350	50.60	0.42	13.45	7.13	13.96	13.15	1.29	0.224	ol,op,sp	B&S
#22	1	1360	50.73	0.42	13.06	7.33	14.57	12.76	1.13	0.239	ol,op,sp	B&S
#26	1	1390	51.49	0.35	12.22	7.47	15.85	11.61	1.01	0.274	ol,op,sp	B&S

know the mineral proportion of mantle peridotite. Mantle lherzolite change its mineral proportion from plagioclase lherzolite to spinel and garnet lherzolite as pressure increase. McKenzie and O'Nions (1991) have proposed that the changes from plagioclase to spinel lherzolite, and from spinel to garnet lherzolite occurred over the depth ranging from spinel-in to plagioclase-out, and from garnet-in to spinel-out, respectively (Fig. 4.9 a). They have assumed that mineral proportion of plagioclase lherzolite changes linearly from the depth of spinel-in to the depth of plagioclase-out (Fig. 4.9 b). The mineral proportion of spinel lherzolite from the depth of garnet-in to spinel-out is also assumed to change linearly. This assumption is also accepted in this study, and pressure and temperature relationship of each boundary is assumed as follows (McKenzie and O'Nions, 1991).

sp-in: 0.833 GPa (=25 km)
pl-out: 1.17 GPa (=35 km)
gar-in: T=666.7P-400
sp-out: T=666.7P-533 (4.2)

where, T is the temperature in degrees of centigrade and P is the pressure in GPa.

The relationship among pressure, temperature and degree of melting for each mantle lherzolite is estimated from the results of melting experiments by Hirose and Kushiro (1993). I estimated the value of T given by

$$T=1026+136.1P+631.2X-155.5PX \quad (4.3)$$

for primitive mantle (HK-66), where X is degree of partial melting, and

$$T=1108+113.0P+699.8X-158.6PX \quad (4.4)$$

for MORB source mantle (KLB-1). The calculated solidus and the line of X=0.5 using equation (4.3) are shown in Fig. 4.9 a.

b. Major element constraint

The pristine magma of Deccan Traps is tholeiite basalts. Parental magma of the

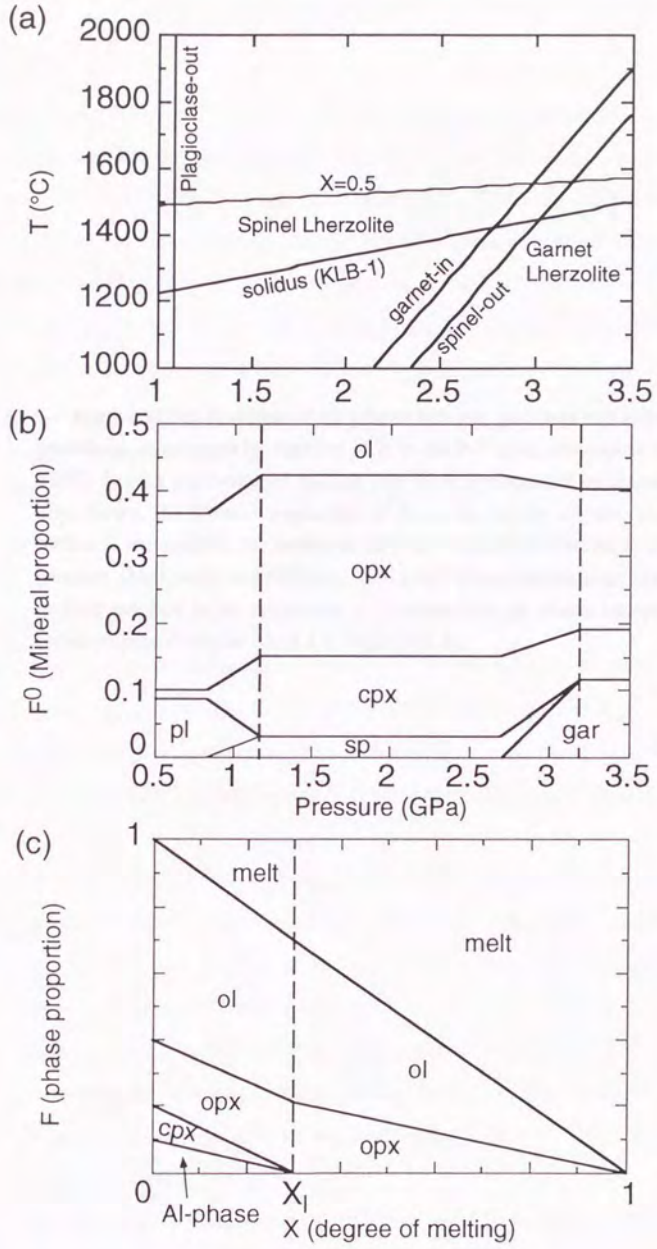

Fig. 4.9 (See next page for explanations)

Fig. 4.9 (--- continued) (a) Positions of the plagioclase-out, garnet-in and spinel-out phase boundaries represented by equation (4.2) in the P-T space (McKenzie and O'Nions, 1991). Solidus and isodegree melting line (X=0.5) calculated by equation (4.4) are also shown. (b) Mineral proportion of lherzolite on the solidus, shown against pressure, and used in the inversion method. Mineral proportion is a function of pressure (McKenzie and O'Nions, 1991). (c) Phase proportions with degree of melting assumed in the calculation. It is assume that all phases except olivine and orthopyroxene disappear when X is larger than X_l.

pristine magma of Deccan Traps may have not been alkalic but tholeiitic basalts.

It has been reported that the partial melts formed at low degree of melting at high pressure (> 1 GPa) show compositions of alkalic basalts. Contrarily, melts formed at high degree of melting are tholeiitic basalts at various pressures (*e.g.*, Falloon *et al*, 1988; Green and Ringwood, 1967; Takahashi and Kushiro, 1983). Compositions of partial melts determined by previous workers (Baker and Stolper, 1994; Hirose and Kushiro, 1993) are plotted on an Ol-Di-Qz ternary projection (Walker *et al.*, 1979) in Fig. 4.10a. It is clear that the partial melts formed at low degree of melting have compositions of alkalic basalts.

Yoder and Tilley (1962) suggested that alkalic basalts could be generated by the fractionation of tholeiitic basalts at high pressures. Grove *et al.* (1992) also suggested that tholeiitic magmas at high pressure ($\geq$ 0.8 GPa) evolved to SiO_2-undersaturated compositions. When Qz component of tholeiitic magma is lower than that of tie line connecting olivine and clinopyroxene compositions, subtractions of olivine and clinopyroxene could derive alkalic magma from tholeiitic magma (Fig. 4.11). On the other hand, tholeiitic basalts could not be generated by the fractionation of alkalic basalts at any pressures. Therefore, the parental magma of tholeiitic magma should be also tholeiitic.

Fig. 4.10b shows the estimated degree of melting of mantle lherzolites, plotted against the Qz component of the melts (Baker and Stolper, 1994; Hirose and Kushiro, 1993). We can recognize that the Qz components of the partial melts decrease with increasing pressure at a given degree of melting. This is mainly caused by the decreasing SiO_2 contents in the partial melts with increasing pressure (Hirose and Kushiro, 1993). It is also clear that melts formed by partial melting of primitive mantle (HK-66) have lower Qt components than those of MORB-source mantle (KLB-1, MM3) at a given pressure and a given degree of melting.

Partial melts plotted on the area of alkalic magma (Qz component < 0 in Fig. 4.10b) might not be the primary magma of the pristine magma of Deccan Traps. Primary magma of the pristine magma of Deccan Traps must be formed at high degree of partial

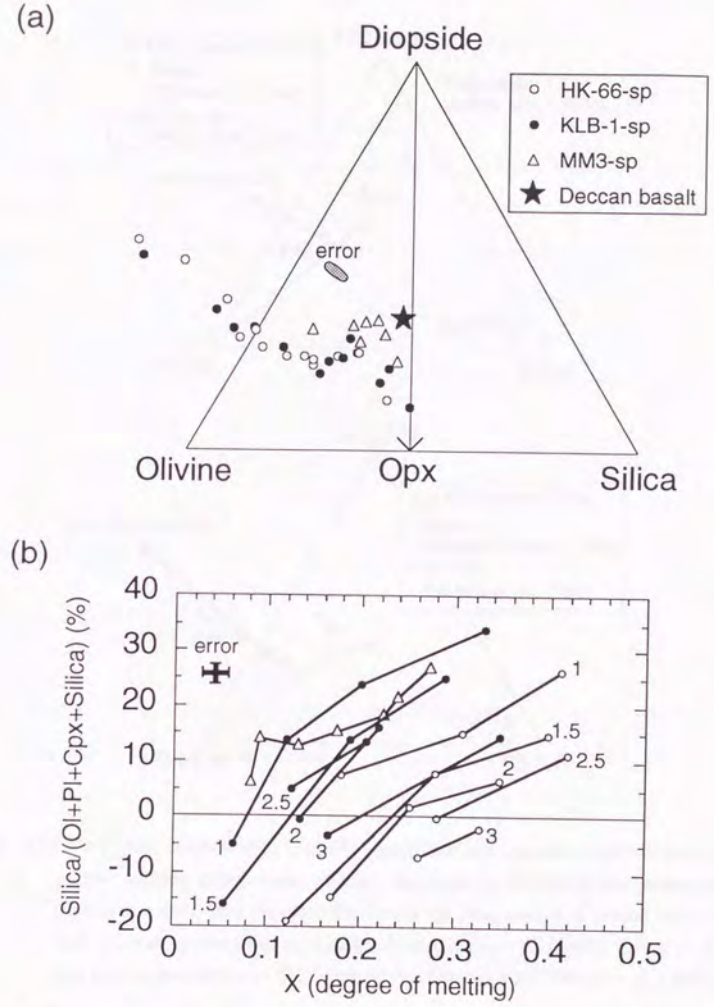

Fig. 4.10 Compositions of melts formed experimentally by partial melting of lherzolite by Baker and Stolper (1994) and Hirose and Kushiro (1993). Composition of Deccan pristine magma is also shown. (a) The compositions are projected from the plagioclase apex onto the base plane, Olivine-Diopside -Silica. (b) Plots of Silica components of the melt compositions versus degree of partial melting (X). Projection scheme is after Walker *et al.* (1979). error: 2 sigma error is calculated based on the melt compositions of Baker and Stolper (1994).

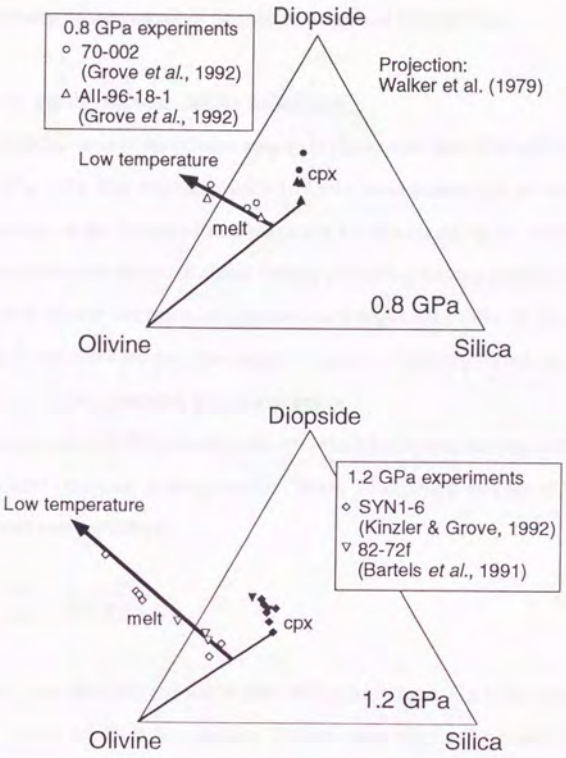

Fig. 4.11 Normative compositions of melts (open) and clinopyroxene (solid) determined by partial melting experiments at high pressures ($\geq$ 0.8 GPa). Projection from the plagioclase apex onto the plane Ol-Di-Qz. Qz components of partial melts decrease with decreasing temperature. Data are from Bartels *et al.* (1991), Grove *et al,* (1992) and Kinzler and Grove (1992). Projection scheme is after Walker *et al.* (1979).

melting so as to be tholeiitic magma (Qz component ≥ 0 in Fig. 4.10b). This is the major element constraint on the genesis of the pristine magma of Deccan Traps.

c. Rare earth element (REE) constraint

LREE/HREE ratio of the pristine magma is higher than that of MORB and mantle lherzolites (Fig. 4.8). The minimum value of La/Lu ratio normalized to the primitive mantle, $(La/Lu)_N$, of the Deccan pristine magma is 2.2, even if taking the analytical error into account. Either low degree of partial melting or melting leaving garnet as a residual phase in typical mantle lherzolite can generate such high La/Lu ratio. In the following discussions, I will estimate possible range of degree of melting by which $(La/Lu)_N$ magma of > 2.2 can be generated at a given pressure.

Concentrations of REE in basalt melts are calculated by two melting models, batch and accumulated fractional melting models (Shaw, 1970) using data set of Table 4.6. The equation of batch melting is

$$\frac{C_{im}}{C_{i0}} = \frac{1}{D + X(1-D)} \qquad (4.5)$$

where, C_{im} is the concentration of element i in the magma, C_{i0} is the concentration of element i in the source before melting, D is the bulk distribution coefficient of an element between the magma and the residue, X is weight fraction of the magma.

When phases enter into the melt in proportions different from those present in the solid, the D for any element changes as a function of X. Shaw (1970) and McKenzie and O'Nions (1991) have shown that

$$D = \frac{D_0 - PX}{1-X} \qquad (4.6)$$

where,

$$D_0 = \sum_{\alpha=1}^{N} F_\alpha^0 D_\alpha \qquad (4.7)$$

$$P = \sum_{\alpha=1}^{N} p_\alpha D_\alpha \tag{4.8}$$

$$p_\alpha = F_\alpha^0 / X_l \qquad (\alpha \geq 3) \tag{4.9}$$

$$p_\alpha = \left(1 - \sum_{\beta=3}^{M} p_\beta\right) F_\alpha^0 \Big/ \left(F_1^0 + F_2^0\right) \qquad (\alpha < 3) \tag{4.10}$$

where, D_0 is the bulk distribution coefficient of an element when X is zero, P is the distribution coefficient weighted according to proportions of the phase entering the magma and $F_\alpha{}^0$ are the proportions by weight of the N minerals in the source before melting, each with the partition coefficient D_α, with n=1 being olivine and n=2 orthopyroxene. p_α are the proportions of different minerals entering the melt. Equations (4.9) and (4.10) show that all phase except olivine and orthopyroxene disappear when $X > X_l$, and that the abundance of p_α varies linearly with X when $X \leq X_l$ (Fig. 4.9c).

By substituting equation (4.6) into equation (4.5), we arrive at:

$$\frac{C_{im}}{C_{i0}} = \frac{1}{D_0 + X(1-P)} \tag{4.11}$$

Equations (4.7) to (4.11) can be applied only when $X \leq X_l$. When degree of melting is larger than X_l, $(La/Lu)_N$ is almost equal to 1.0 (Fig. 4.12) because of the absence of garnet and clinopyroxene as residual phases. This $(La/Lu)_N$ is extremely lower than that of the Deccan pristine magma. Therefore, we need not discuss the La/Lu ratio when $X > X_l$.

When degree of melting is smaller than X_l, the equation of accumulated fractional melting is

$$\frac{C_{im}}{C_{i0}} = \frac{1}{X}\left[1 - \left(1 - \frac{PX}{D_0}\right)^{\frac{1}{P}}\right] \tag{4.12}$$

The REE concentrations in melts (C_{im}) formed by partial melting of primitive and

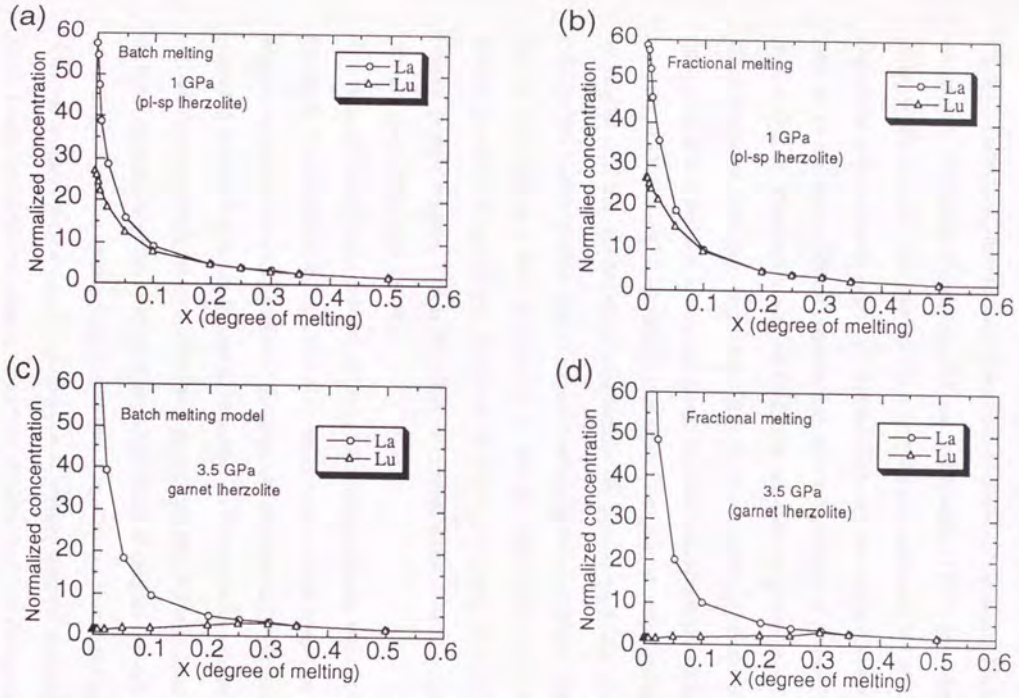

Fig. 4.12 Normalized La and Lu concentrations of melts formed by partial melting of primitive mantle plotted against degree of partial melting. Concentrations are calculated by equations (4.2)-(4.12). (a) Plots of the concentrations of melts generated at 1 GPa. The concentrations are calculated by batch melting model. (b) Plots of the concentrations of melts generated at 1 GPa. The concentrations are calculated by fractional melting model. (c) Plots of the concentrations of melts generated at 3.5 GPa. The concentrations are calculated by batch melting model. (d) Plots of the concentrations of melts generated at 3.5 GPa. The concentrations are calculated by fractional melting model. Normalizing values are based on a primitive mantle model (McKenzie and O'Nions, 1991).

MORB-source mantle lherzolite can be calculated by equations (4.2)-(4.12) using data set of Table 4.6.

The calculated concentrations of La and Lu are plotted against degree of melting in Fig. 4.12. Considering the relationship between the degree of melting and residual phase assemblage of melting experiments (Hirose and Kushiro, 1993), the value of 0.3 is given for X_l. At small melt fractions ($X < 0.1$), the concentrations of LREEs decrease drastically with increasing degree of melting. However, the concentrations of HREEs such as Yb and Lu are almost constant with increasing degree of melting at 3.5 GPa (Fig. 4.12 c, d). High partitioning of HREEs to the residual garnet brings this trend. When degree of melting is larger than 0.05, the concentrations calculated by batch melting are almost the same as those calculated by accumulated fractional melting.

Fig. 4.13 shows the normalized La/Lu ratios, $(La/Lu)_N$, of melts formed by partial melting of primitive and MORB-source mantle. We can recognize that the $(La/Lu)_N$ (>2.2) of the Deccan pristine magma can be satisfied by melts extremely low degree of melting (< 0.001) at 1 GPa (Fig. 4.13 a, c). On the other hand, at 3.5 GPa, melts formed by relatively high degree of melting ($X > 0.1$) may satisfy the $(La/Lu)_N$ of the Deccan pristine magma. This is the effect of residual garnet which appears at high pressure (more than about 2.6 GPa).

The calculated results in Fig. 4.13 treat partial melting process without subsequent fractional crystallization process. However, the pristine magma cannot be a primary magma and should have experienced subsequent fractional crystallization if it is originated from melt of mantle lherzolite. Therefore, we have to discuss the modification of $(La/Lu)_N$ by the fractional crystallization of partial melt (Fig. 4.14a). Clinopyroxene is the most appropriate phase to increase the La/Lu ratio of magma through fractional crystallization process among main phases which crystallized from basaltic magmas. When we consider the fractional crystallization of primary magma, it is impossible to subtract only clinopyroxene without subtraction of olivine (*e.g.*, Bender *et al.*, 1978). I compiled numerous melting experiments of basaltic magma (MgO > 7 wt.%), and found that olivine occupies at least 6 % in crystallizing phases when olivine and clinopyroxene

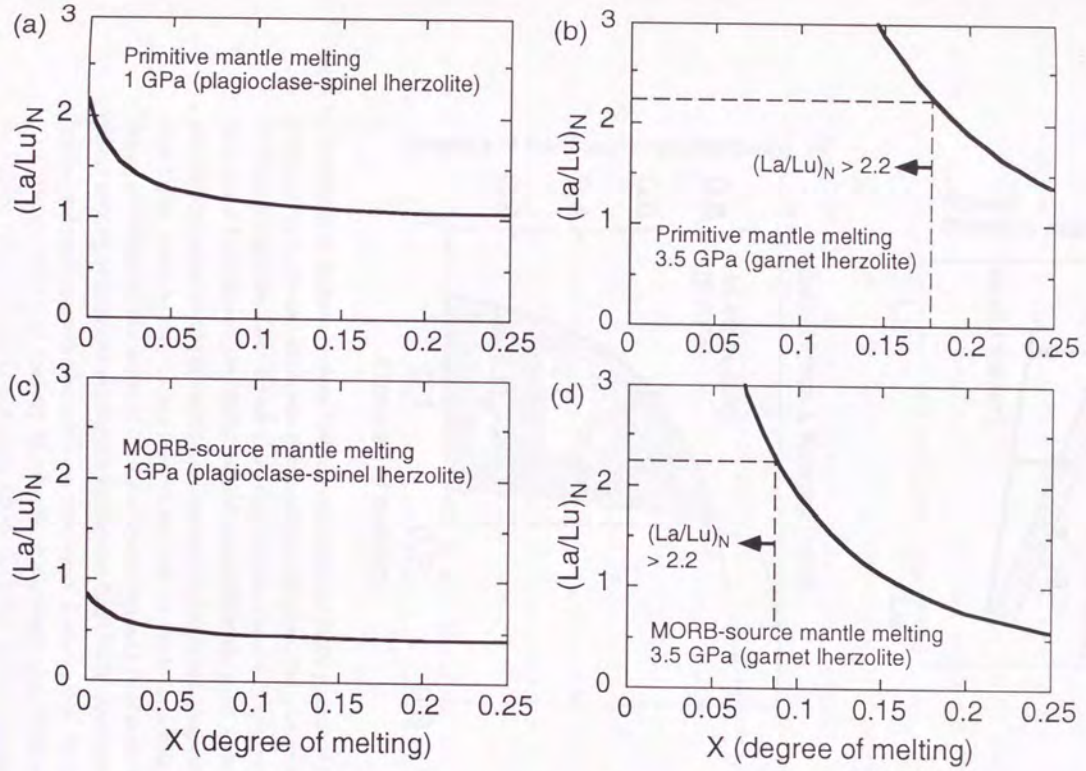

Fig. 4.13 Normalized La/Lu ratios, $(La/Lu)_N$, of melts calculated by batch partial melting model plotted against degree of melting (X). $(La/Lu)_N$ of melts formed by partial melting of primitive mantle at 1 GPa (a) and 3.5 GPa (b), and of MORB-source mantle at 1 GPa (c) and 3.5 GPa (d). Normalizing values are based on a primitive mantle model (McKenzie and O'Nions, 1991).

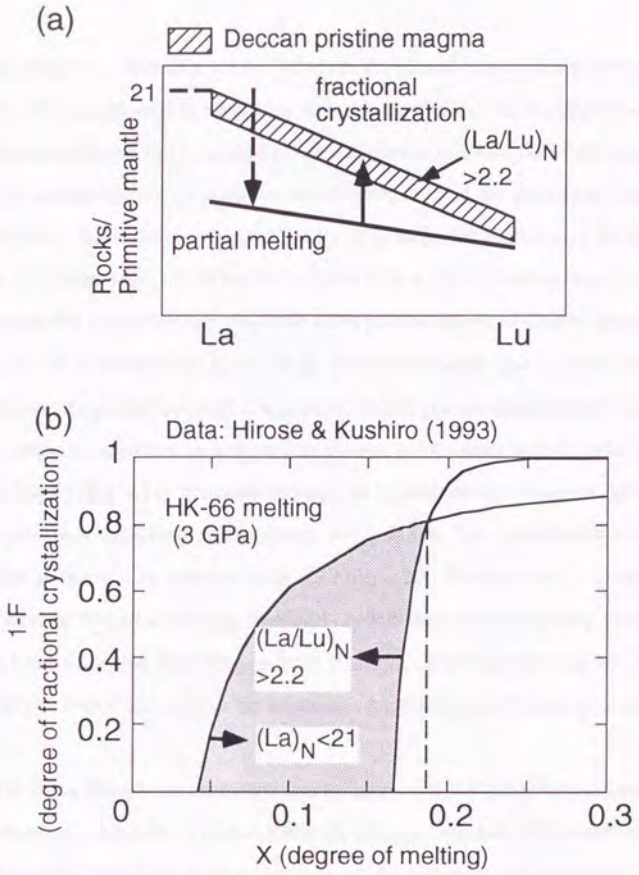

Fig. 4.14 (a) Schematic diagram to show REE concentrations of melts generated by partial melting of lherzolite and subsequent fractional crystallization. The pristine magma of the Deccan Traps has 2.2 as the minimum ratio of $(La/Lu)_N$ and 21 as the maximum normalized La concentration, $(La)_N$, even if we consider analytical error. Magma generated by partial melting of lherzolite and subsequent fractional crystallization must have higher $(La/Lu)_N$ than 2.2 and lower $(Lu)_N$ than 21. (b) Relationship between degree of melting (X) and degree of fractional crystallization (1-F) of melt formed by partial melting of primitive mantle and subsequent fractional crystallization. The hatched area shows the area where melt can have higher $(La/Lu)_N$ than 2.2 and lower $(Lu)_N$ than 21. Even if we consider the subsequent fractional crystallization process, the highest value of degree of melting to satisfy $(La/Lu)_N$ of 2.2 increases only by about 0.02. The concentrations of melts are calculated by batch partial melting at 3 GPa.

are coexisting with melts (Fig. 4.15). Therefore, the subtracted phase proportion of ol : cpx = 6 : 94 was adopted to obtain the largest La/Lu ratio. The Rayleigh fractional crystallization equation (4.1) was used for the calculation. Fig. 4.14 shows the calculated results of partial melting of primitive mantle (HK-66) and the following fractional crystallization. When degree of crystallization is so large, the $(La/Lu)_N$ of the pristine magma of Deccan Traps (>2.2) can be achieved (Fig. 4.14b). However, the calculated La concentration becomes larger than those of the pristine magma of Deccan Traps when the degree of crystallization is too large. It was estimated that La concentration normalized to the primitive mantle, $(La)_N$, of the Deccan pristine magma should be lower than 21 taking the analytical uncertainty into account, and the calculated $(La)_N$ have to be smaller than 21 (Fig. 4.14). We could estimate the highest value of degree of melting to reach $(La/Lu)_N$ of the Deccan pristine magma in Fig. 4.14b. This value is the intersection of the line of $(La)_N = 21$ and the line of $(La/Lu)_N = 2.2$. We can notice, however, the rate of increase of La/Lu ratios by fractional crystallization process is very small. The highest value of degree of melting to reach $(La/Lu)_N$ of 2.2 increase only 0.02 (from 0.17 to 0.19), even if we consider the subsequent fractional crystallization process (Fig. 4.14b).

The above discussions treated the case of subtraction of olivine and clinopyroxene only. However, subtraction of garnet effectively increase La/Lu ratio of basaltic magma. When fractional crystallization of the primary magma took place at high pressure (> 2.5 GPa), garnet may have been subtracted from basaltic magma. Previous melting experiments did not report any proportion of garnet phase in equilibrium with olivine, clinopyroxene and melt phases, and we can not quantitatively discuss the subtraction of garnet from basaltic magma. However, I will suggest that the La/Lu ratio of the Deccan pristine magma can not be generated by subtraction of garnet. When we consider phase relationships of basaltic magma and crystallizing minerals, garnet crystallizes after olivine and clinopyroxene (Fig. 4.16).

Qz component of the basaltic magma must be higher than that of tie lines which connect the olivine and the clinopyroxene compositions, so as not to generate alkalic

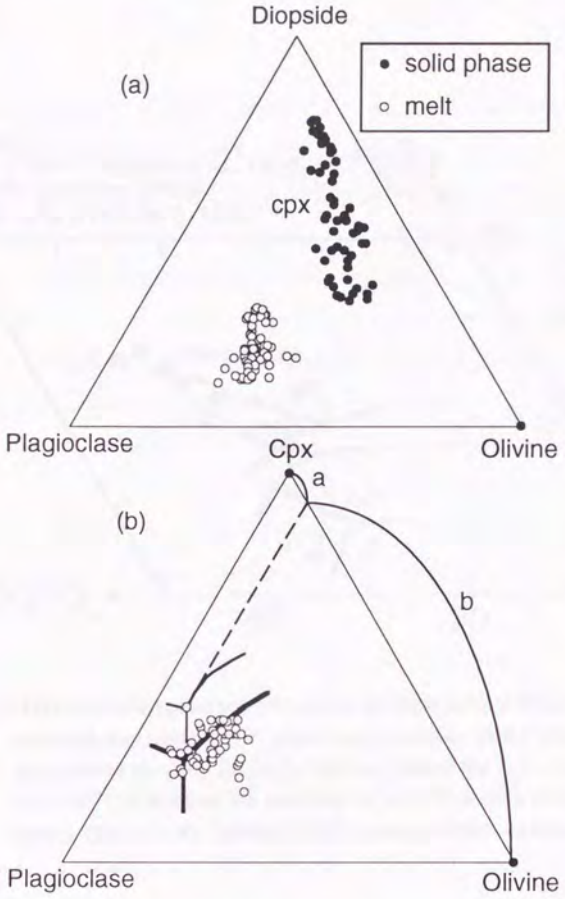

Fig. 4.15 Compositions of minerals and basaltic magma (> 7 wt.%) reported by melting experiments, plotted in Walker's ternary projections (Walker *et al.*, 1979). (a) Plots of the compositions projected from Quartz on to the base; Diopside-Plagioclase-Olivine. (b) Plots of the compositions projected from Quartz onto the base plane; Cpx-Plagioclase-Olivine. Compositions of clinopyroxene coexisting with melt are plotted onto the apex. When I examined the ratio of olivine to cpx plus plagioclase, the weight fraction of a (=a/(a+b)) is more than 6 % . Mineral compositions are from Baker and Eggler (1987), Baker *et al.* (1994), Bartels *et al.* (1991), Bender *et al.* (1978), Elthon and Scarfe (1984), Fujii and Bougault (1983), Grove and Bryan (1983), Grove *et al.* (1982), Grove *et al.* (1992), Johnston (1986), Kinzler and Grove (1992), Panjasawatwong *et al.* (1995), Putirka *et al.* (1996), Tormey *et al.* (1987), Walker *et al.* (1979), Yang *et al.* (1996) and this study.

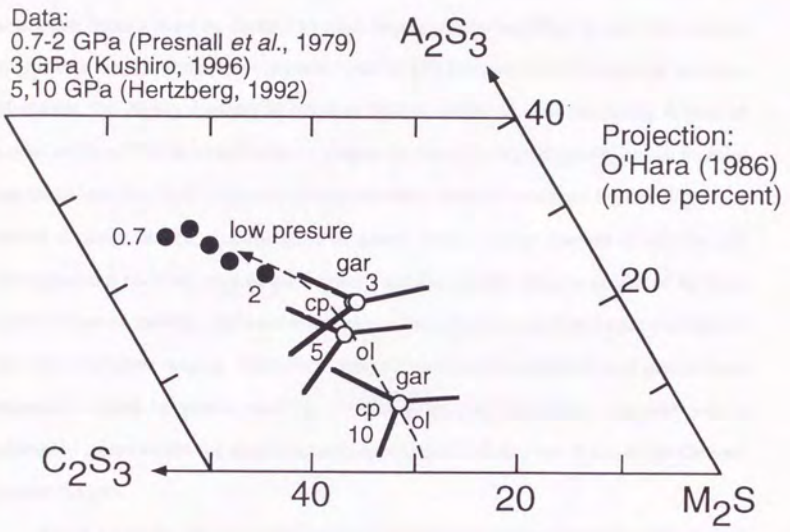

Fig. 4.16 Projection of invariant points at various pressures in CaO-MgO-Al_2O_3-SiO_2 system, projected from enstatite (MS) onto a part of the plane M_2S-C_2S_3-A_2S_3. The invariant point moves parallely the A_2S_3-M_2S and toward the A_2S_3 apex with decreasing pressure. The numbers are pressures in GPa. Projection scheme is after O'Hara (1968). Data are from Herzberg (1992), Kushiro (1996) and Presnall *et al.* (1979).

magma by the subtractions of these phases (Fig. 4.11). As described before, high Qz-normative basalts must be formed by high degree of melting (Fig. 4.10). This magma might have low $(La/Lu)_N$ ratio (almost equal to 1.0) because of high degree of melting. Moreover, the Al_2O_3 contents in magmas become depleted with increasing degree of partial melting. This fact implies that a magma produced by high degree of partial melting has small stability field of garnet compared with a magma produced by low degree of partial melting. Before crystallization of garnet phase, a large amount of olivine and clinopyroxene minerals may be subtracted from the basaltic magma produced by high degree of partial melting, and La concentration of the magma would be larger than that of the Deccan pristine magma. Therefore, when we consider the subtraction of garnet from magmas formed by partial melting of typical mantle lherzolites, magmas which subtracted garnet could not simultaneously satisfy the $(La/Lu)_N$ and $(La)_N$ of the Deccan pristine magma.

Fig. 4.17 shows the calculated results of partial melting and subsequent fractional crystallization of MORB-source mantle. La content of MORB-source mantle is lower than that of primitive mantle. In order to obtain the $(La)_N$ of 21, a large amount of crystals can be subtracted from the partial melt of MORB-source mantle compared to the partial melt of primitive mantle. This implies the partial melting and subsequent fractional crystallization of MORB-source mantle might form basaltic magma which has higher La/Lu ratio compared to primitive mantle. On the other hand, La/Lu ratio of MORB-source mantle is lower than that of primitive mantle. This implies La/Lu ratio of melt formed by partial melting of MORB-source mantle might be lower than that of primitive mantle at a given degree of partial melting. Fig. 4.17 shows that primitive mantle has high degree of partial melting compared with MORB-source mantle so as to satisfy $(La/Lu)_N$ and $(La)_N$ of the Deccan pristine magma simultaneously. This fact suggests that the effect of fractional crystallization process to change La/Lu ratio is small compared to that of partial melting process.

I have estimated the range of degree of partial melting which satisfy $(La/Lu)_N$ and $(La)_N$ of the Deccan pristine magma for primitive and MORB-source mantle at each

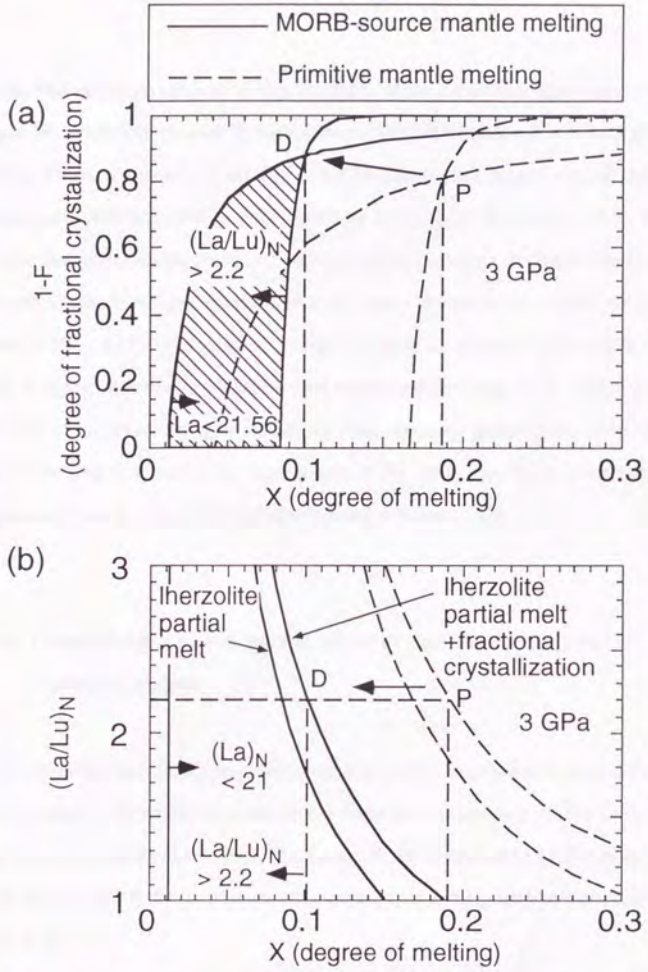

Fig. 4.17 (a) Relationship between degree of melting (X) and degree of fractional crystallization (1-F) of melts formed by partial melting of MORB-source mantle and subsequent fractional crystallization. The hatched area shows the area which has $(La/Lu)_N$ higher than 2.2 and $(Lu)_N$ lower than 21. The concentrations of melts are calculated by batch partial melting at 3 GPa. The calculated results for primitive mantle (Fig. 4.14b) are also shown by dotted line. (b) Plots of $(La/Lu)_N$ of melts formed by partial melting of MORB-source mantle and subsequent fractional crystallization versus degree of partial melting (X). The highest value of degree of melting to satisfy $(La/Lu)_N$ of 2.2 for partial melts of MORB-source mantle (D) is less than that of primitive mantle (P).

pressure. The estimated range of degree of partial melting is plotted against the pressure in Fig. 4.18. When the pressure is higher than 3 GPa, the fraction of residual garnet is high (Fig. 4.9 b), so that high $(La/Lu)_N$ of the Deccan pristine magma can be explained by fractional crystallization of magma formed by high degree of melting (> 0.1). We can recognize that accumulated fractional melting model calculates the higher La/Lu ratios compared to batch melting model under the same pressure and degree of melting conditions (Fig. 4.18). The possible range of degree of melting of primitive mantle melting is higher than that of MORB-source mantle melting (Fig. 4.18). In any case, the La/Lu ratio of the pristine magma of Deccan Traps has to be generated by relatively low degree of melting as shown in the hatched area in Fig. 4.18. This is the constraints from REE concentration to generate the pristine magma of Deccan Traps.

B. Comparison between partial melts of lherzolites and Deccan pristine magma

As described before, the important petrological and geochemical characters of the Deccan pristine magma are as follows; (1) tholeiitic basalts and (2) the La/Lu ratio normalized to the primitive mantle, $(La/Lu)_N$ (>2.2), is extremely higher than that of MORB (about 0.6) (3) the La concentration normalized to the primitive mantle, $(La)_N$ is as high as 21.

In order to form tholeiitic magma by partial melting of mantle lherzolite, degree of melting must be high enough at a given pressure (Fig. 4.10). On the contrary, in order to generate a magma with high $(La/Lu)_N$ more than 2.2, degree of partial melting must be low enough (Fig. 4.18). Therefore, it is necessary to satisfy the above contradictory requirements on the degree of melting to form the Deccan pristine magma from typical mantle lherzolites. The possible degree of melting to generate tholeiitic magma and high $(La/Lu)_N$ (> 2.2) at various pressures are shown in Fig. 4.19. It can be recognized that there is no overlapping region to satisfy the both requirements for each mantle lherzolite.

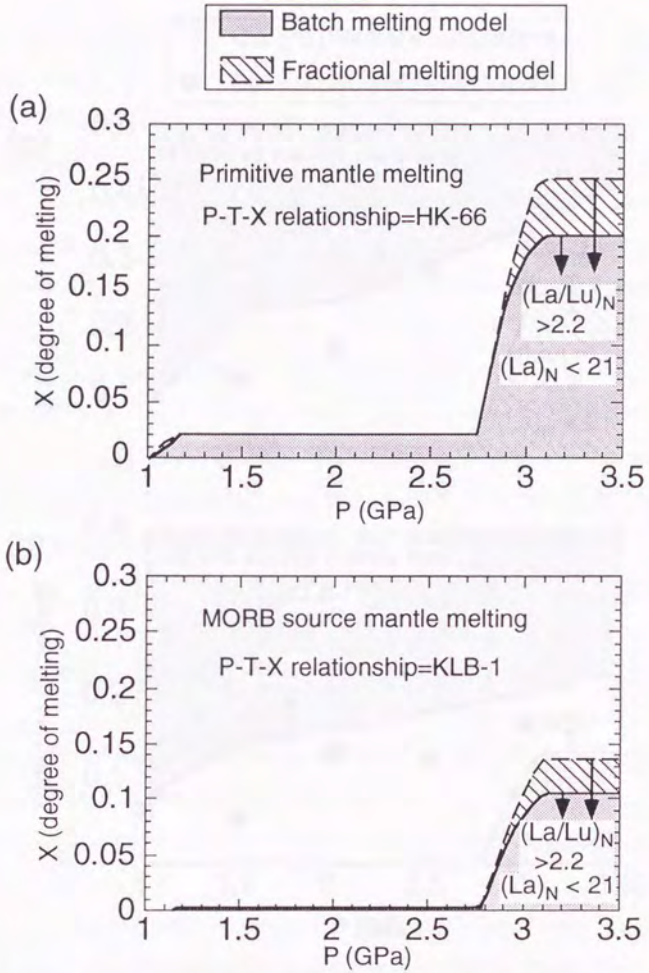

Fig. 4.18 Probable range of degree of melting to satisfy $(La/Lu)_N$ of the Deccan pristine magma ($\geq$ 2.2), shown with the pressure of melting. A source material is primitive mantle (a) and MORB-source mantle (b).

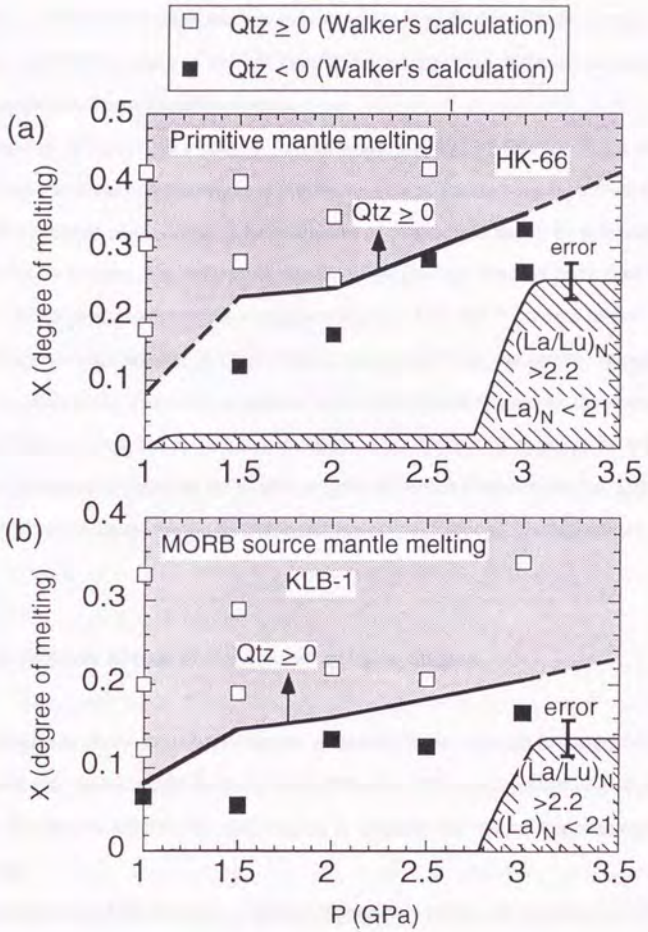

Fig. 4.19 Plots of the possible degree of melting to generate the major element composition (tholeiitic basalts) of the Deccan pristine magma determined at Fig. 4.11, and the possible degree of melting to generate the $(La/Lu)_N$ of the Deccan pristine magma determined at Fig. 4.18 shown with pressures. Error bar shows 2 sigma uncertainties witch include those for the source chemistry (McKenzie and O'Nions, 1991).

Therefore, it can be concluded that the pristine magma of Deccan Traps cannot be generated by partial melting of typical mantle lherzolites, even if we consider the subsequent fractional crystallization process.

Moreover, if the pristine magma (= Ambenali magma) of Deccan Traps was generated by fractional crystallization of picritic magma at shallow depth (Cohen and Sen, 1994; Lightfoot *et al.*, 1990), a large amount of plagioclase has to be subtracted from the picritic magma. The subtracted amount of plagioclase must be more than 20 wt.% in order to generate the pristine magma which has high FeO* content (about 13 wt.%). When so large amount of plagioclase is subtracted from the picritic magma, negative anomaly of Eu should be recognized in the REE pattern. However, the pristine magma of Deccan Traps has no negative anomaly of Eu in the REE pattern (Fig. 4.8). Therefore, the author believe that the pristine magma of Deccan Traps can not be formed by partial melting of typical mantle lherzolite and subsequent fractional crystallization.

C. A suitable source of the Deccan pristine magma

As described above, the pristine magma of Deccan Traps could not be produced by partial melting of typical mantle lherzolite and subsequent fractional crystallization at any pressures. We have to propose the other sources to generate Deccan pristine magma by their melting.

Extraordinary LREE enriched mantle peridotite may have been the source of the pristine magma of Deccan Traps. Subcontinental lithospheric mantle (Hawkesworth *et al.*, 1988; Turner and Hawkesworth, 1995) is the candidate of the source. It is proposed that the subcontinental mantle is the metasomatized mantle formed by addition of fluid. Previous workers have suggested that the subcontinental lithospheric mantle had higher $^{87}Sr/^{86}Sr$ ratio and lower ε_{Nd} value compared to the typical mantle lherzolite. They have proposed that the additional fluid has high Rb/Sr and low Sm/Nd ratios compared to the typical mantle lherzolite. When we can accept that the occasion of the fluid addition was

old enough, the metasomatized mantle should have extraordinary high $^{87}Sr/^{86}Sr$ and low ε_{Nd} ratios. As a result, the metasomatized mantle should become enriched in highly incompatible elements, especially in LREE. However, I have already defined that the pristine magma of Deccan Traps was isotopically depleted and the isotope ratios were lower in $^{86}Sr/^{87}Sr$ and higher in ε_{Nd} than those of primitive mantle (Chapter IV-2). The source of the Deccan pristine magma must have the same isotope ratios with the magma. Therefore, it is impossible to generate the pristine magma of Deccan Traps by partial melting of the subcontinental lithospheric mantle.

Moreover, MgO contents of tholeiitic magmas formed by partial melting of mantle lherzolite are always higher than those of the Deccan pristine magma (*e.g.*, Hirose and Kushiro, 1993). To explain this compositional difference, fractional crystallization process might be one possibility. As discussed above, however, the negative anomaly of Eu might generate when the magma underwent large amount of fractional crystallization. Therefore, it has been concluded that the pristine magma of Deccan Traps could not be generated by partial melting of mantle lherzolite.

Magma formed by partial melting of the subducted MORB may be a candidate of the pristine magma of Deccan Traps. This is because the mass fraction of the subducted MORB is estimated as about 5 % in the whole mantle (*e.g.*, Hess, 1989). The subducted MORB is one of the most important candidate for the source of LIPs which erupted all over the world. Compositional characteristics of the pristine magma described above might be generated by the partial melting of MORB, because of the following reasons. Most of melts formed by partial melting of dry-MORBs at various pressures were tholeiitic magma (*e.g.*, Johnston, 1986).

Paying attention to these characteristics of MORB, Yasuda and Fujii (1994) proposed that magmas formed by partial melting of a plume which consists of the subducted MORB and lherzolite would be the magmas of LIPs. This is called the composite plume model. This model was petrologically investigated by Yasuda and Fujii (1994), while the exact compositions of partial melts of MORB had not been reported. There were not known the exact pressure and temperature conditions under which LIP's

magma is generated. Petrological investigations of this model will be reported in the following chapter.

V. Magma genesis of Deccan pristine magma

1. Purpose

Deccan Trap is one of the most famous area among the Large Igneous Provinces (LIPs). LIPs are continua of voluminous mafic rock emplacements which originate via process other than normal sea-floor spreading (Coffin and Eldholm, 1994). The activity of LIPs is characterized by their huge magma supply during relatively short time scale such as < 2 Ma (*e.g.*, Tolan *et al.*, 1989; Vandamme *et al.*, 1991). It has been proposed that mantle plume incident at the base of the lithosphere generates huge amount of magma of LIPs, and a hot spot represents successive magmatism associated with the mantle plume (*e.g.*, Duncan and Richards, 1991; Richards *et al.*, 1989).

Three plume models have been proposed to explain the emplacement of LIPs (Fig. 5.1). The first model is called the mantle plume initiation model (Campbell and Griffiths, 1990; Farnetani and Richards, 1994; Griffiths and Campbell, 1990). According to this model, the first massive volcanic event corresponds to melting of large leading "head" of the plume, while the following magmatic activity of the hot spot is associated with the remaining plume "tail" (Fig. 5.1a). It has been proposed that mantle plumes originate from a thermal boundary layer in the mantle, the core mantle boundary. The large scale melting is induced by impact of the mantle plume head at the base of the lithosphere (Fig. 5.1a). The second model is called the rifting/decompression model (White and McKenzie, 1989, 1995). This model proposes adiabatic upwelling and decompressional melting of hot asthenosphere as a result of extending lithosphere. The plume-derived thermal mushroom (Fig. 5.1b) causes dynamic uplift. The magmatism is not driven by the plume but is response to lithospheric extension such as continental break-up.

The above two models assumed partial melting of mantle lherzolites. In chapter IV, however, it has been concluded that partial melting of mantle lherzolites and subsequent fractional crystallization can not generate the pristine magma of Deccan Traps, even if we considered subcontinental lithospheric mantle as the source. Moreover, it has been

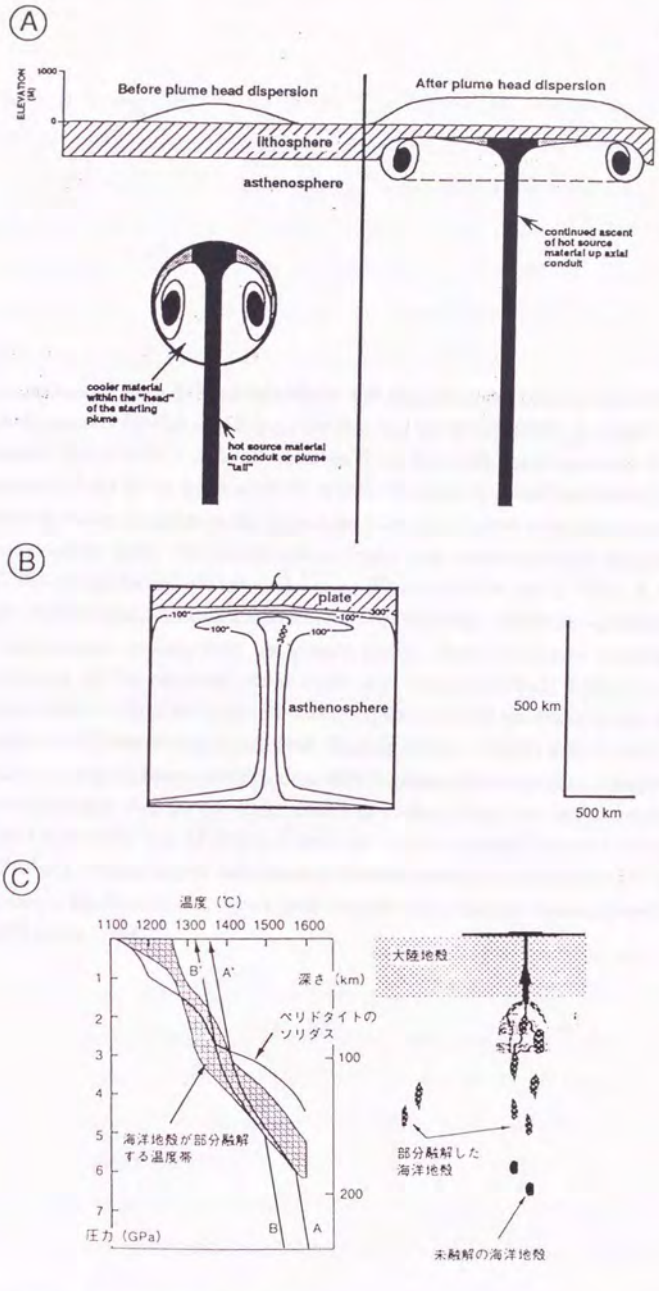

Fig. 5.1 (See next page for explanations)

Fig. 5.1 (--- continued) Three different models for LIP generation and emplacement: (a) The mantle plume initiation model (*e.g.*, Griffiths and Campbell, 1990). A mantle plume (excess temperature > 300 °C) detaches from the weak, heterogeneous thermal boundary layer D" at the base of the mantle. The mantle plume entraining mantle material during its ascent to the base of the lithosphere where large transient plume head develops (left), rifts the lithosphere (right), and causes excessive magmatism. (b) The rifting/decompression model (*e.g.*, White and McKenzie, 1989). A steady state thermal plume (excess temperature > 170 °C) exists. Adiabatic upwelling and decompression melting over the mantle plume causes excessive melting and volcanism. (c) The composite plume model (*e.g.*, Yasuda and Fujii, 1994). A mantle plume entrains subducted basaltic blocks or layers at the 660 km discontinuity during its ascent and form a composite plume. Basaltic blocks or layers start to melt when plume temperature becomes higher than MORB solidus. When the plume temperature becomes higher than the peridotite solidus at shallow depth, the excess amount of hybrid melts from both MORB and peridotite can be separated from the composite plume and erupted (right). Relationship between pressure and temperature of the composite plume were also shown (left). (a) and (b) models are compiled by Coffin and Eldholm (1994).

suggested that the subducted MORB is suitable for the source of the pristine magma of Deccan Traps. This suggestion has been supported by the following facts. First, compositions of melts formed by partial melting of MORB at high pressures (> 2 GPa; *e.g.*, Jhonston, 1986) are akin to the composition of the Deccan pristine magma. We need not consider the fractional crystallization process. Second, the voluminous magmas of LIPs could be produced by partial melting of the subducted MORB (plus ambient lherzolite) in the mantle plume, whereas the voluminous magma could not be produced by partial melting of a plume which consists of only lherzolite at a given melting model. This is because degree of melting of MORB is extremely higher than that of lherzolite at a given pressure and temperature. Third, it has been believed that a large quantity of the subducted MORBs existed in the mantle. For example, Hess (1989) has estimated that the subducted MORB represented about 5 % of the mass of the whole mantle. We can suggest that this subducted MORB is the source of LIPs which erupted all over the world.

Considering these characteristics of MORB, Yasuda and Fujii (1994) proposed that the melt produced by partial melting of a composite plume which consists of basaltic block (= subducted MORB) and ambient lherzolite, represented the magma of LIPs. The subducted MORBs (basaltic blocks or layers) stagnated at the boundary between the upper and lower mantles were caught by an upwelling mantle plume, and the hybrid mixture form a composite plume (Fig. 5.1c). A large volume of magma can be produced as pockets in the composite plume during adiabatic upwelling, because degree of melting of basalt is enormously higher than that of mantle peridotite at a given pressure and temperature. This partial melting model is called the composite plume model. However, the exact compositions of partial melts of MORB at high pressures are very little known, such that Yasuda and Fujii (1994) did not exactly evaluate the possibility of the composite plume model petrologically and geochemicaly.

In this section, therefore, the exact compositions of melts formed by partial melting of MORB at high pressures ($\geq$ 3 GPa) have been determined using the diamond aggregate

method (Baker and Stolper, 1994; Hirose and Kushiro, 1993). Moreover, the composite plume has been investigated petrologically based on the melting experiments.

2. Partial melting of the subducted oceanic crust (MORB)

Numerous partial melting experiments were performed to determine the phase relations for MORB at low pressures ($\leq$ 2 GPa; *e.g.*, Green, 1969; Green and Ringwood, 1967). On the other hand, only a little phase relations and partial melt compositions of MORB were reported at high pressures (> 2 GPa; *e.g.*, Jhonston, 1986; Yasuda *et al.*, 1993). They showed only the partial melt compositions near the liquidus. In order to evaluate whether the composite plume model is suitable for magma genesis of LIPs or not, we have to know the exact phase relations and partial melt compositions of MORB at high pressures. In this section, compositions of partial melts formed by various degrees of melting of MORB have been determined to know the effect of pressure and temperature. The experiments were conducted at high pressure ($\geq$ 3 GPa) which correspond to the depth of the top of the continental asthenosphere. Compositions of residual phases have been also determined.

A. Starting material and experimental method

The starting material used in the experiments is an abyssal tholeiite (49-2-2,13-17) from the Mid-Atlantic Ridge (Deep Sea Drilling Project (DSDP): Leg 45 Site 395A; Melson *et al.*, 1978). The abyssal tholeiite is aphyric glassy basalt. Fig. 5.2 shows bulk chemical compositions of the starting material and the other abyssal tholeiites. Composition of the starting material is similar to the average composition of MORB except that CaO content may be close to the poorest extreme of MORB glass. The starting material is, therefore, considered to represent the average composition of MORB.

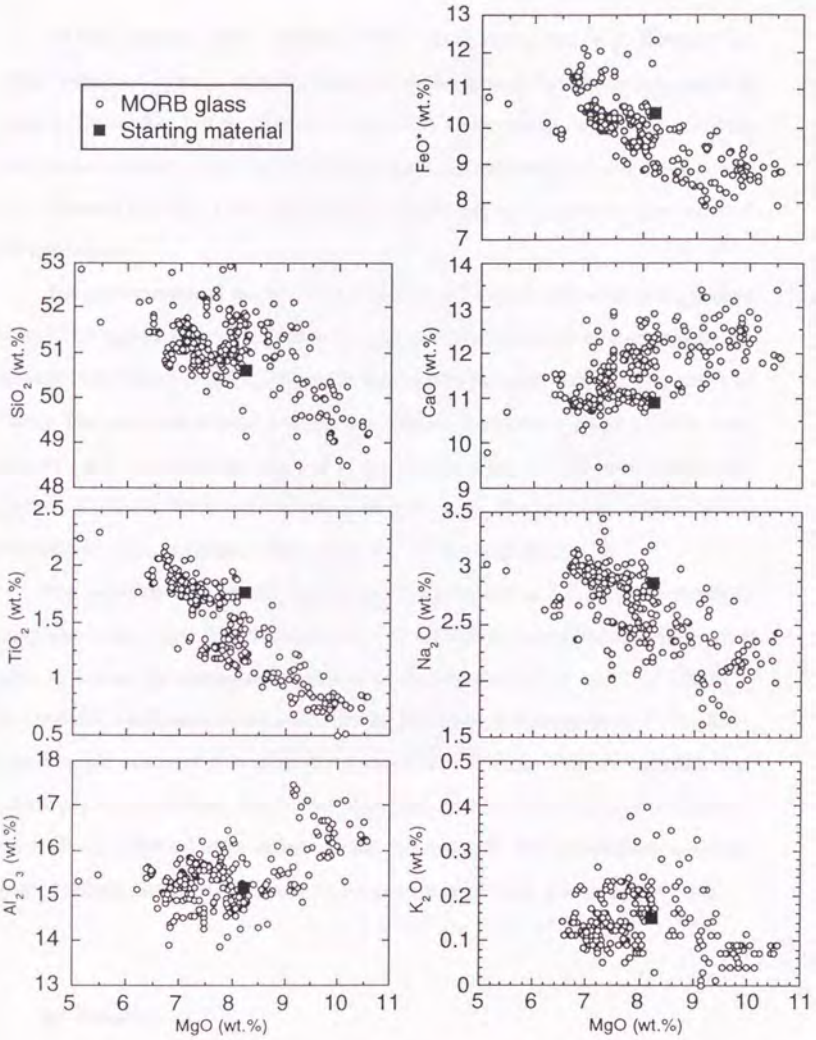

Fig. 5.2 Plots of major oxides versus MgO for a stating material (Leg45-395A-49-2-2, 13-17). 257 analyses for N-MORBs are also shown (Melson *et al.*, 1976). It can be seen that composition of the starting material falls within the cluster of MORBs.

MORBs contain a little amount of H_2O before subduction (*e.g.*, Dixon *et al.*, 1988). However, hydrous minerals such as hornblende must have been dehydrated at depth shallower than 110 km (Tatsumi *et al.*, 1989). Consequently, water contents of the subducted oceanic crust may be small except the water retained in lawsonite and zoisite (*e.g.*, Schmidt and Poli, 1994). All melting experiments were, therefore, performed at dry conditions.

The starting material was prepared in powder. All experiments were accomplished by an MA 8 type multi-anvil high pressure apparatus driven by a pair of guide blocks in a uniaxial 2000 ton press (ERI 2000) at the Earthquake Research Institute, University of Tokyo. The experiments were done in three different pressures 3, 4 and 5.5 GPa using the anvils with truncated edge length of 12 mm. Twelve pieces of preformed pyrophyllite gaskets of 3.0 mm thick and 6.0 mm wide were used. The pressure medium was a semisintered zirconium oxide octahedron with an 18 mm edge length.

The assembly used in this experiments is shown in Fig. 5.3. Graphite heater is composed of five parts. The thick central tube of graphite is sandwiched between thin tubes to reduce the temperature gradient in the sample cell (< 15 °C at 1500°C). Temperature was measured and controlled by two types of thermocouple. Pt/$Pt_{87}Rh_{13}$ thermocouple was used to measure the temperature difference between a capsule and surface of pressure medium. Temperature difference between surface of pressure medium and room was corrected using alumel-chromel thermocouple. Pressure calibration and the detailed descriptions of experimental procedure were reported by Yasuda *et al.* (1990).

B. Results

Experimental details and phase assemblage in each charge are shown in Table 5.1. The melting phase relations of the experiments are shown in Fig. 5.4. The liquidus phase is clinopyroxene followed by garnet at pressure range in this study (3.0-5.5 GPa). Liquidus temperature is about 1480 °C at 3 GPa and rises to about 1575 °C at 5.5 GPa.

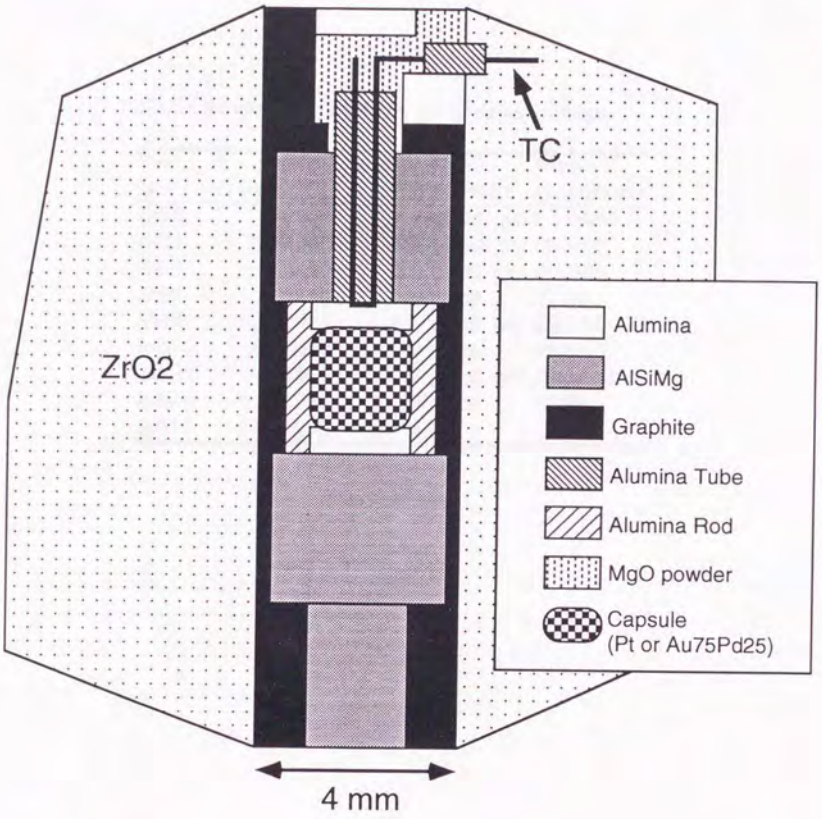

Fig. 5.3 Cross section of truncation 12 mm cell assembly.

Table 5.1 Experimental conditions and phase assemblages.

Run No.	P (G Pa)	T (°C)	Duration (hours)	Run products	Phase proportions
MB6	3	1300	7	gl, cp, gar	23:64:13
MB7	3	1350	12	gl, cp, gar	29:66:5
MB5	3	1400	3.5	gl, cp, gar	60:34:5
MB8	3	1440	6	gl, cp	77:23
MB9	4	1450	6.5	gl, cp, gar	29:63:8
MB10	4	1500	5	gl, cp	45:55
MB21	5.5	1500	7	gl, cp, gar	28:57:15
MB20	5.5	1550	6	gl, cp	62:38
MB13	5.5	1600	6	gl	100

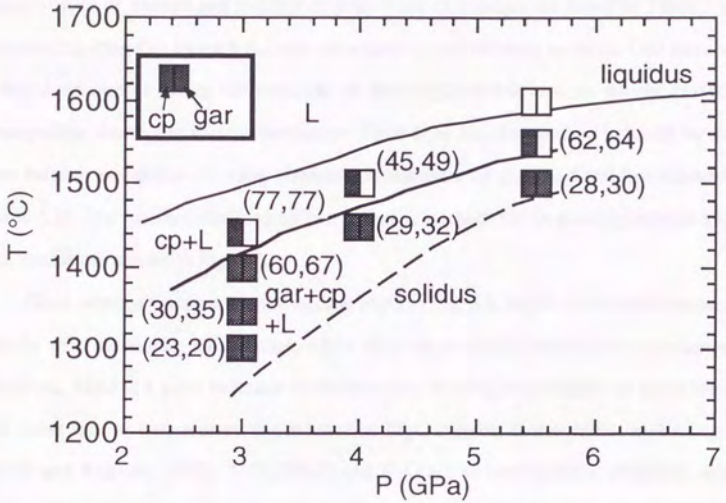

Fig. 5.4 Melting phase relations of a MORB (Leg 45-395A-49-2-2 ,13-17). The numbers in parentheses are the values of degree of melting calculated based on K_2O content (left) and on the mass balance calculation of major element for glass and residual minerals (right).

Compositions of glasses and residual crystals from all charges are listed in Table 5.2. Degree of melting (X) for each run was calculated by two different methods. One method is based on simply using the contents of only K_2O which acts as nearly perfect incompatible element in these experiments (Table 5.2). Another method is based on the mass balance calculation of major element compositions for glass and residual minerals (Table 5.1). The results calculated by two different methods are in good agreement and both results are shown in Fig. 5.4.

Glass compositions are plotted against MgO in Fig. 5.5. MgO in the melt increases linearly with increasing temperature, while they are relatively insensitive to pressure. Therefore, MgO is a good indicator of temperature. Melting experiments of peridotites also show similar temperature dependence of MgO content in the partial melts (*e.g.*, Hirose and Kushiro, 1993). TiO_2, Na_2O and K_2O act as incompatible elements, and consequently, they decrease with increasing temperature (= MgO). SiO_2 also decreases with increasing MgO. On the other hand, CaO which constitutes both residual phases, clinopyroxene and garnet, increase with increasing MgO. Because Al_2O_3 and FeO contents in garnet phases are higher than those in liquidus clinopyroxene, those contents in the melts decrease after garnet disappear with increasing MgO. In this study, they have maximum values when garnet phases disappear.

TiO_2 content for a given value of MgO increases with increasing pressure (Fig. 5.5). This character would be generated by decreasing TiO_2 contents in the residual garnet and clinopyroxene (Table 5.2). On the contrary, Al_2O_3 content decreases according to the decreasing of the clinopyroxene/garnet ratios of residual phases with increasing pressure. The maximum value of FeO content shifts to the MgO-rich side. This fact is consistent with the increasing of the liquidus temperature of garnet with increasing pressure.

In all runs, clinopyroxene and garnet crystals are homogeneous, respectively, except that some garnet crystals have inclusions of clinopyroxene. Glass is also homogeneous. The crystal-liquid Fe-Mg exchange coefficient for clinopyroxene, $K_D^{cp\text{-}gl}$, and that for garnet, $K_D^{gar\text{-}gl}$, are nearly constant throughout all runs (Table 5.3). These

Table 5.2 Electron microprobe analyses of run products of experiments reported in Table 5.1.

Leg45-395A-49-2-2(13-17) phase	Run No.	P (GPa)	T (°C)	n	SiO2 (wt.%)	TiO2	Al2O3	FeO*	MnO	MgO	CaO	Na2O	K2O	P2O5	F (fraction)
gl	MB6	3	1300	3	58.10	3.48	14.96	8.45	0.12	2.64	6.98	3.92	0.73	0.62	0.21
					0.17	0.04	0.06	0.39	0.02	0.06	0.03	0.14	0.03	0.02	0.02
	MB7	3	1350	5	54.86	3.29	14.78	11.10	0.15	3.66	7.95	3.37	0.43	0.41	0.35
					0.34	0.11	0.20	0.23	0.01	0.07	0.13	0.07	0.02	0.05	0.04
	MB5	3	1400	7	51.72	2.39	15.60	11.59	0.17	5.55	9.18	3.37	0.22	0.21	0.67
					0.35	0.08	0.21	0.53	0.02	0.07	0.29	0.11	0.02	0.05	0.09
	MB8	3	1440	10	50.93	2.07	15.77	10.99	0.19	6.52	10.08	3.09	0.19	0.17	0.77
					0.30	0.09	0.10	0.37	0.02	0.09	0.14	0.11	0.01	0.05	0.10
	MB9	4	1450	4	54.10	3.51	14.15	11.54	0.15	4.06	8.75	2.85	0.47	0.42	0.32
					0.34	0.14	0.06	0.11	0.02	0.13	0.07	0.05	0.01	0.03	0.04
	MB10	4	1500	5	51.52	2.89	15.13	12.93	0.19	5.15	9.05	2.56	0.30	0.28	0.49
					0.35	0.09	0.05	0.15	0.01	0.13	0.08	0.25	0.03	0.04	0.07
	MB21	5.5	1500	6	54.61	3.83	13.28	11.13	0.14	4.13	9.19	2.75	0.49	0.45	0.31
					0.42	0.09	0.20	0.32	0.03	0.06	0.19	0.13	0.03	0.03	0.04
	MB20	5.5	1550	10	50.32	2.33	15.35	12.85	0.19	6.21	9.51	2.79	0.23	0.22	0.64
					0.31	0.09	0.29	0.53	0.03	0.12	0.24	0.25	0.01	0.05	0.08
	MB13	5.5	1600	8	50.40	1.76	15.13	10.33	0.19	8.18	10.84	2.86	0.15	0.16	1
					0.47	0.06	0.12	0.26	0.03	0.15	0.19	0.12	0.02	0.03	
cp	MB6	3	1300	5	49.56	1.36	14.28	8.99	0.16	9.47	13.03	3.15			
					0.65	0.16	1.04	0.52	0.02	0.33	0.97	0.09			
	MB7	3	1400	7	49.45	1.01	14.76	9.48	0.16	9.79	12.49	2.86			
					0.27	0.06	0.37	0.40	0.03	0.28	0.28	0.08			
	MB5	3	1400	6	49.69	0.69	12.80	7.84	0.18	12.00	14.29	2.51			
					0.59	0.06	0.57	0.17	0.03	0.27	0.37	0.10			
	MB9	4	1450	6	50.23	0.89	15.03	8.67	0.16	9.45	12.30	3.27			
					0.73	0.59	0.84	0.85	0.54	0.78	0.76	0.61			
	MB10	4	1500	6	50.00	0.67	14.87	8.25	0.17	10.53	12.50	3.03			
					0.41	0.06	0.21	0.17	0.03	0.26	0.39	0.18			
	MB21	5.5	1500	6	51.19	0.87	14.36	8.14	0.15	9.19	12.56	3.54			
					0.48	0.04	0.55	0.55	0.03	0.12	0.33	0.11			
	MB20	5.5	1550	6	50.29	0.53	14.66	6.44	0.15	11.39	13.25	3.29			
					0.34	0.06	0.20	0.39	0.02	0.26	0.18	0.15			
gar	MB6	3	1300	6	39.85	1.09	21.74	18.63	0.42	10.98	7.18	0.11			
					0.82	0.14	0.33	0.58	0.03	0.35	0.19	0.02			
	MB7	3	1400	9	39.24	1.18	21.84	18.37	0.44	11.87	6.97	0.09			
					0.31	0.08	0.22	0.43	0.04	0.15	0.18	0.03			
	MB5	3	1400	6	39.83	0.98	22.31	15.23	0.43	13.82	7.32	0.08			
					0.21	0.06	0.29	0.40	0.03	0.34	0.16	0.02			
	MB9	4	1450	1	39.27	1.11	21.83	18.13	0.41	11.71	7.40	0.14			
	MB21	5.5	1500	6	39.43	1.24	21.63	17.71	0.41	11.59	7.84	0.15			
					0.18	0.10	0.13	0.53	0.04	0.27	0.22	0.03			

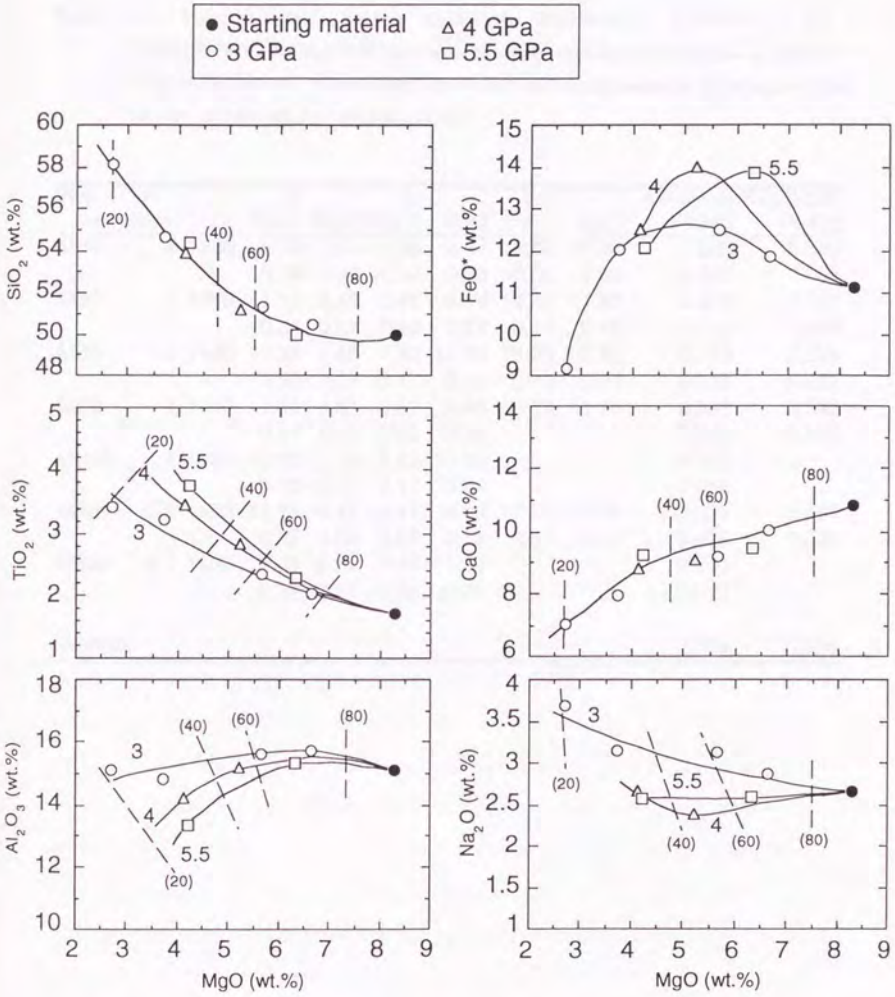

Fig. 5.5 Plots of major elements versus MgO for partial melts of a MORB (Leg 45-395A-49-2-2, 13-17). Solid curves with numbers are experimentally determined isobaric liquid compositions. Dotted lines with numbers in parentheses show the estimated degrees of melting.

Table 5.3 Mineral-liquid Fe-Mg exchange distribution coefficient, $K_D = (Fe/Mg)^{mineral}/(Fe/Mg)^{liquid}$, for run products of experiments reported in Table 5.1. Weight fractions of minerals and liquids are calculated based on least-square mass balance calculations for major elements.

Run	P	T	gl		cp		gar		KD(gl-cp)	KD(gl-gar)
No.	(GPa)	(°C)	FeO*	MgO	FeO*	MgO	FeO*	MgO	Fe-Mg	Fe-Mg
MB6	3	1300	8.45	2.64	8.99	9.47	18.63	10.98	0.297	0.530
			0.39	0.06	0.52	0.33	0.58	0.35	0.025	0.036
MB7	3	1350	11.10	3.66	9.48	9.79	18.37	11.87	0.319	0.510
			0.23	0.07	0.40	0.28	0.43	0.15	0.018	0.020
MB5	3	1400	11.59	5.55	7.84	12.00	15.23	13.82	0.313	0.528
			0.53	0.07	0.17	0.27	0.40	0.34	0.018	0.031
MB9	4	1450	11.54	4.06	8.67	9.45	18.13	11.71	0.323	0.545
			0.11	0.13	0.85	0.78			0.043	0.018
MB10	4	1500	12.93	5.15	8.25	10.53			0.312	
			0.15	0.13	0.17	0.26			0.013	
MB21	5.5	1500	11.13	4.13	8.14	9.19	17.71	11.59	0.329	0.567
			0.32	0.06	0.55	0.12	0.53	0.27	0.025	0.028
MB20	5.5	1550	12.85	6.21	6.44	11.39			0.273	
			0.53	0.12	0.39	0.26			0.022	
average									0.309	0.536

facts suggest that all charges attained almost chemical equilibrium. The grain size of the clinopyroxene crystals is about 10-30 μm and that of garnet crystals varies from about 30 to 150 μm.

3. Petrological and geochemical investigations of the composite plume model

A. Introduction of the model

Yasuda and Fujii (1994) have proposed the eruption of voluminous magma formed by adiabatic upwelling of the composite plume. When we assume the existence of the composite plume, the following question arises. Where do the basaltic blocks incorporate into the plume in mantle? It bas been suggested that the subducted lithosphere is denser than ambient mantle lherzolite (pyrolite) except in the 660 km discontinuity (Irifune and Ringwood, 1987, 1993). This 660 km discontinuity is caused by the endothermic transformation of γ-spinel into perovskite and magnesiwüstite (Ito and Takahashi, 1989). Irifune and Ringwood (1993) have reported that the MORB layer of the subducted lithosphere was less denser than ambient mantle lherzolite between 660 and 800 km, and therefore, the subducted MORB may have been accumulated above 660 km. However, whether subducted slabs accumulate above the 660 km discontinuity or penetrate straightforward to the lower mantle, depends on many geophysical parameters such as viscosity, density contrast and viscosity step at 660 km, velocity of trench migration, the existence of 400 km discontinuity, and so on (*e.g.*, Bunge *et al.*, 1996; Christensen and Yuen, 1984; Christensen, 1996; Tackley *et al.*, 1994).

Yasuda and Fujii (1994) have assumed that blocks or layers of the subducted MORB were accumulated along the 660 km discontinuity. In this model, small size is desirable for the subducted MORB. The proposed composite plume model is shown in Fig. 5.6. They have suggested that the magmas of LIPs were formed by the following

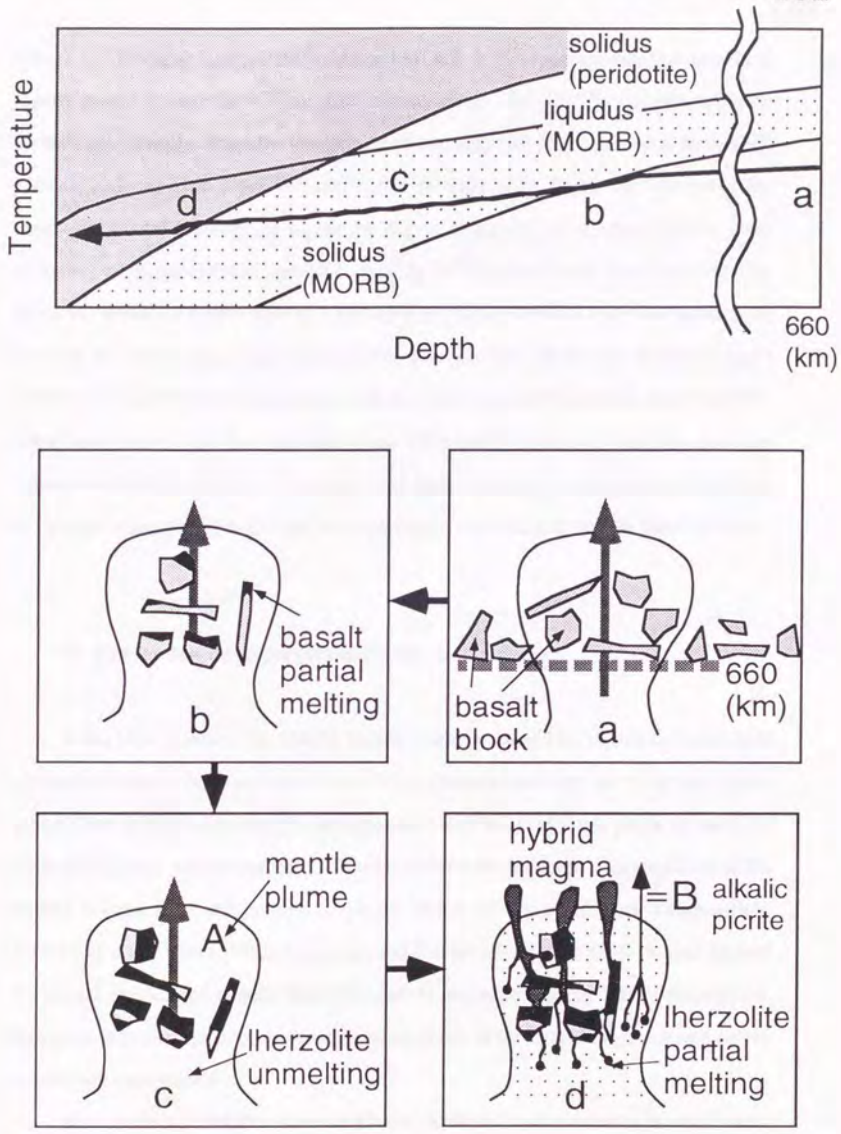

Fig. 5.6 Schematic diagrams based on the composite plume model of Yasuda and Fujii (1994), showing the melting process during its ascent. See text for the explanation.

model. (1) Block or layer of the subducted MORB is incorporated into the upwelling mantle plume around the 660 km discontinuity (Fig. 5.6a). (2) The composite plume ascends adiabatically. When the temperature of the composite plume intersects the MORB solidus, only basaltic block or layer melts partially (Fig. 5.6b). (3) The more the composite plume ascends, the higher the degree of melting of basaltic block or layer becomes, while the ambient lherzolite part (Fig. 5.6A) of the plume does not melt (Fig. 5.6c). (4) When the temperature of the composite plume intersects lherzolite solidus, the ambient lherzolite part of the plume melts partially (Fig. 5.6d). (5) Hybrid magma consists of partial melt of basaltic block or layer and that of the ambient lherzolite (Fig. 5.6A) is separated from the composite plume when the melt phase of lherzolite becomes connected (McKenzie, 1984). This model can explain the high eruption rates of LIPs by the sudden release of melts formed by a high degree of melting of basaltic block or layer.

B. Estimation of segregation depth

It has been proposed that hybrid magma would be formed by mixing of partial melt of basaltic block or layer and partial melt of the ambient lherzolite part in the composite plume. The hybrid magma may have segregated from the composite plume in the wide range of pressure and temperature. We want to estimate the depth of segregation of the hybrid magma from the composite plume, based on the whole rock composition. McKenzie and O'Nions (1991) have proposed that the segregation depth of melt formed by partial melting of mantle lherzolite can be calculated using REE composition. However, it is difficult to estimate segregation depth of the hybrid magma based on the whole rock composition.

It has been reported that there are alkalic picrite lavas which can be in equilibrium with mantle lherzolite on the Kathiawar area of Deccan Traps (Alexander and Gibson, 1977; Krishnamurthy and Cox, 1977; Melluso *et al.*, 1995). The whole rock compositions of the alkalic picrites are shown in Table 5.4. Compositions of olivine

Table 5.4 Major and rare earth element compositions of alkalic picrite produced on Kathiawar area in Deccan Traps. Data of major element compositions are from Krishnamurthy and Cox (1977). Data of rare earth element compositions are from Alexander and Gibson (1977).

Sample	SiO2	TiO2	Al2O3	FeO*	MnO	MgO	CaO	Na2O	K2O	P2O5
D10	46.66	2.55	12.27	11.29	0.17	10.82	12.57	2.16	1.15	0.36
D12	47.60	2.01	10.11	10.75	0.14	13.26	13.25	1.65	0.92	0.31
average	47.13	2.28	11.19	11.02	0.15	12.04	12.91	1.91	1.04	0.33

sample	Ce	Nd	Eu	Gd	Tb	Tm	Yb	Lu
D5	44.7	23.3	1.64	4.18	0.7	0.31	1.56	0.23
D6	50.4	25.2	1.7	3.85	0.7		1.56	0.23
D7	54.5	26.9	1.69	4.39	0.68	0.34	1.54	0.25
D8	54.3	27.6	1.85	6.16	0.74		1.88	0.26
D10	68.3	34.1	2.23	7.26	0.87	0.39	2.25	0.31
D12	51.3	25.6	1.69		0.7		1.6	0.27
D30	42.6	18.1	1.18	3.01	0.53	0.24	1.33	0.18
D32	50.6	26.2	1.6	4.9	0.73	0.3	1.86	0.21
average	52.09	25.85	1.70	4.82	0.71	0.32	1.70	0.24

Sample	Q	or	ab	an	ne	di	hy	ol	il	ap
D10	0	6.8	9.75	20.4	4.62	32.3	0	20.4	4.84	0.83
D12	0	5.44	10.2	17.5	2.04	37.5	0	22.9	3.82	0.72

phenocrysts in the alkalic picrites are ranging from Fo_{90} to Fo_{87}. NiO contents of the whole rocks range from 0.28 and 0.39 wt.% (Krishnamurthy and Cox, 1977). This composition relationships shows that the alkalic picrites can be in equilibrium with mantle lherzolite (Takahashi, 1986b). We can estimate the segregation pressures and temperatures of the alkalic picrites based on the method proposed by McKenzie and O'Nions (1991).

Both the alkalic picrite lavas and the uncontaminated basalts the latter of which constitute main part of Deccan Traps erupted on the same province, Deccan Traps. Moreover, it was reported that eruption of the alkalic picrite lavas was coeval with the eruption of basalts in the main part of Deccan Traps. Therefore, we can propose that the alkalic picrites and the pristine magma of Deccan Traps were segregated from the same plume. The alkalic picrites were considered as the magma formed by partial melting of the ambient lherzolite part of the composite plume and erupted without mixing with partial melt of basaltic block or layer in the same composite plume (Fig. 5.6B). Assuming that the segregation depth of the alkalic picrite magma was the same as that for the hybrid magma, the segregation depth of the hybrid magma can be estimated.

It is known that alminous phase in mantle lherzolite changes from spinel to garnet when pressure increases from 2.5 to 3.5 GPa. Assuming the proportion of garnet vs. spinel varies linearly over the depth range garnet-in to spinel-out (Fig. 4.9b), the segregation depth of magma was calculated using the REE pattern of the alkalic picrites. The REE concentrations of partial melts were calculated according to batch melting model using equations (4.7)-(4.11) and data set of Table 4.6. Pressure and temperature relationships of garnet-in and spinel-out boundaries were calculated by equation (4.2). Relationships among pressure, temperature and degree of melting for mantle lherzolite were calculated by equation (4.3), because the lherzolite part of the composite plume can be assumed to be primitive mantle. The calculated results are shown in Fig. 5.7. If the segregation pressure is lower than 2.5 GPa, the calculated composition shows almost flat pattern (Fig. 5.7a) because of the absence of garnet as residual phase. On the contrary, if that pressure is higher than 3.5 GPa, the calculated composition shows a steeper pattern

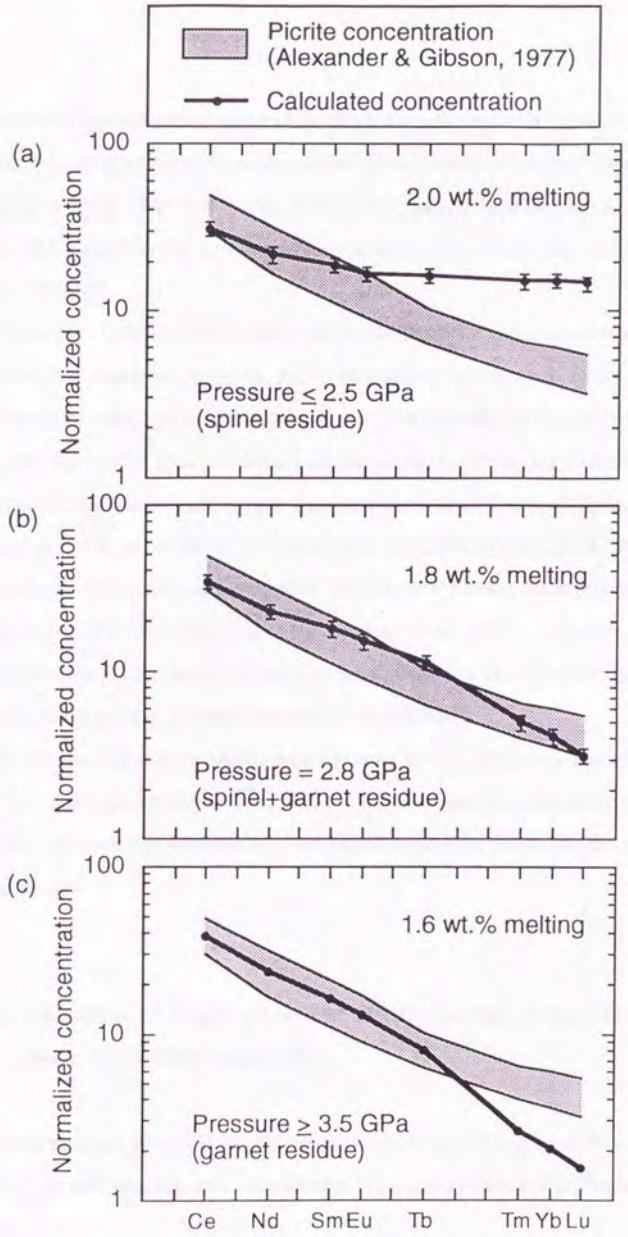

Fig. 5.7 Normalized REE abundances for alkalic picrites erupted on the Kathiawar area in Deccan Traps (Alexander and Gibson, 1977). Bold lines show REE patterns calculated by batch partial melting of primitive mantle at the pressure lower than 2.5 GPa (a), at 2.8 GPa (b) and at higher than 3.5 GPa (c). Normalized values are from the primitive mantle model (McKenzie and O'Nions, 1991).

compared with those of alkalic picrites (Fig. 5.7c). The calculated composition is closest to the average composition of the alkalic picrites, when pressure and degree of melting are 2.8 GPa and 0.018, respectively (Fig. 5.7b). Thus, we can estimate that segregation pressure and temperature of the alkalic picrite magma in Kathiawar area are about 2.8 GPa and 1410 °C.

The depth of segregation estimated with major element composition was similar to that calculated above by inverting REE composition. In Fig. 5.8, major element compositions of alkalic picrites were compared with those of liquids in equilibrium with mantle lherzolite which were determined experimentally by Hirose and Kushiro (1993). Assuming that the alkalic picrites were generated under anhydrous conditions, they are estimated to have been equilibrated with lherzolite at 2-3 GPa. Melluso *et al.* (1995) also showed that the picrite magma generated by low degree of melting could be equilibrated with lherzolite at 2.5-3.0 GPa (Fig. 15 in Melluso *et al.*, 1995). Therefore, we can conclude that the alkalic picrites erupted on the Kathiawar area of Deccan Traps were formed by partial melting of mantle lherzolite at about 2.8 GPa.

As we assumed that the alkalic picrite magma and the pristine magma of Deccan Traps were segregated from the same plume at the same pressure and temperature, the segregation pressure and temperature of the hybrid magma are about 2.8 GPa and 1410 °C, respectively.

C. Estimation of weight fraction of MORB material in the composite plume using REE composition

Assuming that the hybrid magma was generated by partial melting of the composite plume, major and trace element concentration ($C_{im,cal}$) is calculated by the following equation.

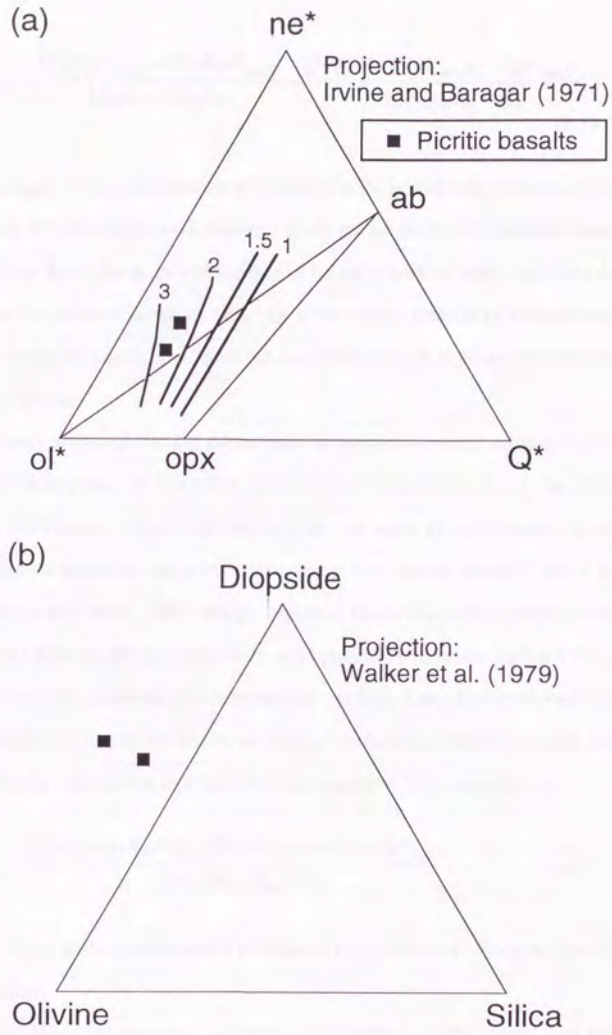

Fig. 5.8 Normative compositions of alkalic picrites erupted in the Kathiawar area in Deccan Traps (Krishnamurthy and Cox, 1977). (a) Plots of the compositions onto normative Nepheline (ne) - Olivine (ol) - Quartz (*Q) plane. Projection scheme is after Irvine and Baragar (1971). Lines with numbers are experimentally determined isobaric liquid compositions for primitive mantle (HK-66) after Hirose and Kushiro (1993). The numbers are pressures in GPa. (b) Plots of the compositions from Plagioclase onto normative Olivine-Diopside-Quartz plane. Projection scheme is after Walker *et al.* (1979).

$$C_{im,cal} = \frac{M_B X_B C_{im,B} + M_P X_P C_{im,P}}{M_B X_B + M_P X_P} = \frac{(M_B/M_P) X_B C_{im,B} + X_P C_{im,P}}{(M_B/M_P) X_B + X_P} \quad (5.1)$$

where, $C_{im,B}$ is the concentration of element i in the partial melt of basaltic block or layer, $C_{im,P}$ is the concentration of element i in the partial melt of the ambient lherzolite part (Fig. 5.6A), X_B is the degree of melting of basaltic block or layer, X_P is the degree of melting of the ambient lherzolite part, M_B is the weight fraction of basaltic block or layer in the composite plume, and M_P is the weight fraction of ambient lherzolite part of the composite plume.

It has been proposed that the partial melt of mantle lherzolite separated from the source when melt phase of lherzolite becomes connected because of the effect of compaction (McKenzie, 1984). It is believed that net work of melt formed by partial melting of mantle lherzolite becomes connected at low degree (about 2 %) of partial melting (Bargen and Waff, 1986) at high pressure. However, partial melts of basaltic block or layer might not be separated from solid phases, because the ambient lherzolite part of the composite plume has not been melted, yet (Fig. 5.6c). Compositions of melts formed by partial melting of basaltic block or layer could be calculated by batch melting equation (4.5). By substituting equation (4.5) into equation (5.1), we arrive at:

$$C_{im,cal} = \frac{(M_B/M_P) X_B C_{i0,B} / (D + X_B(1-D)) + X_P C_{im,P}}{(M_B/M_P) X_B + X_P} \quad (5.2)$$

where, $C_{i0,B}$ is the concentration of element i in the basaltic block or layer in the composite plume.

The difference between the calculated composition of the hybrid magma and observed compositions ($C_{im,obs}$) is described as H:

$$H = \left[\frac{1}{N} \sum_{i=1}^{N} \left\{ \frac{Cim,obs}{\sigma_i C_{i,PM}} - \frac{(M_B/M_P) X_B \left(C_{im,B}/\sigma_i C_{i,PM}\right) + X_P \left(C_{im,P}/\sigma_i C_{i,PM}\right)}{(M_B/M_P) X_B + X_P} \right\}^2 \right]^{\frac{1}{2}}$$

(5.3)

where,

$$C_{im,B} = \frac{C_{i0,B}}{D + X_B(1-D)}$$

where, N is the number of element using the calculation. $C_{i,PM}$ is the concentration of element i in the primitive mantle. σ_i is the standard deviation of $C_{im,obs}/C_{i,PM}$. The calculations were conducted using only REE data.

The following parameters were used for the calculation. The average REE composition of MgO-rich (> 6.6 wt.%) basalts in the uncontaminated basalts was assumed as that of the Deccan pristine magma (= observed composition). The standard deviation of $C_{im,obs}$ was calculated using compositions of MgO-rich (> 6.6 wt.%) basalts in the uncontaminated basalts. The calculated REE composition and standard deviation of the pristine magma are shown in Table 5.5. Results of melting experiments show that degree of melting is about 0.6-0.77 when at 3 GPa and 1400-1440 °C (Table 5.1). These conditions are similar to the segregated condition (2.8 GPa and 1410 °C) of the hybrid magma estimated by inverting REE compositions of the alkalic picrites. Assuming X_B as about 0.6-0.77, the composition ($C_{i0,B}$) of basaltic block or layer within the composite plume can be replaced with the composition of N-type MORB (Sun and McDonough, 1989). The bulk distribution coefficient, D, was calculated based on phase proportion and degree of melting of the melting experiments. The average composition of the alkalic picrites in the Kathiawar area (Alexander and Gibson, 1977; Krishnamurthy and Cox, 1977) was referred to the partial melt composition ($C_{im,P}$) of the ambient lherzolite part of the composite plume. Calculated degree of melting for the alkalic picrites using the REE pattern was applied for X_P. Substituting these parameters into equation (5.3), H is considered to be in function of M_B/M_P. When H was minimized using REE data, the calculated value of M_B/M_P was the best fit value.

The calculated results are listed in Table 5.5. Fig. 5.9a shows the calculated REE compositions of the hybrid magmas and the Deccan pristine magma. We can recognize

Table 5.5 Major and trace element compositions for the hybrid magma calculated in the batch melting model by inverting REE concentrations. Major and trace element compositions of the Deccan pristine magma are also shown. Degree of melting for basaltic block or layer (X_B) and ambient lherzolite part (X_P), mixing ratio (M_B/M_P) of basaltic block or layer and ambient lherzolite part in the composite plume, weight fractions of partial melts of basaltic block or layer (F_{MB}) and ambient lherzolite part (F_{PM}) are also shown.

parameter	XP	XB	MB/MP	FPM	FBM
3 GPa,1400°C	0.018	0.60	0.09	0.25	0.75
3 GPa,1440°C	0.018	0.77	0.05	0.33	0.67

REE	La	Ce	Nd	Sm	Eu	Tb	Yb	Lu
3 GPa,1400°C	9.26	22.04	14.88		1.53	0.83	2.84	0.41
3 GPa,1440°C	10.35	23.52	14.60		1.40	0.77	2.94	0.44
Pristine magma	9.57	23.05	16.35	4.87	1.90	0.96	3.12	0.43
1 signa (N=3)	0.84	1.90	1.66	0.42	0.17	0.08	0.26	0.05

trace element	Rb	Ba	Th	Nb	K	Sr	P	Zr	Y
3 GPa,1400°C	9	97	1	8	2893	261	1067	124	31
3 GPa,1440°C	12	122	1	9	4046	279	1059	116	31
Pristine magma	3	42	1.8	10	1970	212	930	142	32
1 sigma (N=27)	3	16	0.6	2	743	13	92	14	3
XRF error	3	18	2.2	1.1	83	11	44	6	2

major element	SiO2	TiO2	Al2O3	FeO*	MnO	MgO	CaO	Na2O
3 GPa,1400°C	50.18	2.32	14.47	12.11	0.17	7.24	10.27	2.82
3 GPa,1440°C	49.33	2.10	14.24	11.56	0.18	8.39	11.16	2.55
Pristine magma	49.68	2.35	13.93	12.93	0.18	6.95	11.68	2.16
1 sigma (N=29)	0.45	0.24	0.27	0.70	0.01	0.18	0.48	0.12
MORB glass								
1sigma (N=256)	0.80	0.42	0.63	0.89		1.04	0.72	0.36

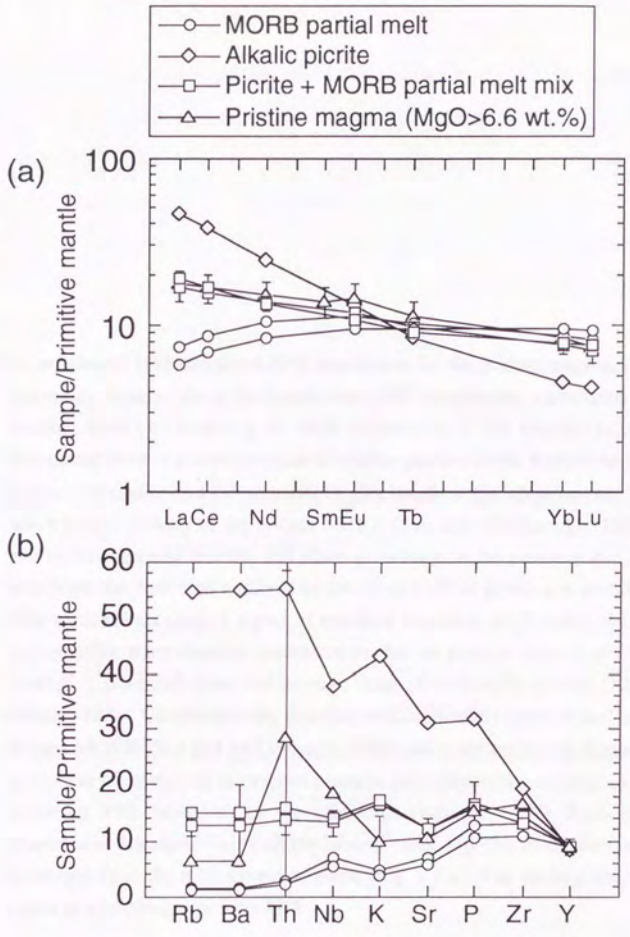

Fig. 5.9 (See next page for explanations)

Fig. 5.9 (--- continued) (a) Normalized REE abundances for the pristine magma, Deccan Traps (triangle). Squares show the normalized REE abundances, calculated in the batch melting model by inverting the REE abundances of the Deccan pristine magma. Diamonds show the average value of alkalic picrites in the Kathiawar area, Deccan Traps (Alexander and Gibson, 1977). Circles show the abundances calculated by batch partial melting of the N-type MORB (Sun and McDonough, 1989) using the estimated degree of melting and phase proportion at the pressure and temperature, which are the condition obtained by inverting REE of the alkalic picrites (Fig. 5.7). The vertical bars show 2 sigma of standard deviation for 3 rocks. (b) Normalized incompatible trace element concentrations for the pristine magma of Deccan Traps (triangle). Diamond shows the average value of the alkalic picrites (Alexander and Gibson, 1977). Circles show the abundances calculated by batch partial melting of the N-type MORB (Sun and McDonough, 1989) using the estimated degree of melting and phase proportion at segregated pressure and temperature conditions obtained by inverting REE inversion of the alkalic picrites (Fig. 5.7). Squares show the abundances calculated based on the mixing ratio, M_B/M_P, in the composite plume, estimated from the REE inversion alone (Fig. 5.9 a). The vertical bar shows the 2 sigma of analytical error with XRF.

that calculated compositions of the hybrid magmas are in good agreement with the composition of the Deccan pristine magma. The calculated M_B/M_P was 0.05-0.09 (Table 5.5). The fraction of partial melt of MORB in the hybrid magma was calculated to be 0.67 to 0.75 (Table 5.5).

D. Major and trace element compositions

The M_B/M_P ratios obtained by inverting REE compositions are applied to estimate major and trace element composition of the hybrid magma. Major element compositions of the hybrid magmas were calculated by equation (5.1). Trace element compositions of the hybrid magmas were calculated by equation (5.2).

The following parameters were used for the calculations. X_B and X_P used in the above calculation which estimates the M_B/M_P ratios were applied for the X_B and X_P of the calculations. Experimentally determined major element compositions of melts formed by partial melting of MORB (3 GPa, 1400 and 1440 °C) were used as major element compositions ($C_{im,B}$) of partial melts of basaltic block or layer in the composite plume. Trace element composition ($C_{im,0}$) of the basaltic block or layer in the composite plume was that of the N-type MORB (Sun and McDonough, 1989). The bulk distribution coefficient, D, was calculated based on the estimated phase proportions of the melting experiments (3 GPa and 1400-1440 °C). The average major and element composition of the alkalic picrites in the Kathiawar area (Alexander and Gibson, 1977; Krishnamurthy and Cox, 1977) was applied to composition ($C_{im,P}$) of the partial melt of the ambient lherzolite part of the composite plume. Trace element composition ($C_{im,P}$) of the partial melt of the ambient lherzolite part of the composite plume was calculated based on batch melting model (equations 4.7-4.11) using estimated degree of melting (= 0.018) and data of Table 4.6. Substituting these parameters and estimated M_B/M_P ratios into equations (5.1) or (5.2), major and trace element compositions of hybrid magma were calculated.

Calculated hybrid magma compositions (Table 5.5) almost coincide with the pristine magma composition of Deccan Traps (Fig. 5.9b, 5.10). CaO content of the calculated hybrid magma is a little lower (about 1 wt.%) than that of the pristine magma. This might be due to depletion in CaO of the starting composition. The starting material has lower CaO content (about 1 wt.%) than the average composition of MORB (Fig. 5.2). This composite plume model can, therefore, produce the pristine magma of Deccan Traps.

E. Isotopes

It is important to show whether the model discussed above is also consistent in terms of the Nd, Sr and Pb isotope data.

Each isotope ratio is a function of age, and shown by the following equations:

$$\left(\frac{^{87}Sr}{^{86}Sr}\right)_P = \left(\frac{^{87}Sr}{^{86}Sr}\right)_0 + \left(\frac{^{87}Rb}{^{86}Sr}\right)_P \left(e^{\lambda_1 t} - 1\right)$$
$$\left(\frac{^{143}Nd}{^{144}Nd}\right)_P = \left(\frac{^{143}Nd}{^{144}Nd}\right)_0 + \left(\frac{^{147}Sm}{^{144}Nd}\right)_P \left(e^{\lambda_2 t} - 1\right)$$
$$\left(\frac{^{206}Pb}{^{204}Pb}\right)_P = \left(\frac{^{206}Pb}{^{204}Pb}\right)_0 + \left(\frac{^{238}U}{^{204}Pb}\right)_P \left(e^{\lambda_3 t} - 1\right)$$
$$\left(\frac{^{207}Pb}{^{204}Pb}\right)_P = \left(\frac{^{207}Pb}{^{204}Pb}\right)_0 + \left(\frac{^{235}U}{^{204}Pb}\right)_P \left(e^{\lambda_4 t} - 1\right) \qquad (5.4)$$

where the subscript p refers to the ratio of the corresponding isotopes as they exist present, the ratios with the subscript of 0 are called the initial ratios at some time t, λ_i is the characteristic radioactive decay constant of element i. Table 5.6 lists the decay constants, isotope ratios and trace element concentrations used in the calculations.

Isotope ratios of basaltic block or layer in the composite plume must be different from those of MORB generated at 66 Ma. Because the basaltic block or layer was the subducted material, a long time must have passed after the birth of the basalt at mid

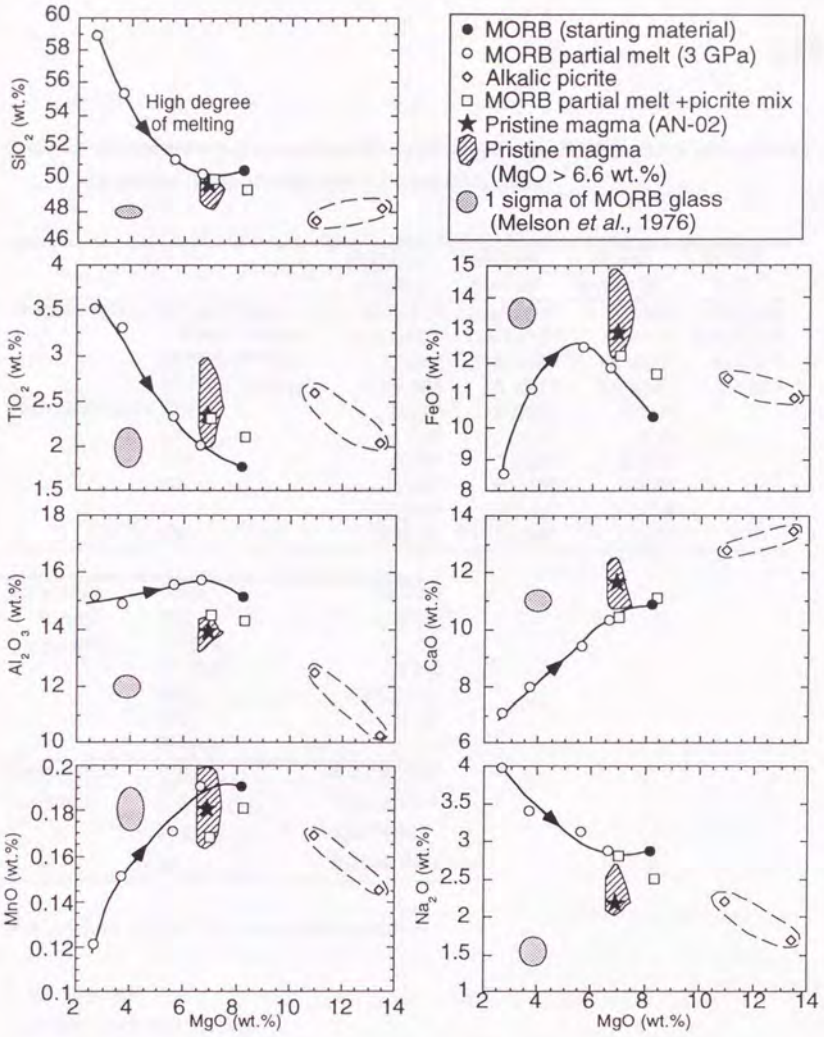

Fig. 5.10 Plots of major elements versus MgO for the pristine magma of Deccan Traps (AN-02). Also shown are the compositions of the hybrid magma calculated based on the mixing ratio, M_B/M_P, in the composite plume, which was estimated from the REE inversion alone (Fig. 5.9 a). Solid curves show isobaric compositional trends of the partial melts of MORB which were generated at 3 GPa. Ellipse is 1 sigma error for 257 analyses of MORBs (Melson *et al.*, 1976).

Table 5.6 Isotope ratios and concentrations of end components (MORB-source and primitive mantle) and decay constant used in isotope calculations.

		Primitive mantle	MORB source	MORB average	MORB S.D.
Isotope ratio	$(^{87}Sr/^{86}Sr)_P$	0.7050[a]	0.70264[b]	0.70264[b]	0.00022[b]
	$(^{143}Nd/^{144}Nd)_P$	0.51262[a]	0.51313[b]	0.51313[b]	0.00007[b]
	$(^{206}Pb/^{204}Pb)_P$	17.55[a]	18.300[b]	18.300[b]	0.335[b]
	$(^{207}Pb/^{204}Pb)_P$	15.38[a]	15.486[b]	15.486[b]	0.037[b]
Concentration	Rb	0.62[c]	0.062[c]	0.56[d]	
	Sr	20[c]	14.7[c]	90[d]	
	Sm	0.35[c]	0.299[c]	2.63[d]	
	Nd	1.08[c]	0.815[c]	7.3[d]	
	U	0.018[c]	0.0018[c]	0.047[d]	
	Pb	0.155[c]	0.016[c]	0.3[d]	

Existence ratio (mole ratio)	^{87}Rb	27.835
	^{86}Sr	9.86
	^{147}Sm	15
	^{144}Nd	23.8
	^{238}U	99.2745
	^{235}U	0.72
	^{204}Pb	1.4
Destraction constant	^{87}Rb (λ_1)	4.88×10^{10}
	^{147}Sm (λ_2)	1.06×10^{11}
	^{238}U (λ_3)	4.47×10^{9}
	^{235}U (λ_4)	7.04×10^{8}

P = present value; S.D.= standard deviation.

Data sources

[a] Zindler and Hart (1986)

[b] Ito *et al.* (1987)

[c] McKenzie and O'Nions (1991, 1995)

[d] Sun and McDonough (1989)

oceanic ridge. The magma produced by partial melting should have Sm/Nd ratio smaller than that of the source material. ε_{Nd} of the magma must be smaller than that of unmelted source which spent a long time (Fig. 5.11a). Therefore, ε_{Nd} of the basaltic block or layer in the composite plume might be smaller than that of MORB generated at 66 Ma. On the contrary, $^{87}Sr/^{86}Sr$ ratio of the basaltic block or layer of the composite plume was higher than that of MORB generated at 66 Ma because of the Rb enrichment rather than Sr. ε_{Nd} value and $^{87}Sr/^{86}Sr$ ratio of basaltic block or layer in the composite plume are sorts of the function of time (equation 5.4).

In the above discussions, I have proposed that the pristine magma of Deccan Traps was the hybrid magma composed of partial melt of basaltic block or layer and partial melt of the ambient lherzolite part of the composite plume. When we know isotope ratios of the pristine magma and the mixing ratio of the hybrid magma, we can calculate the age of the basaltic block or layer in the composite plume based on isotope mixing calculation using data set of Table 5.6.

The following parameters were used for the calculations. The average Nd and Sr isotope ratios of the uncontaminated basalts (= Ambenali basalts) of Deccan Traps were used as those of the hybrid magma. The uncontaminated magmas (= Ambenali magma) of Deccan Traps are depleted in Nd and Sr isotopes compared to primitive mantle which has isotope ratios of $\varepsilon_{Nd} > 0$ and $^{86}Sr/^{87}Sr < 0.7050$ at 66 Ma (Chapter IV). Weight fraction of the partial melt of the ambient lherzolite part in the hybrid magma has been estimated to be 0.25-0.33 using the REE composition of the Deccan pristine magma. This value was used here. The isotope ratios of the ambient lherzolite part were defined as those of primitive mantle of 66 Ma. The average Nd and Sr isotope ratios of N-MORBs (Ito *et al.*, 1987) were applied to those of the basaltic block or layer in the composite plume.

The age of the basaltic block or layer in the composite plume was calculated to be about 300 Ma (Fig. 5.11b). This age is consistent with the Pb isotope data (Fig. 5.11c), although Pb isotope data have been reported a little for the uncontaminated basalts (= Ambenali basalts) of Deccan Traps.

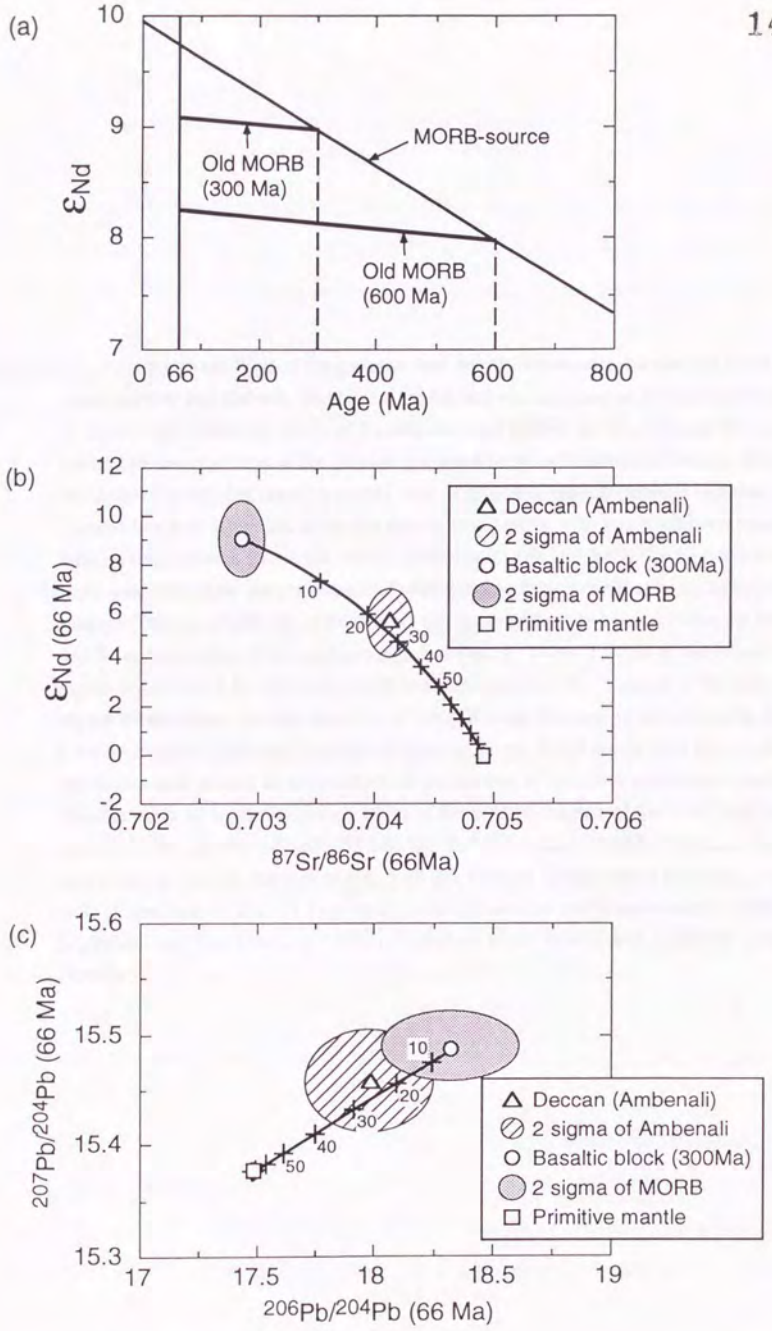

Fig. 5.11 (See next page for explanations)

Fig. 5.11 (--- continued) (a) Plots of ε_{Nd} versus time for MORB-source mantle and MORB produced 300 and 600 Ma. The subducted MORB was assumed to be basaltic block or layer in the composite plume of Yasuda and Fujii (1994). (b) The average Nd- and Sr-isotope compositions of the pristine magma (Ambenali basalts) of Deccan Traps (triangle). The mixing between partial melt of primitive mantle (square) and that of basaltic block or layer (circle) is also shown. Solid curve with tick marks represents bulk mixing between the partial melt of primitive mantle and that of basaltic block or layer. Numbers show weight fraction of partial melts of primitive mantle in the hybrid magma. The age of 300 Ma of MORB for the basaltic block or layer satisfies the Nd- and Sr-isotope ratios of the pristine magma of Deccan Traps. 2 sigma of Ambenali: 2 sigma error ellipse for the analyses of Ambenali basalts. The 2 sigma of MORB: 2 sigma error ellipse for the analyses of MORBs. (c) Pb-isotope variations in the pristine magma (Ambenali basalts) of Deccan Traps. Solid curve with tick marks represents bulk mixing between estimated partial melt of primitive mantle and that of basaltic block or layer. Pb-isotope ratios of the pristine magma of Deccan Traps are also satisfied by the age of 300 Ma for the subducted MORB. Numbers and abbreviations are the same as in Fig. 5.23 (b). Data of MORB taken from Ito *et al.* (1987), and data of Deccan Trap basalts taken from Cox and Hawkesworth (1985), Lightfoot and Hawkesworth (1988), Lightfoot *et al.* (1990) and Mahoney *et al.* (1982).

F. Temperature and size of the composite plume

Previous workers have proposed temperature of the plume according to mantle plume initiation model (Farnetani and Richard, 1994; Griffiths and Campbell, 1990) and rifting/decompression model (White and McKenzie, 1989, 1995). In order to compare the composite plume with the previously proposed models, I estimated plume temperature in the composite plume.

When physical parameters of basaltic block or layer, such as specific heat, thermal expansion coefficient, density and entropy change on melting of basaltic block or layer are almost the same as those of the ambient lherzolite part of the composite plume, we can calculate a potential temperature, T_P, of the composite plume from McKenzie (1984). The potential temperature of the composite plume which produced the pristine magma of Deccan Traps has been calculated based on the method of McKenzie (1984). Before calculation, we have to know the following parameters. (1) The segregation pressure and temperature of the pristine magma and (2) the mixing ratio ($=M_B/M_P$) in the composite plume. As described before, these parameters were estimated by inverting REE composition of the Deccan pristine magma. Therefore, when we assume that the composite plume ascended adiabatically (McKenzie, 1984), the potential temperature can be calculated (Appendix F) using the segregation condition (=2.8 GPa and 1410 °C) and the mixing ratio ($X_B/M_P = 0.09$). It can be calculated that the composite plume intersected the MORB solidus at 5.11 GPa and 1456 °C (Fig. 5.12). Estimated potential temperature of the composite plume is about 1370 °C. The excess temperature, ΔT_P, which is the temperature over the adiabatic geotherm (about 1280 °C; McKenzie and Bickle, 1988) is about 90 °C.

Based on the rifting/decompression melting model (*e.g.*, White and McKenzie, 1989), the potential temperature of the mantle plume which generated the Deccan Trap magma was estimated to be more than 1450 °C (White and McKenzie, 1995) using REE composition of Deccan Trap basalts (Ambenali basalts). We can estimated that the excess

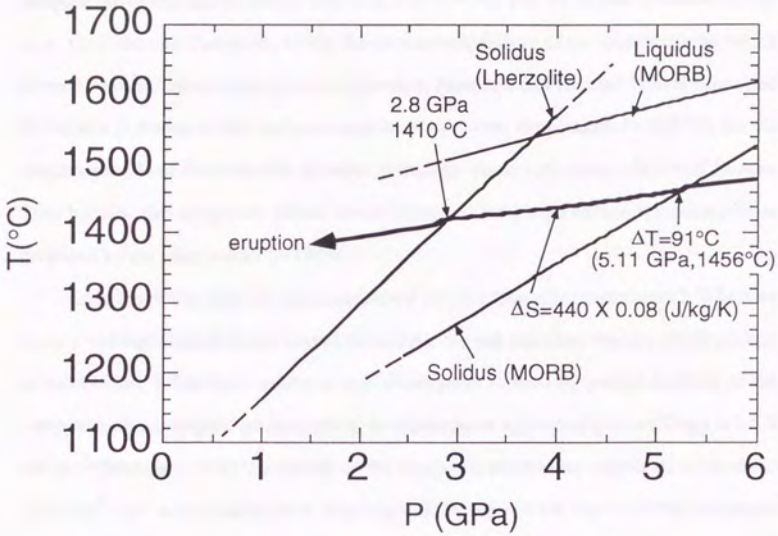

Fig. 5.12 Estimated temperature of the composite plume. Isoentropic path for the composite plume was calculated by the method of McKenzie (1984) (Appendix F), using his parameterizations and the entropy of melting of 440 J/kg/K of Fukuyama (1985).

temperature of the mantle plume was more than 170 °C. For the mantle initiation model (*e.g.*, Griffiths and Campbell, 1990), the excess temperature of the mantle plume which formed Deccan Trap magma was not estimated. Farnetani and Richard (1994) supported the mantle initiation model and proposed the high excess temperature (> 300 °C) for the magma genesis of flood basalts. In order to explain whole rock compositions of Deccan Trap basalts, the composite plume model does not need high excess temperatures as proposed by the other model (> 170 °C).

Last, the plume size was estimated based on the composite plume model. When we know a volume of magma and degree of melting, we can calculate volume of the source. In calculation, it has been assumed that all magmas formed by partial melting of the composite plume erupted on the surface. As the eruption volume of Deccan Traps is 1.5×10^6 km^3 (Mahoney, 1988), a volume of the composite plume was calculated to be about 2.2×10^7 km^3 using parameters ($M_B/M_P = 0.09$, $X_B = 0.65$, $X_P = 0.018$) estimated above. If we assume that the shape of the plume was a spherical diapir, the radius was estimated to be about 210 km.

Conclusions

The geological and petrological studies presented in this thesis were summarized as follows:

(1) In order to establish chemical stratigraphy, basalt flows exposed in 27 sections in whole Deccan Traps were divided into several stratigraphic groups. Thick lava piles in Western Ghats was assigned into ten formations among twelve formations previously established. Lava piles of each section on the central and eastern Deccan were divided into several stratigraphic groups. I could not establish the continuity of the stratigraphic formations recognized in the Western Ghats into central and eastern sectors, but could recognize the presence of stratigraphic formations in the latter sectors which are chemically analogous to the Poladpur, Ambenali and Mahabaleshwar Formations in Western Ghats. Two key groups, "Eastern Ambenali Formation" and "Eastern low-Ti Formation", could be identified. They have a large regional extent in the central and eastern Deccan. A possible stratigraphic relationship between the central and eastern Deccan Traps were established using these key groups.

(2) Review of data from the previous studies resulted in the recognition of a clear positive correlation between Ba/Nb and $^{87}Sr/^{86}Sr$ ratios and reverse correlation between Ba/Nb and ε_{Nd} ratios in the Western Ghats area. Based on these relationships, the uncontaminated basalts which have low $^{87}Sr/^{86}Sr$ and high ε_{Nd} ratios, can be discriminated using Ba/Nb ratios. Although almost of contaminated rocks ($\varepsilon_{Nd} < 0$ and $^{87}Sr/^{86}Sr > 0.705$) could be discriminated by Ba/Nb ratios, some TiO_2-poor (≤ 1.95 wt.%) basalts could not be detected using Ba/Nb ratio. The TiO_2-poor basalts with low Ba/Nb ratio were also regarded as contaminated basalts. Major and trace element compositions of this defined uncontaminated basalts in the central and eastern Deccan area are similar to those of Ambenali basalts in the Western Ghats area.

(3) Chemical trend of the uncontaminated basalts can be explained by low pressure

fractional crystallization under the condition of QFM and temperature of 1155-1130 °C. One of the most evolved uncontaminated basalts can be generated by removal of phenocrystic phases (olivine = 4 wt.%, plagioclase = 16 wt.%, augite = 15 wt.%) from the most primitive aphyric basalt. The most primitive aphyric basalts in the uncontaminated basalts was called the pristine magma.

(4) The dissolved H_2O contents in basalt glass inclusions in olivine phenocrysts from an uncontaminated basalt (0.5-0.7 wt.%) were as small as those of mid-oceanic ridge basalts (MORBs). This fact shows that the effect of H_2O is not important on magma genesis of the uncontaminated basalts.

(5) The Deccan pristine magma is tholeiitic basalts. La/Lu value normalized to primitive mantle, $(La/Lu)_N$, of the Deccan pristine magma is more than 2.2. Melting experiments for mantle lherzolites, previously reported, show that partial melts formed by low degree of melting do not have the compositions of tholeiitic basalts but alkalic basalts. Calculated results showed that partial melts formed by high degree of melting could not satisfy the $(La/Lu)_N$ of the Deccan pristine magma, taking the subsequent fractional crystallization into account. These quantitative evaluations suggested that partial melting of typical mantle lherzolite (primitive and MORB-source mantles) and subsequent fractional crystallization at any pressures cannot produce the Deccan pristine magma.

(6) Yasuda and Fujii (1994) have proposed the composite plume model for the magma genesis of LIPs. However, quantitative discussion has not been applied yet. In order to evaluate the model on the genesis of Deccan Trap magma, melting experiments on an abyssal tholeiite from the Mid-Atlantic Ridge were performed at pressures between 3 and 5.5 GPa. The liquidus phase was clinopyroxene and was followed by garnet in the above pressure range. Compositions of melts formed by partial melting were also determined and they were used to estimate the composition of hybrid magma which can be formed by mixing of partial melts of basaltic blocks and of ambient peridotite.

(7) Assuming that the alkalic picrite from the Kathiawar area of Deccan Traps represents a magma formed by partial melting of the ambient lherzolite part, segregation depth and temperature of magma which can explain its REE pattern was estimated. It was found that the segregation pressure and temperature of 2.8 GPa and 1410 °C are appropriate to explain the REE and major element compositions of the alkalic picrites. Combining these parameters with the results of melting experiments on MORB, the mixing ratio (=M_B/M_P) of basaltic block or layer and the ambient lherzolite part in the composite plume was calculated to satisfy the REE composition of the pristine magma. Thus calculated mixing ratio is 0.05-0.09. Calculated major and trace element compositions based on the composite plume model using the above estimated pressure, temperature and mixing ratio (M_B/M_P) agreed with the Deccan pristine magma composition. The estimated excess temperature of the composite plume is about 90 °C.

These studies give rise to further problems as follows:

(A) Almost all previous workers suggested that LIPs were generated by fractionation of picritic magma at the base of the continental lithosphere. The picritic magma can be in equilibrium with mantle lherzolite. However, fractionation of the picritic magma was not examined based on partial melting experiments at high pressure (> 2 GPa). Although this thesis concluded that the pristine magma of Deccan Traps cannot be generated by partial melting of typical mantle lherzolite and subsequent fractional crystallization at any pressures (conclusion 5), evaluation of this conclusion should be made by melting experiments at high pressure.

(B) Assuming the composite plume model, we could estimate the geophysical parameters such as segregation pressure and temperature, weight fraction of basaltic block or layer,

potential temperature of the composite plume. However, only Deccan Traps were studied in this thesis. There are so many LIPs all over the world. Many LIPs may have generated by partial melting of the composite plume. When we can calculate the geological parameters of these LIPs, the world wide distribution of subducted MORBs will be estimated.

Acknowledgments

I am grateful to Prof. T. Fujii, University of Tokyo, for discussions and constructive comments. I would also like to thank Dr. S.S. Deshmukh of the Geological Survey of India, for the geologic information. I am very grateful Dr. T. Fukuoka for INAA at Gakushuin University. Dr. K. Hirose, Tokyo Institute of Technology, taught me the diamond aggregates method for the melting experiments at high pressure. Prof. S. Aramaki, Nippon university, provided the some whole rock analysis data. During the course of this study I have benefited from discussions with Prof. T. Koyaguchi, Prof. I. Kaneoka, Prof. S. Nakada, Prof. H. Nagahara, Prof. K. Ozawa, Dr. A. Yasuda, Drs. T. and K. Kanekos, Mr. N. Iwata, Mr. T. Miura, Mr. T. Hanyu and Miss M. Ichihara, University of Tokyo. I thank them.

References

Alexander, P.O. and Gibson, I.L. (1977) Rare earth abundances in Deccan trap basalts. Lithos, 10: 143-147.

Allmukhamedov, A.I. and Zolotukhin, V.V. (1988) Geochemistry of low- potassic basalts from Siberian and Deccan Traps. In: Subbarao K.V. (ed.) Deccan flood basalts. Geol. Soc. India, Mem. 10: 341-351.

Aoki, K, Yoshida, T., Aramaki, S. and Kurasawa, H. (1992) Low-pressure fractional crystallization origin of the tholeiitic basalts of the Deccan plateau, India. J. Min. Petr. Econ. Geol., 87: 375-387.

Baker, D.R. and Eggler, D.H. (1987) Compositions of anhydrous and hydrous melts coexisting with plagioclase, augite, and olivine or low-Ca pyroxene from 1 atm to 8 kbar: Application to the Aleutian volcanic center of Atka., Am. Mineral., 72: 12-28.

Baker, M.B., Grove, T.L. and Price, R. (1994) Primitive basalts and andesites from the Mt. Shasta region, N. California: products of varying melt fraction and water content. Contrib. Mineral. Petrol., 118: 111-129.

Baker, M.B. and Stolper, E.M. (1994) Determining the composition of high-pressure mantle melts using diamond aggregates. Geochim. Cosmochim. Acta, 58: 2811-2827.

Baksi, A.K. (1994) Geochronological studies on whole-rock basalts, Deccan Traps, India: Evaluation of the timing of volcanism relative to the K-T boundary. Earth Planet Sci. Lett., 121: 43-56.

Bargen, N. and Waff, H.S. (1986) Permeabilities, interfacial areas and curvature of partially molten system: Results of numerical computations of equilibrium microstructures. J. Geophys. Res., 91: 9261-9276.

Bartels, K.S., Kinzler, R. and Grove, T.L. (1991) High pressure phase relations of primitive high-alumina basalts from Medicine Lake volcano, northern California. Contrib. Mineral. Petrol., 108: 253-270.

Beane, J.E. and Hooper, P.R. (1988) A note on the picrite basalts of the Western Ghats, Deccan Traps, India. In: Subbarao, K.V. (ed.) Deccan food basalts. Geol. Soc. India, Mem. 10:117-133.

Beane, J.E., Turner, C.A., Hooper, P.R., Subbarao, K.V. and Walsh, J.N. (1986) Stratigraphy, composition and form of the Deccan basalts, Western Ghats, India. Bull. Volcanol., 48: 61-83.

Bender, J.F., Hodges, F.N. and Bence, A.E. (1978) Petrogenesis of basalts from the project FAMOUS area: Experimental study from 0 to 15 kbars. Earth Planet. Sci. Lett., 41: 277-302.

Bhattacharji, S., Chatterjee, N. Wampler, J.M. and Gazi, M. (1994) Mafic dikes in Deccan volcanics: Indicator of India intraplate rifting, crustal extension and Deccan flood basalt volcanism. In: Subbarao, K.V. (ed.) Volcamism. Wiley Eastern Ltd., 253-276.

Bodas, M.S., Khadri, S.F.R. and Subbarao, K.V. (1988) Stratigraphy of the Jawhar and Igatpuri Formations, western Deccan basalt province. In: Subbarao, K.V. (ed.) Deccan food basalts. Geol. Soc. India, Mem. 10: 235-252.

Bunge, H.P., Richards, M.A. and Baumgardner, J.R. (1996) Effect of depth-dependent viscosity on the planform of mantle convection. Nature, 379: 436-438.

Campbell, I.H. and Griffiths, R.W. (1990) Implications of mantle plume structure for the evolution of food basalts, Earth Planet. Sci. Lett., 99: 79-93.

Campbell, I.H., Griffiths, R.W. and Hill, R.I. (1989) Melting in an Archaean mantle plume: heads it's basalts, tails it's komatiites. Nature, 339: 697-699.

Christensen, U.R. (1996) The influence of trench migration on slab penetration into the lower mantle. Earth Planet. Sci. Lett., 140: 27-39.

Christensen, U.R. and Yuen, D.A. (1984) The interaction of a subducting lithospheric slab with a chemical or phase boundary., 89: 4389-4402.

Coffin, M.F. and Eldholm, O. (1994) Large igneous provinces: Crustal structure, dimensions, and external consequences, Rev. Geophys, 32: 1-36.

Cohen, T.H. and Sen, G. (1994) Fractionation and ascent of Deccan Trap magmas: an experimental study at 6 kilobar pressure. In: In: Subbarao, K.V. (ed.) Volcamism. Wiley Eastern Ltd., 173-186.

Cox, K.G. (1980) A model for food basalt volcanism. J. Petrol, 21: 629-650.

Cox, K.G. (1989) The role of mantle plumes in the development of continental drainage patterns. Nature, 342: 873-877.

Cox, K.G. and Hawkesworth, C.J. (1984) Relative contribution of crust and mantle to flood basalt magmatism, Mahabaleshwar area, Deccan Traps. Phil. Trans. R. Soc. Lond., A310: 627-641.

Cox, K.G. and Hawkesworth, C.J. (1985) Geochemical stratigraphy of the Deccan Traps at Mahabaleshwar, Western Ghats, India, with implications for open system magmatic processes. J. Petrol., 26: 355-377.

Cox, K.G. and Mitchell, C. (1988) Importance of crystal settling in the differentiation of Deccan Trap basaltic magmas. Nature, 333: 447-449.

Courtillot, V., Besse, J., Vandamme, D., Montigny, R., Jaeger, J.-J. and Cappetta, H. (1986) Deccan flood basalt at the Cretaceous/ Tertiary boundary? Earth Planet Sci. Lett., 80: 361-374.

Courtillot, V., Féraud, G., Maluski, H., Vandamme, D. Moreau, M.G. and Besse, J. (1988) Deccan flood basalts and the Cretaceous/ Tertiary boundary. Nature, 333: 843-846.

De, A. (1994) Fractionation trends of the Deccan Trap magmas in parts of Western Gujarat and the Satpuras. In: Subbarao, K.V. (ed.) Volcamism. Wiley Eastern Ltd., 277-294.

Deshmukh, S.S. (1977) A critical petrological study of the Deccan basalts and associated high level laterites in parts of the Western Ghats, Maharashtra state. Ph.D. thesis, Nagpur Univ., 306p.

Deshmukh, S.S. (1982) Volcanological and petrological appraisal on Deccan basalts. Sci. Lecture Ser., 1: 30-56, Gondwana Geol. Soc., India.

Deshmukh, S.S. (1988) Petrographic variations in compound flows of Deccan Traps and their significance. In: Subbarao, K.V. (ed.) Deccan food basalts. Geol. Soc. India, Mem. 10: 305-319.

Deshmukh, S.S., Aramaki, S., Shimizu, N., Kurasawa, N. and Konda, T. (1977) Petrography of the basalt flows exposed along Mahabaleshwar and Amboli sections in Western Ghats, India. Rec. Geol. Surv. Ind., 108, Pt.2: 81-103.

Deshmukh, S.S., Sano, T., Fujii, T., Nair, K.K.K, Yedekar, D.B., Umino, S., Iwamori, H. and Aramaki, S. (1996a) Chemical stratigraphy and geochemistry of the basalts flows from the central and eastern parts of the Deccan Volcanic Province of India., Gondwana Geol. Mag. Spl., 2: 145-170.

Deshmukh, S.S., Sano, T. and Nair, K.K.K. (1996b) Geology and chemical stratigraphy of the Deccan basalts of Chikaldara and Behramghat sections from the eastern part of the Deccan Traps Province, India. Gondwana Geol. Mag. Spl., 2: 1-22.

Deshmukh, S.S. and Sehgal, M.N. (1988) Mafic dyke swams in Deccan volcanic province of Madhya Pradesh and Maharashtra. In: Subbarao K.V. (ed.) Deccan flood basalts. Geol. Soc. India, Mem. 10: 323-340.

Devey, C.W. and Lightfoot, P.C. (1986) Volcanological and tectonic control of stratigraphy and structure in the western Deccan Traps. Bull. Volcanol., 48: 195-207.

Dixon, J.E., Stolper, E. and Delaney, J.R. (1988) Infrared spectroscopic measurements of CO_2 and H_2O in Juan de Fuca Ridge basaltic glasses. Earth Planet. Sci. Lett., 90: 87-104.

Duncan, R.A. and Pyle, D.G. (1988) Rapid eruption of the Deccan flood basalts at the Cretaceous/ Tertiary boundary. Nature, 333: 841-843.

Duncan, R.A. and Richards, M. A. (1991) Hotspots, mantle plumes, flood basalts, and true polar wander. Rev. Geophys, 29: 31-50.

Elthon, D. and Scarfe, C.M. (1984) High-pressure phase equilibria of a high-magnesia basalt and the genesis of primary oceanic basalts. Am. Mineral., 69: 1-15.

Falloon, T.J., Green., D.H., Hatton, C.J. and Harris, K.L. (1988) Anhydrous partial melting of a fertile and depleted peridotite from 2 to 30 kb and application to basalt petrogenesis. J. Petrol., 29: 1257-1282.

Farnetani, C.G. and Richards, M.A. (1994) Numerical investigations of the mantle plume initiation model for flood basalt events. J. Geophys. Res., 99: 13813-13833.

Fujii, T. and Bougault, H. (1983) Melting relations of a magnesian abyssal tholeiite and the origin of MORBs., Earth Planet. Sci. Lett., 62: 283-295.

Fukuyama, H. (1985) Heat of fusion of basaltic magma. Earth Planet. Sci. Lett.., 73: 407-414.

Green, D.H. (1969) A review of experimental evidence on the origin of basaltic and nephelinitic magmas. Phys. Earth Planet. Interiors, 3: 221-235.

Green, D.H. and Ringwood, A.E. (1967) The genesis of basaltic magmas. Contrib. Mineral. Petrol., 15: 103-190.

Griffiths, R.W. and Campbell, I.H. (1990) Stirring and structure in mantle starting plumes. Earth Planet Sci. Lett., 99: 66-78.

Grove, T.L. and Bryan, W.B. (1983) Fractionation of pyroxene-phyric MORB at low pressure: An experimental study. Contrib. Mineral. Petrol., 84: 293-309.

Grove, T.L., Gerlach, D.C. and Sando, T.W. (1982) Origin of calc-alkaline series lavas at Medicine Lake volcano by fractionation, assimilation and mixing. Contrib. Mineral. Petrol., 80: 160-182.

Grove, T.L., Kinzler, R.J. and Bryan, W.B. (1992) Fractionation of Mid-Oceanic Ridge Basalt (MORB) In: Morgan, J.P., Blackman, D.K. and Sinton, J.M. (ed.) Mantle flow and melt generation at mid-ocean ridges. Geophysical Monograph, 71: 281-310.

Godbole, S.M. and Ray, B. (1992) Petrographic and geochemical studies of the intrusive rocks in the western part of Deccan volcanic province. Rep. Geol. Surv. India, 32p.

Gupta, M.L. and Gaur, V.K. (1984) Surface heat flow and probable evolution of Deccan volcanism. Tectonophys., 105: 309-318.

Hart, S.R. and Zindler, A. (1986) In search of a bulk-Earth composition. Chem. Geol., 57: 247-267.

Hawkesworth, C., Mantovani, M., and Peate, D. (1988) Lithosphere remobilization during Parana magmatism. In: Menzies, M.A. and Cox, K.G. (ed.) Oceanic and continental lithosphere: Similarities and Differences, J. Petrol. Spec. Vol., 205-224.

Helz, R.T. and Thornber, C.R. (1987) Geothermometry of Kilauea Iki lava lake, Hawaii. Bull. Volcanol., 49: 651-668.

Herzberg, C. (1992) Depth and degree of melting of Komatiites. J. Geophys. Res., 4521-4540.

Hess, P.C. (1989) Origin of igneous rocks. Harvard Univ. Press., 336p.

Hirose, K. and Kushiro, I. (1993) Partial melting of dry peridotite at high pressures: determination of compositions of melts segregated from peridotite using aggregates of diamond. Earth Planet Sci. Lett., 114: 477-489.

Hooper, P.R. (1990) The timing of crustal extension and the eruption of continental flood basalts. Nature, 345: 246-249.

Hooper, P.R. (1994) Sources of continental flood basalts: the lithospheric component. In: Subbarao, K.V. (ed.) Volcamism. Wiley Eastern Ltd., 29-53.

Hooper, P.R., Subbarao, K.V. and Beane J.E. (1988) The giant plagioclase basalts (GPBs) of the Western Ghats, Deccan Traps. In: Subbarao K.V. (ed.) Deccan flood basalts. Geol. Soc. India, Mem. 10: 135-144.

Imai, N., Terashima, S., Itoh, S. and Ando, A. (1995) 1994 compilation values for GSJ reference samples, "Igneous rock series". Geochem. J., 29: 91-95.

Irifune, T. and Ringwood, A.E. (1987) Phase transformations in a harzburgite composition to 26 GPa: implications for dynamical behavior of the subducting slab. Earth Planet. Sci. Lett., 86: 365-376.

Irifune, T. and Ringwood, A.E. (1993) Phase transformations in subducted oceanic crust and buoyancy relationships at depths of 600-800 km in the mantle. Earth Planet. Sci. Lett., 117: 101-110.

Irvine, T.N., Baragar, W.R.A. (1971) A guide to the chemical classification of the common volcanic rocks. Canadian J. Earth. Sci., 8: 523-548.

Ito, E. and Takahashi, E. (1989) Postspinel transformations in the system Mg_2SiO_4-Fe_2SiO_4 and some geophysical implications. J. Geophys. Res., 94: 10637-10646.

Ito, E., White, W.M. and Göpel, C. (1987) The O, Sr, Nd and Pb isotope geochemistry of MORB. Chem. Geol., 62: 157-176.

Johnston, A.D. (1986) Anhydrous P-T phase relations of near-primary high-alumina basalt from the South Sandwich Islands. Contrib. Mineral. Petrol., 92: 368-382.

Kaila, K.L. (1988) Mapping the thickness of Deccan Trap flows in India from DSS studies and inferences about a hidden Mesozoic basin in the Narmada-Tapti region. In: Subbarao, K.V. (ed.) Deccan flood basalts. Geol. Soc. India, Mem. 10: 91-116.

Kailasam, L.N., Murthy, B.G.K. and Chayanulu, A.Y.S.R. (1972) Regional gravity studies of Deccan trap areas of Peninsular India. Science, 41: 400-407.

Kaneko, T. (1995) Geochemistry of Quaternary basaltic lavas in the Norikura area, central Japan: Influence of the subcontinental upper mantle on the trace elements and Sr isotope compositions. J. Volcanol. Geotherm. Res., 64: 61-83.

Kaneoka, I. (1980) ^{40}Ar-^{39}Ar dating on volcanic rocks of the Deccan Traps, India. Earth Planet Sci. Lett., 46: 233-243.

Kaneoka, I. and Haramura, H. (1972) K/Ar ages of successive lava flows from the Deccan Traps, India. Earth Planet Sci. Lett., 18: 229-236.

Kent, R.W., Storey, M. and Saunders, A.D. (1992) Large igneous provinces: Sites of plume impact or plume incubation? Geology, 20: 891-894.

Khadri, S.F.R., Subbarao, K.V., Hooper, P.R. and Walsh, J.N. (1988) Stratigraphy of Thakurvadi Formation, Western Deccan basalt province, India. In: Subbarao K.V. (ed.) Deccan flood basalts. Geol. Soc. India, Mem. 10: 281-304.

Kinzler, R. and Grove, T.L. (1992) Primary magmas of mid-ocean ridge basalts 1. Experiments and methods., J. Geophys. Res., 97: 6885-6906.

Klootwijk, C.T., Gee, J.S., Peirce, J.W., Smith, G.M. and McFadden, P.L. (1992) An early India-Asia contact: Paleomagnetic constraints from Ninetyeast Ridge, ODP Leg 121. Geology, 20: 395-398.

Krishnamurthy, P. and Cox, K.G. (1977) Picrite basalts and related lavas from the Deccan Traps of Western India. Contrib. Mineral. Petrol., 62: 53-75.

Kushiro, I. (1996) Partial melting of fertile mantle peridotite at high pressures: An experimental study using aggregates of diamond. In: Basu, A. and Hart, S. (ed.) Earth processes: reading the isotopic code. Geophysical Monograph, 95: 109-122.

Lightfoot, P.C. and Hawkesworth, C.J. (1988) Origin of Deccan Trap lavas: evidence from combined trace element and Sr-, Nd-, and Pb-isotope studies. Earth Planet Sci. Lett., 91: 89-104.

Lightfoot, P.C., Hawkesworth, C.J., Devey, C.W., Rogers, N.W. and VanCalsteren, P.W.C. (1990) Source and Differentiation of Deccan Trap lavas: Implications of geochemical and mineral chemical variations. J. Petrol., 31: 1165-1200.

Maaløe, S. and Aoki, K. (1977) The major element composition of the upper mantle estimated from the composition of lherzolites. Contrib. Mineral. Petrol., 63: 161-173.

Mahoney, J.J. (1988) Deccan traps. In: Macdougall, J.D. (ed.) Continental flood basalts. Kluwer Academic Publishers., 151-194.

Mahoney, J., Macdougall, J.D., Lugmair, G.W., Murali, A.V., SankarDas, M. and Gopalan, K. (1982) Origin of the Deccan Trap flows at Mahabaleshwar inferred from Nd and Sr isotopic, and chemical evidence. Earth Planet Sci Lett., 60: 47-60.

Matsuhisa, Y., Bhattacharya, S.K., Gopalan, K., Mahoney, J. and Macdougall, J.D. (1986) Oxygen isotope evidence for crustal contamination in Deccan basalts. Terra Cognita, 6: 181.

McDonough, W.F. and Sun, S.-S. (1995) The composition of the Earth. Chem. Geol., 120: 223-253.

McKenzie, D (1984) The generation and compaction of partially molten rock. J. Petrol., 25: 713-765.

McKenzie, D. and Bickle, M.J. (1988) The volume and composition of melt generated by extension of the lithosphere. J. Petrol., 29: 625-679.

McKenzie, D. and O'Nions (1991) Partial melt distributions from inversion of rare earth element concentrations. J. Petrol., 32: 1021-1091.

McKenzie, D. and O'Nions (1995) The source regions of ocean island basalts. J. Petrol., 36: 133-159.

Melluso, L., Beccaluva, L., Brotzu, P., Gregnanin, A., Gupta, A.K., Morbidelli, L. and Traversa, G. (1995) Constraints on the mantle sources of the Deccan Traps from the petrology and geochemistry of the basalts of Gujarat State (Western India). J. Petrol., 36: 1393-1432.

Melson, W.G., Wright, T.L., Byerly, G. and Nelen, J. (1976) Chemical diversity of abyssal volcanic glass erupted along Pacific, Atlantic, and Indian Ocean sea-floor spreading centers. In: Sutton, G.M., Manghnani, M.H. and Moberly, R. (ed.) The Geophysics of the Pacific Ocean Basin and Its Margin. Geophys. Monogr. Ser., 19: 351-367.

Melson, W.G., *et al.* (1978) Site 395: 23°N, Mid-Atlantic Ridge, Proc. Ocean Drill. Program Initial Rep., 45: 131-264.

Mitchell, C. and Cox, K.G. (1988) A geological sketch map of the southern part of the Deccan province. In: Subbarao K.V. (ed.) Deccan flood basalts. Geol. Soc. India, Mem. 10: 27-33.

Mitchell, C. and Widdowson, M. (1991) A geological map of the southern Deccan Traps, India and its structural implications. J. Geol. Soc. Lond., 148: 495-505.

Morgan, W.J. (1981) Hotspot tracks and the opening of the Atlantic and Indian oceans. In: Emiliani, C. (ed.) The Sea 7 : 443-487. The Oceanic Lithosphere. Wiley Interscience, New York.

Müller, R.D., Royer J.-Y. and Lawver, L.A. (1993) Revised plate motions relative to the hotspots from combined Atlantic and Indian Ocean hotspot tracks. Geology, 21: 275-278.

Mysen, B.O. and Boettcher, A.L. (1975) Melting of a hydrous mantle: 1. Phase relations of natural peridotite at high pressures and temperatures with controlled activities of water, carbon dioxide, and hydrogen. J. Petrol., 16: 520-548.

Nair, K.K.K. and Chatterjee, A.K. (1993) Report of the Petrographic and geochemical studies of the Narmada-Satpura dyke system between 74° and 76° E longitudes, Dhulia dist., Maharashtra and Khargone and Khandwa districts, Madhya Pradesh. Rep. Geol. Surv. India, 24p.

Nair, K.K.K., Chatterjee, A.K. and Sano, T. (1996) Stratigraphy and geochemistry of the Deccan basalts along Toranmal section, Western Satpura region. Gondwana Geol. Mag. Spl., 2: 23-48.

Nair, K.K.K and Roi, B. (1994) Report on the synthesis and compilation of field, petrographic and geochemical studies of the basalt flows along different sections between 74° and 80° longitudes in Narmada-Tapti-Satpura zone. Rep. Geol. Surv. India, 23p.

Norton, I.O. and Sclater, J.G. (1979) A model for the evolution of the Indian Ocean and the breakup of Gondwanaland. J. Geophys. Res., 84: 6803-6830.

O'Hara, M.J. (1968) The bearing of phase equilibria studies in synthetic and natural systems on the origin and evolution of basic and ultrabasic rocks, Earth Sci. Rev., 4: 69-133.

Panjasawatwong, Y., Danyushevsky, L.V., Crawford, A.J. and Harris, K.L. (1995) An experimental study of the effects of melt composition on plagioclase-melt equilibria at 5 and 10 kbar: implications for the origin of magmatic high-An plagioclase. Contrib. Mineral. Petrol., 118: 420-432.

Peng, Z.X., Mahoney, J., Hooper, P., Harris, C. and Beane, J. (1994) A role for lower continental crust in flood basalt genesis?: Isotopic and incompatible element study of the lower six formations of the western Deccan Traps. Geochim. Cosmochim. Acta, 58: 267-288.

Presnall, D.C., Dixon, J.R., O'Donnell, T.H. and Dixon, S.A. (1979) Generation of mid-oceanic ridge tholeiites. J. Petrol., 20: 3-35.

Putirka, K., Johnson, M., Kinzler, R., Longhi, J. and Walker, D. (1996) Thermobarometry of mafic igneous rocks based on clinopyroxene-liquid equilibria, 0-30 kbar. Contrib. Mineral. Petrol., 123: 92-108.

Raja Rao, C.S., Sahasrabudhe, Y.S., Deshmukh, S.S. and Raman, R. (1978) Distribution, structure and petrography of the Deccan Trap, India. Rep. Geol. Surv. India, 43p.

Richards, M.A., Duncan, R.A. and Courtillot, V.E. (1989) Flood basalts and hot-spot tracks: Plume heads and tails, Science, 246: 103-107.

Roeder, P.L. and Emslie, R.F. (1970) Olivine-liquid equilibrium. Contrib. Mineral. Petrol., 29: 275-289.

Schmidt, M.W. and Poli, S. (1994) The stability of lawsonite and zoisite at high pressures: Experiments in CASH to 92 kbar and implications for the presence of hydrous phases in subducted lithosphere. Earth Planet. Sci. Lett., 124: 105-118.

Scotese, C.R., Gahagan, L.M. and Larson, R.L. (1988) Plate tectonic reconstructions of the Cretaceous and Cenozoic ocean basins. Tectonophysics, 155: 27-48.

Sen, G (1986) Mineralogy and petrogenesis of the Deccan Trap lava flows around Mahabaleshwar, India. J. Petrol, 27: 627-663.

Sen, G (1988) Possible depth of origin of primary Deccan tholeiite magma. In: Subbarao K.V. (ed.) Deccan flood basalts. Geol. Soc. India, Mem. 10: 35-51.

Sen, G and Cohen, T.H. (1994) Deccan intrusion, crustal extension, doming and the size of the Deccan- Reunion plume head. In: Subbarao, K.V. (ed.) Volcamism. Wiley Eastern Ltd., 201-216.

Shaw, D.M. (1970) Trace element fractionation during anatexis. Geochim. Cosmochim. Acta, 34: 237-243.

Srivastava, R.K., Pandit, M.K. and Rajani Upadhyaya (1988) Petrography and chemical stratigraphy of Deccan basalts from a part of the Malwa Plateau: Use of cluster analysis in chemical stratigraphy. In: Subbarao K.V. (ed.) Deccan flood basalts. Geol. Soc. India, Mem. 10: 181-197.

Subbarao, K.V., Chandrasekharam, D., Navaneethakrishnan, P. and Hooper, P.R. (1994) Stratigraphy and structure of parts of the central Deccan basalt province: Eruptive models. In: Subbarao, K.V. (ed.) Volcamism. Wiley Eastern Ltd., 321-332.

Subbarao, K.V. and Hooper, P.R. (1988) Reconnaissance map of the Deccan Basalt Group in the Western Ghats, India. In: Subbarao, K.V. (ed.) Deccan food basalts. Geol. Soc. India, Mem. 10: (enclosure).

Sun, S.-S. and McDonough, W.F. (1989) Chemical and isotopic systematics of oceanic basalts: implications for mantle composition and processes. In: Saunders, A.D. and Norry, M.J. (ed.) Magmatism in the Ocean Basins. Geol., Soc. London. Spec. Pub.., 42: 313-345.

Tackley, P.J., Stevenson, D.J., Glatzmaier, G.A. and Schubert, G. (1994) Effects of multiple phase transitions in a three-dimensional spherical model of convection in Earth's mantle. J. Geophys. Res., 99: 15877-15901.

Takahashi, E. (1986a) Melting of a dry peridotite KLB-1 up to 14 GPa: Implications on the origin of peridotitic upper mantle. J. Geophys. Res., 91: 9367-9382.

Takahashi, E. (1986b) Origin of basaltic magmas: Implications from peridotite melting experiments and an olivine fractionation model (in Japanese). Bull. Volcanol. Soc. Jpn., 30: s17-s40.

Takahashi, E. and Kushiro, I. (1983) Melting of a dry peridotite at high pressures and basalt magma genesis, Am. Mineral., 68: 859-879.

Tatsumi, Y. (1989) Migration of fluid phases and genesis of basalt magmas in subduction zones, J. Geophys. Res., 94: 4697-4707.

Tolan, T.L., Reidel, S.P., Beeson, M.H., Anderson, J.L. Fecht, K.R. and Swanson, D. A. (1989) Revisions to the estimates of the aerial extent and volume of the Columbia River Flood-Basalt Province. In: Reidel, S.P. and Hooper, P.R. (ed.) Spec. Pap. Geol. Soc. Am., 239: 1-20.

Tormey, D.R., Grove, T.L. and Bryan, W.B. (1987) Experimental petrology of normal MORB near the Kane Fracture Zone: 22°-25°N, mid-Atlantic ridge. Contrib. Mineral. Petrol., 96: 121-139.

Turner, S.T. and Hawkesworth, C. (1995) The nature of the sub-continental mantle: constraints from the major-element composition of continental flood basalts. Chem. Geol., 120: 295-314.

Vandamme, D., Courtillot, V., Besse, J. and Montigny, R. (1991) Paleomagnetism and age determinations of the Deccan Traps (India): Results of a Nagpur-Bombay traverse and review of earlier work. Rev. Geophys., 29: 159-190.

Venkatesan, T.R., Pande, K. and Gopalan, K. (1993) Did Deccan volcanism pre-date the Cretaceous/ Tertiary transition? Earth Planet Sci. Lett., 119: 181-189.

Verma, R.K. and Banerjee, P. (1992) Nature of continental crust along the Narmada-Son Lineament inferred from gravity and deep seismic sounding data. Tectonophysics, 202: 375-397.

Vink, G.E, Morgan, W.J. and Zhao, W.L., (1984) Preferential rifting of continents: A source of displaced terranes. J. Geophys. Res., 89: 10072-10076.

Walker, D., Shibata, T and DeLong, E. (1979) Abyssal tholeiites from the oceanographic fracture zone II, Phase equilibria and mixing. Contrib. Mineral. Petrol. 70: 111-125.

Walker, G.P.L. (1972) Compound and simple lava flows and flood basalts. Bull. Volcanol., 35: 579-590.

White, R. and McKenzie, D. (1989) Magmatism at rift zones: The generation of volcanic continental margins and flood basalts, J. Geophys. Res., 94: 7685-7729.

White, R.S. and McKenzie, D. (1995) Mantle plumes and flood basalts. J. Geophys. Res., 100: 17543-17585.

Yang, H.-J., Kinzler, R.J. and Grove, T.L. (1996) Experiments and models of anhydrous, basaltic olivine-plagioclase-augite saturated melts from 0.001 to 10 kbar. Contrib. Mineral. Petrol., 124: 1-18.

Yasuda, A. and Fujii, T. (1994) Continental flood basalts and Oceanic plateau (in Japanese). Gekkan-Chikyu, s9: 153-158.

Yasuda, A., Fujii, T. and Kurita, K. (1990) Melting relations of an anhydrous abyssal basalt at high pressures. In: Marumo, F. (ed.) Dynamic Processes of Material Transport and Transformation in the Earth's Interior. Terrapub, Tokyo., 327-337.

Yasuda, A., Fujii, T. and Kurita, K. (1993) Melting phase relations of an anhydrous mid-oceanic ridge basalt from 3 to 20 GPa: Implications for the behavior of subducted oceanic crust in the mantle. J. Geophys.. Res., 99: 9401-9414.

Yedekar, D.B., Aramaki, S., Fujii, T. and Sano. T. (1996) Geochemical signature and stratigraphy of the Chhindwara-Jabalpur-Seoni-Mandla sector of the eastern Deccan volcanic province and problems of its correlation. Gondwana Geol. Mag. Spl., 2: 49-68.

Yoder, H.S., Jr. and Tilley, C.E. (1962) Origin of basalt magmas: an experimental study of natural and synthetic rock systems., J. Petrol., 3: 342-532.

Zindler, A. and Hart, S. (1986) Chemical geodynamics. Ann. Rev. Earth Planet. Sci., 14: 493-571.

Appendix A: Petrographical descriptions

The "formation" in the table indicates Formations in the Western Ghats area and stratigraphic groups in the central and eastern area (chapter III).

Table A1 Petrographical descriptions of the Deccan Trap basalts. pl: plagioclase, cp: augite, ol: olivine, opq: opaque mineral, gl: glass, a.m.: ambiguous altered mineral or glass. Abbreviation for each formation is same as Fig. 3.2.

Sample No.	Phenocryst (size=mm)	Mode (vol.%)	Groundmass (size=micron)	Tecture etc.	height (m)	flow No.	forma-tion
AB01-21	pl (1.0)	5	cp>pl>opq>ol (80-300)		604	1	Mah
AB02-21	pl (1.2-2.0)	8	cp>pl>opq>ol?>a.m. (80-250)		610	2	Mah
AB03-61	pl (2.0)>cp (2.0)>ol? (1.0)	18	cp>pl>opq>a.m. (80-300)		640	3	Mah
AB04-21		0	cp>pl>opq>a.m. (80-400)		671	4	Mah
AB04-22	pl (1.0)	7	cp>pl>opq>a.m. (80-250)		702	4	Mah
AB04-23	pl (0.8-1.0)>>cp (0.5)	8	cp>pl>opq>a.m. (50-150)		702	4	Mah
AB04-24	pl (0.8)	2	cp>pl>opq>a.m. (80-300)		702	4	Mah
AB04-25	pl (1.0-1.2)> ol? (0.5)	10	cp>pl>opq>a.m. (40-120)		702	4	Mah
AB05-21	pl (1.0-2.0)>cp (0.8)	30	cp>pl>opq>a.m. (80-300)		725	5	Pan
KP-02-51	pl (0.5)=ol? (0.5)	1	cp>pl>opq.a.m. (80-150)		730	2	Mah
KP-03-51	pl (1.0)>ol? (0.5)	5	cp>pl>opq.a.m. (40-120)		835	3	Pan
KP-04-51	pl (1.5)>ol? (1.5)>cp (0.5)	8	cp>pl>opq.a.m. (40-120)		880	4	Pan
AG-02-51	pl (1.0)>ol? (0.5)	12	cp>pl>opq>a.m. (40-120)		123	2	Amb
AG-03-51	pl (1.5)>cp (0.8)	20	cp>pl>opq>a.m. (40-120)		190	3	Amb
AG-04-51	pl (1.5)>cp (0.8)	25	cp>pl>opq>a.m. (40-120)		200	4	Amb
AG-05-51		0	cp>pl>opq>a.m. (120-400)		244	5	Amb
AG-05-52		0	cp>pl>opq=ol?=gl (100-800)		244	5	Amb
AG-06-51		0	cp>pl>opq>a.m. (100-400)		259	6	Amb
AG-07-51	ol? (0.8)	3	cp>pl>opq.a.m. (40-120)		290	7	Amb
AG-08-51		0	cp>pl>opq.a.m. (100-400)		302	8	Amb
AG-09-51	pl (1.0)>ol? (0.5)	3	cp>pl>opq.a.m. (80-120)		335	9	Amb
AG-10-51		0	cp>pl>opq>ol? (80-200)		382	10	Amb
AG-11-51	ol? (0.5)>pl (0.5)	3	cp>pl>opq>ol? (40-120)		427	11	Amb
AG-12-51	pl (4.0)	30	cp>pl>opq>ol? (40-120)		442	12	Amb
AG-12-52	pl (0.8)>cp (0.8)	12	cp>pl>opq>ol? (40-120)		457	12	Amb
AG-12-53	pl (0.8)>cp (0.8)	20	cp>pl>opq>ol? (40-120)		495	12	Amb
AG-13-51	pl (2.0-3.0)	30	cp>pl>opq>ol? (40-120)		504	13	Amb
AG-14-51	pl (0.5)	1	cp>pl>opq>ol? (40-120)		594	14	Mah
MA-001-51	pl (0.5-1.0)	7	cp>pl>opq>a.m. (100-400)		40	1	Bus
MA-002-51		0	pl=cp>opq>ol? (100-500)		46	2	Bus
MA-A-51		0	cp>pl>opq (100-500)		149	A	Pol
MA-B-51		0	cp>pl>opq>ol? (100-500)		168	B	Pol
MA-F-51	pl (0.5)	10	cp>pl>opq>a.m. (50-120)		272	F	Pol
MA-G-51	pl (0.5)=cp (0.5)	10	cp>pl>opq>a.m. (50-120)		309	G	Pol
MA-H-51	ol (0.5)=pl (0.5)=cp (0.5)	15	cp>pl>opq>a.m. (50-160)		336	H	Amb
MA-I-55	pl (0.5)=cp (0.5)	15	cp>pl>opq>a.m. (50-160)		387	I	Amb
MA-K-55	pl (0.5)>cp (0.5)	7	cp>pl>opq>a.m. (50-120)		428	K	Amb
MA-L-55	pl (0.5)	7	cp=pl>opq>a.m. (80-200)		459	L	Amb
MA-N-55	pl (0.5)>>ol? (0.5)	7	cp>pl>opq>a.m. (40-120)		529	N	Amb
MA-O-55	pl (0.5-1.0)>cp (0.5)>ol? (0.5)	12	cp>pl>opq>a.m. (40-120)		548	O	Amb
MA-P-51		0	cp>pl>opq>ol (120-300)		568	P	Amb
MA-Q-55	pl (1.0)>cp (0.5)	7	cp>pl>opq>a.m. (40-120)		593	Q	Amb
MA-R-56	pl (1.0)>cp (0.5)	12	cp>pl>opq>a.m. (40-120)		625	R	Amb
MA-T-55	pl (1.0)>cp (0.5)	18	cp>pl>opq>a.m. (40-120)		655	T	Amb
MA-U-55		0	cp>pl>opq>a.m. (40-150)		694	U	Amb
MA-V-55	pl (1.0-1.5)	2	cp>pl>opq>a.m. (40-120)		701	V	Amb
MA-W-21		0	cp>pl>opq>ol (40-200)		734	W	Amb
MA-W-22		0	cp>pl>opq>ol (40-200)		734	W	Amb
MA-W-23		0	cp>pl>opq>ol (40-200)		734	W	Amb
MA-W-24		0	cp>pl>opq>ol (40-200)		734	W	Amb
MA-W-25	pl (0.3)>cp (0.3)>ol (0.3)	3	cp>pl>opq>ol (40-200)		734	W	Amb
MA-W-26	pl (0.3)>cp (0.3)>ol (0.3)	3	cp>pl>opq>ol (40-200)		734	W	Amb
MA-W-27	pl (0.3)>cp (0.3)>ol (0.3)	3	cp>pl>opq>ol (40-200)		734	W	Amb
MA-W-29	pl (0.3)>cp (0.3)>ol (0.3)	3	cp>pl>opq>ol (40-200)		734	W	Amb
MA-W-31	pl (0.3)>cp (0.3)>ol (0.3)	2	cp>pl>opq>ol (40-200)		734	W	Amb
MA-W-51	pl (0.3)>cp (0.3)>ol (0.3)	3	cp>pl>opq>a.m. (40-120)		734	W	Amb
MA-X-51		0	cp>pl>opq>ol? (40-120)		773	X	Amb
MA-Y-51	pl (1.0-1.5)>cp (0.5)=ol (0.5)	8	cp>pl>opq>a.m. (40-120)		803	Y	Amb

Table A1 (---continued)

Sample No.	Phenocryst (size=mm)	Mode (vol.%)	Groundmass (size=micron)	Tecture etc.	height (m)	flow No.	forma-tion
MA-Z2-51		0	cp>pl>opq>a.m. (40-160)		883	Z2	Amb
MA-Z3-51	ol (0.3)=pl (0.3)	10	cp>pl>opq>a.m. (40-160)		916	Z3	MK
MA-Z5-51	ol (0.5)=pl (0.5-1.0)>cp (0.5)	20	cp>pl>opq>a.m. (40-120)		959	Z5	Mah
MA-Z6-55	ol (0.5)=pl (0.5-1.0)>cp (1.0)	20	cp>pl>opq>a.m. (80-200)		987	Z6	Mah
MA-Z7-51	pl (1.0)	2	cp=pl>opq>a.m. (40-120)		1016	Z7	Mah
MA-Z8-51	pl (1.2-3.0)	5	cp>pl>opq>a.m. (40-120)		1058	Z8	Mah
MA-Z10-51	pl (1.0)>cp (1.0)	15	cp>pl>opq>a.m. (80-200)		1091	Z10	Mah
MA-Z11-51	pl (1.0)	15	cp>pl>opq>a.m. (80-200)		1130	Z11	Mah
MA-Z12-51	pl (1.0)	20	cp>pl>opq>a.m. (80-200)		1197	Z12	Mah
BM-01-51		?	cp>pl>opq (100-400)	doleritic	120	1	Bus
BM-02-51	amp (0.5)	2	cp>pl>a.m. (120-300)		135	2	Bus
BM-04-51	pl (1.5)	?	cp>pl>a.m. (80-200)	doleritic	255	4	Pol
BM-05-51	pl (0.5)>cp (0.5)	8	cp>pl>opq>a.m. (80-200)		300	5	Pol
BM-06-51	pl (0.5)>ol? (0.5)	8	cp>pl>opq>a.m. (80-200)		420	6	Pol
BM-07-51	pl (0.5-1.0)	12	cp>pl>opq>a.m. (80-200)		490	7	Pol
BM-08-51	pl (1.0)>cp (1.0)>ol? (1.0)	12	cp>pl>opq>a.m. (80-200)		540	8	Amb
BM-09-51	pl (0.8)>cp (0.8)>ol? (0.8)	12	cp>pl>opq>a.m. (40-120)		565	9	Amb
BM-10-51	pl (0.5)>cp (0.5)>ol? (0.5)	3	cp>pl>a.m. (40-120)		590	10	Amb
BM-11-51	pl (0.8)>cp (0.8)>ol? (0.8)	8	cp>pl>a.m. (40-120)		660	11	Amb
BM-12-51	pl (0.8)>ol? (0.8)	8	cp>pl>a.m. (40-120)		680	12	Amb
BM-13-51	pl (1.0)>cp (1.0)>ol? (1.0)	17	cp>pl>a.m. (40-120)		710	13	Amb
BM-14-51	pl (0.8)>ol? (0.8)>cp (0.5)	8	cp>pl>a.m. (40-120)		740	14	Amb
BM-15-51	pl (0.8)>ol? (0.8)	8	cp>pl>a.m. (80-200)		780	15	Amb
BM-16-51		0	cp>pl>a.m. (80-300)		815	16	Amb
KK-02-51	pl (1.0)>cp (1.0)>ol (1.0)	12	cp>pl>opq>ol?>a.m. (80-200)		695	2	Amb
KK-03A-51		0	cp>pl>opq>ol?>a.m. (80-200)		740	3	Amb
KK-04-51	pl (1.0)	10	cp>pl>opq>ol?>a.m. (80-200)		765	4	Amb
KK-05-51		0	cp>pl>a.m. (120-400)		785	5	Amb
KK-06-51		0	cp>pl>a.m. (40-120)		810	6	Amb
KK-06-52	pl (0.8)	1	cp>pl>a.m. (80-300)		810	6	Amb
KK-07-51	pl (0.8)	1	cp>pl>a.m. (80-300)		845	7	Amb
KK-08-51	ol? (0.5)>pl (0.5)	3	cp>pl>a.m. (40-120)		865	8	Amb
KK-09-51		0	cp>pl>a.m. (40-200)		890	9	Amb
KK-10-51	pl (0.8)	3	cp>pl>a.m. (120-400)		900	10	Amb
KK-11-51	pl (0.5)	3	cp>pl>a.m. (40-120)		910	11	Amb
KT-02-51	cp (1.2)>pl (1.2)	6	cp>pl>opq>a.m. (200-400)		670	2	Amb
KT-03-51	pl (1.0)>cp (0.5)	3	cp>pl>opq>a.m. (80-120)		700	3	Amb
KT-04-51	pl (1.0)>cp (1.0)>ol? (1.0)	10	cp>pl>opq>a.m. (80-120)		740	4	Amb
KT-05-51	pl (0.8)>cp (0.8)	8	cp>pl>opq>a.m. (80-120)		750	5	Amb
KT-06-51	pl (1.0)>cp (1.0)	8	cp>pl>opq>a.m. (80-120)		770	6	Amb
KT-07-51	pl (1.0)>cp (1.0)	8	cp>pl>opq>a.m. (80-120)		795	7	Amb
KT-09-51	pl (1.0)	1	cp>pl>opq>a.m. (80-120)		850	9	Amb
KT-10-51	pl (1.0-1.5)>cp (1.0-1.5)	18	cp>pl>opq>a.m. (80-120)		880	10	Amb
KT-11-51	pl (1.0-1.5)>cp (1.0-1.5)	18	cp>pl>opq>a.m. (80-120)		900	11	Amb
AK-01-51	ol? (1.0-1.5) >cp (0.5)	8	pl=cp>opq.a.m. (30)		90	1	Tha
AK-02-51	ol? (0.8-1.0)>cp (0.5)	5	pl=cp>opq.a.m. (30)		110	2	Tha
AK-03-51	ol? (0.8-1.0)>cp (0.5)	5	pl=cp>opq.a.m. (30)		130	3	Tha
BH-01	cp (0.5)	3	cp>pl>opq>a.m. (100-300)		153	1	Tha
BH-03	cp (0.5)>ol (0.5)	1	cp>pl>opq>a.m. (40-120)		200	3	Tha
BH-04	cp (0.5)	3	cp>pl>opq>a.m. (100-300)		225	4	Tha
BH-05		0	pl>cp>opq >a.m.(100-300)		270	5	Tha
BH-06	cp (1.0)	40	pl>cp>opq >a.m.(100-300)		290	6	Tha
BH-07	pl (1.0)	1	pl=cp>opq >a.m.(100-300)		310	7	Tha
BH-08	ol (0.5-1.0)>cp (0.5)	7	pl=cp>opq >a.m.(80-300)		316	8	Tha
BH-09	pl (1.0)>ol? (0.8)	12	pl=cp>opq >a.m.(100-300)		343	9	Bhi
BH-10	pl (1.0)>ol? (0.8)	12	pl=cp>opq>a.m. (100-300)		381	10	Bhi
BH-12	pl (0.5)> ol? (0.5)	3	pl>cp>opq >a.m.(40-120)		404	12	Kha
BH-13	ol (0.8)=pl (0.8)	12	pl>cp>ol>opq (40-400)		442	13	Kha

Table A1 (---continued)

Sample No.	Phenocryst (size=mm)	Mode (vol.%)	Groundmass (size=micron)	Tecture etc.	height (m)	flow No.	forma-tion
BH-14	ol (0.5)	2	pl=cp>opq>ol (40-120)		488	14	Kha
BH-15	pl (0.5-1.0)>ol (0.5)>cp (0.5)	3	cp>pl>opq>a.m. (40-120)		508	15	Kha
BH-16-51	pl (1.0-2.5)>0l (0.5)	6	cp>pl>opq>a.m. (40-120)		526	16	Kha
BH-16-52	pl (1.0-2.5)>0l (0.5)	6	cp>pl>opq>a.m. (40-120)		526	16	Kha
IG-01	pl (1.0-2.0)>>cp (1.0)	20	cp>pl>opq>ol (200-500)		250	1	Jaw
IG-02	cp (0.8>ol (0.8)	3	pl>cp>opq>a.m. (120-400)		275	2	Jaw
IG-03		0	pl>cp>a.m. (80-200)		320	3	Jaw
IG-04	pl (1.0-1.5)	2	pl>cp>opq>a.m. (40-120)		332	4	Jaw
IG-05	pl (1.0-1.5)	2	pl>cp>opq>a.m. (120-300)		389	5	Jaw
IG-06	pl (1.0-1.5)	2	pl>cp>opq>a.m. (200-500)		402	6	Jaw
IG-07	cp (1.0-2.5)>ol (1.0-2.0)	25	pl>cp>opq>ol>a.m. (200-500)		431	7	Iga
IG-08	pl (1.0-1.5)>cp (1.0)>ol (0.8)	15	pl>cp>opq>ol>a.m. (120-200)		465	8	Iga
IG-09	pl (1.0-2.5)>ol (1.2)	12	pl=cp>opq>ol>a.m. (120-400)		472	9	Iga
IG-10	pl (1.0-1.5)>ol (0.5)> cp (0.8)	12	pl>cp>opq>ol>a.m. (120-250)		480	10	Iga
IG-11	pl (1.0)	2	pl=cp>opq>ol>a.m. (80-400)		488	11	Iga
IG-12	pl (1.0-1.5)>ol (0.5)>cp (0.8)	25	pl=cp>opq>ol>a.m. (120-400)		497	12	Iga
IG-13	pl (0.8-1.0)>cp (1.0)	12	cp>pl>opq>a.m. (80-200)		512	13	Iga
IG-14	pl (0.5-1.0)>ol (0.5)	12	cp>pl>opq>a.m. (40-120)		526	14	Iga
IG-15		?	cp>pl>opq>a.m. (200-2000)	doleritic	539	15	Tha
EL03A	pl (1.0-2.0)>ol (0.5-1.0)	12	cp>pl>opq>ol>a.m. (120-200)		640		
EL08		?	cp>pl>opq>a.m. (120-600)	doleritic	721		
AJ-01	pl (1.5-3.0)	8	pl>cp>opq>a.m. (80-120)		550	1	AJ I
AJ-02-51	pl (1.0)	1	cp>pl>opq>ol?>a.m. (80-200)		527	2	AJ I
AJ-02-52	pl (1.0)	1	cp>pl>opq>ol?>a.m. (80-200)		527	2	AJ I
AJ-03-51		0	cp>pl>opq>a.m. (200-600)		509	3	AJ I
AJ-03-52		0	cp>pl>opq>a.m. (200-600)		509	3	AJ I
AJ-05		0	cp>pl>opq>ol?>a.m. (200-600)		450	5	AJ I
AJ-07	pl (1.0)	3	cp>pl>opq>a.m. (80-200)		400	7	AJ I
AJ-08	pl (2.0)	12	cp>pl>opq>a.m. (200-600)		350	8	AJ I
BU-03-51		0	cp>pl>opq>a.m. (120-300)		490	3	BU I
BU-04-51	pl (0.5)	1	cp>pl>opq>a.m. (80-300)		507	4	BU I
BU-05-51	pl (0.5)	3	cp>pl>opq>a.m. (80-300)		547	5	BU I
BU-06-51	pl (0.5)	0	cp>pl>opq>a.m. (80-200)		556	6	BU I
BU-07-51	pl (0.5)>cp (0.5)	5	cp>pl>opq>a.m. (80-200)		594	7	BU I
BU-08-51	pl (0.5)>cp (0.5)	8	cp>pl>opq>a.m. (40-120)		634	8	BU I
LC-X1-51	pl (1.0-1.5)	3	cp>pl>opq>a.m. (40-80)		450	1	BU I
LC-04-51	pl (0.5)	1	cp>pl>opq>a.m. (40-80)		510	4	BU I
CK-01		0	cp>pl>opq>a.m. (80-120)				
P1-SF-89-2	pl (1.0)	2	pl=cp>a.m. (80-200)	altered	380	1	P I
P2-P-89-1	pl (0.5)=cp (0.5)	5	pl=cp>a.m. (40-200)	altered	400	2	P I
P3-SF-89-1		0	pl=cp>a.m. (40-200)	altered	430	3	P I
P4-SF-89-1	pl (0.5)	3	pl=cp>opq>a.m. (40-200)		450	4	P I
P5-Aa-89-1	pl (2.0)	1	pl=cp>opq>a.m. (40-200)		475	5	P I
P6-SF-89-2	pl (1.5)	5	pl=cp>a.m, (40-200)		535	6	P II
P7-CP-89-1	pl (2.0)	3	pl=cp>opq (40-200)		570	7	P II
P8-Aa-89-1	pl 91.0-2.0)	3	pl=cp>opq (40-80)		590	8	P II
P9-CP-89-4		?	pl=cp>opq>a.m. (120-400)	doleritic	610	9	P II
P10-SF-89-3	pl (0.5-1.0)	10	pl=cp>opq=a.m. (40-200)		640	10	P II
P11-Aa-89-3	pl (0.5-1.0)	3	pl>cp>opq=a.m. (40-200)		720	11	P II
P12-Aa-89-2	pl (0.5)>cp (0.5)	8	pl=cp>a.m. (40-200)		750	12	MK
P13-Aa-89-1		0	pl=cp>opq=a.m. (40-200)		770	13	P III
P14-Aa-89-2	pl (0.5)	5	pl=cp>a.m. (40-120)		790	14	P III
P15-Aa-89-2		0	pl=cp>opq=a.m. (40-120)		820	15	P III
P16-SF-89-1		?	pl=cp>opq=a.m. (80-400)	dolelitic	830	16	P III
P17-Aa-89-1		0	pl=cp>opq>a.m. (40-80)		860	17	P III
P18-Aa-89-1		0	pl=cp>opq>a.m. (40-200)		930	18	P III
P19-Aa-89-1	pl (0.5-1.0)>cp (0.5-1.0)	8	pl=cp>opq>a.m. (40-120)		1000	19	P VI
P20-Aa-89-1	cp (0.5)>pl (0.5)	5	pl=cp>opq>a.m. (40-200)		1020	20	P VI

Table A1 (---continued)

Sample No.	Phenocryst (size=mm)	Mode (vol.%)	Groundmass (size=micron)	Tecture etc.	height (m)	flow No.	formation
P21-Aa-89-2	pl (2.0)	20	pl=cp>opq>a.m. (120-400)		1040	21	MK
P22-Aa-89-2					1100	22	P V
CH-02	pl (1.2-4.0)	8	cp>pl>opq>a.m. (80-120)		472	2	CH I
CH-03		0	pl>a.m.>opq (120-400)		500	3	CH I
CH-04		0	pl>a.m. (120-1000)		525	4	CH I
CH-05		?	cp>pl>opq>a.m. (200-1000)	doleritic	533	5	MK
CH-06-51	pl (1.0-2.0)	3	pl=cp>opq>a.m. (40-120)		542	6	CH II
CH-06-52	pl (1.0-2.0)>cp (0.5)	3	pl=cp>opq>a.m. (80-200)		542	6	CH II
CH-07	pl (2.0)	3	pl=cp>opq>a.m. (40-120)		567	7	CH II
CH-08	pl (1.0-2.0)	3	pl=cp>opq>a.m. (40-120)		584	8	CH II
CH-09	pl (1.0-2.0)	3	pl=cp>opq>a.m. (40-120)		595	9	CH II
CH-10	pl (1.0-2.0)>cp (1.0)	3	pl=cp>opq>a.m. (200-400)		605	10	CH II
CH-11	pl (2.0)	?	pl=cp>opq>a.m. (200-1000)	doleritic	600	11	CH II
CH-12	pl (1.0-2.0)	3	cp>pl>opq>a.m. (80-200)		608	12	MK
CH-13-52	pl (1.0-2.0)>cp (1.0)	8	cp>pl>a.m. (80-200)		632	13	CH III
CH-13-53		?	cp>pl>opq>a.m. (120-2000)	doleritic	632	13	CH III
CH-14	pl (1.0)>cp (1.0)	5	cp>pl>a.m. (40-120)		670	14	CH III
CH-15	pl (1.0)	2	cp>pl>a.m. (120-400)		693	15	CH III
CH-16	pl (1.0)	2	cp>pl>a.m. (120-400)		707	16	CH III
CH-17		0	cp>pl>opq>a.m. (120-600)		713	17	CH III
CH-18	pl (1.0)	2	cp>pl>opq>a.m. (120-600)		762	18	CH III
CH-19		2	cp>pl>opq>a.m. (120-600)		782	19	CH III
CH-20-51		2	cp>pl>opq>a.m. (120-600)		800	20	CH III
CH-20-52		2	cp>pl>opq>a.m. (120-600)		800	20	CH III
CH-21		2	cp>pl>opq>a.m. (120-600)		823	21	CH III
CH-22		2	cp>pl>opq>a.m. (120-600)		835	22	CH III
CH-23		2	cp>pl>a.m. (120-400)		866	23	CH III
CH-24	pl (0.5-1.0)>cp (0.5)	12	cp>pl>a.m. (80-400)		869	24	CH III
CH-25-51	pl (0.5)>cp (0.5-1.0)	12	cp>pl>a.m. (80-400)		878	25	CH III
CH-25-52	pl (0.5)>cp (0.5-1.0)	18	cp>pl>a.m. (80-400)		880	25	CH III
CH-27		0	cp>pl>opq>a.m. (200-800)		887	27	CH III
CH-28	pl (1.0)>cp (1.0)	12	pl=cp>opq>a.m. (20-800)		899	28	CH IV
CH-30-51		?	pl>cp>opq>a.m. (200-1000)	doleritic	919	30	CH IV
CH-30-52	pl (2.0)>>cp (1.0-1.5)	25	pl=cp>a.m. (40-200)		919	30	CH IV
CH-31-51	pl (1.0)>cp (1.0)	8	pl>cp>a.m. (120-400)		960	31	CH IV
CH-32-51		0	pl=cp>opq>a.m. (120-600)		980	32	CH V
CH-32-52		0	cp>pl>opq>a.m. (120-600)		980	32	CH V
CH-33	cp (1.0)	1	cp>pl>opq>a.m. (120-600)		1013	33	CH V
CH-34		0	cp>pl>opq>a.m. (80-300)		1035	34	CH V
CH-36		0	cp>pl>ol?>a.m. (80-300)		1090	36	CH V
MG-02-51		?	pl>cp>ol>opq (200-800)	doleritic	260	2	MG I
MG-03-51	pl (2.0)>cp (0.5)	12	cp>pl>opq>a.m. (40-120)		340	3	MG I
MG-04-51		?	pl>cp>opq (200-800)	doleritic	370	4	MG I
MG-05-51		0	cp>pl>opq>gl (120-400)		445	5	MG I
MG-06-51		0	cp>pl>opq>gl (80-200)		480	6	MG II
MG-07-51	pl (0.5-1.0)	8	cp>pl>opq>gl (80-200)		510	7	MG II
KV-01-51		0	cp>pl>opq>gl (100-400)		330	1	KV I
KV-02-51		0	cp>pl>opq>gl (100-400)		345	2	KV I
KV-04-51		0	cp>pl>opq>gl (100-400)		375	4	KV I
KV-04-52		0	cp>pl>opq>gl (100-400)		375	4	KV I
KV-04-53		0	cp>pl>opq>gl (100-400)		375	4	KV I
AN-01	pl (1.0-1.5)	3	pl=cp>opq>a.m. (40-150)				
AN-02		0	pl=cp>opq>a.m. (80-200)				
TL-01	ol (0.5-1.0)=cp (0.5-1.0)>pl (0.5)	7	cp>pl>opq>a.m. (40-120)				
TL-52	pl (1.0-1.5)	1	cp>pl>opq>a.m. (30)				
NY-03-51		0	cp>pl>opq>gl (120-300)		330	3	NY I
NY-02-51	pl (0.5)>ol (0.5)>cp (0.5)	10	gl		315	2	NY I
NY-01-51		0	cp>pl>opq>ol?>a.m. (120-300)		290	1	NY I

Table A1 (---continued)

Sample No.	Phenocryst (size=mm)	Mode (vol.%)	Groundmass (size=micron)	Tecture etc.	height (m)	flow No.	forma-tion
NP-01-51	pl (1.0-2.0)	2	cp>pl>opq>a.m. (100-400)				
NP-02-51	pl (0.5)=cp (0.5)	5	cp>pl>opq>a.m. (80-200)				
NP11-51							
NC01-51	pl (0.5-1.5)	10	pl=cp>opq=gl (40-200)		400	1	NC I
NC02-51-01	pl (0.3-0.5)>cp (0.3)>ol (0.3)	15	gl		650	8	YD
NC02-51-02					650	8	YD
NC03-51	pl (1.0)	3	pl=cp>opq=gl (40-120)		630	7	YD
NC04-51	pl (1.0)	3	pl=cp>opq=gl (40-120)		630	7	YD
NC05-51		?	pl=cp>opq=ol=gl (80-800)	doleritic	580	6	YC
NC06-51		?	pl=cp>opq=ol?=gl (200-1200)	doleritic	540	4	YC
NC06-52		?		doleritic	540	4	YC
NJ01-51	pl (0.5-1.0)	3	cp>pl>opq>a.m. (80-200)		585	10	YC
NJ02-51	pl (0.5)>cp (0.5)	3	cp>pl>opq>a.m. (40-120)		440	4	YA
NJ04-51		?	cp>pl>opq>a.m. (200-1200)	doleritic	410	3	YA
NJ04-52		?	cp>pl>opq>a.m. (200-1000)	doleritic	410	3	YA
NJ05-51	pl (1.0)	2	pl>cp>a.m. (50-200)		395	2	NJ I
NJ06-51	pl (1.0)	2	pl>cp>opq>a.m. (40-200)		460	5	YA
NJ07-51		0	pl=cp.opq.a.m. (40-400)		475	6	YB
NJ09-51	pl (1.0-1.2)	2	pl>cp>a.m. (80-200)		630	14	YD
NJ10-51	pl (0.5)	17	pl>cp>a.m. (40-120)		640	15	YD
NJ11-51	pl (1.0)	5	pl>cp>a.m. (80-200)		600	13	YD
NJ12-51	pl (1.0)>cp (1.0)>ol? (0.5)	20	pl>cp>a.m. (80-200)		585	12	YC
NJ13-51	pl (1.0-2.0)>cp (1.0)	20	cp>pl>a.m. (200-500)		575	11	YC
NJ14-51	cp (0.3)>ol (0.3)>pl (0.3)	3	pl=cp>ol>a.m. (40-120)		535	9	YC
NJ15-51	cp (0.3)>pl (0.3)	3	pl=cp>ol>a.m. (40-120)		525	8	YC
NJ17-51	pl (>100)	?	cp>pl>opq>a.m. (120-2500)	GPB	500	7	YB
NJ18-51		0	pl>cp>a.m. (200-400)		460	5	YA
NJ19-51	pl (0.5)>cp (0.5)	18	pl>cp>a.m. (200-400)		440	4	YA
NJ21-51	pl (1.0-1.5)>cp (1.0-1.5)	25	pl>cp>a.m. (200-400)		500	7	YB
JB01-51	pl (0.5-1.0)=cp (0.5)	15	gl>pl=cp (80-200)		450	3	YA
JB02-51	pl (0.5-1.0)=cp (0.5)	20	gl>pl=cp (80-200)		470	5	YA
JB02-52		?	pl=cp>opq=gl (40-600)	doleritic	545	5	YA
JB04-51	pl (>100)	?		GPB	580	9	YC
JB05-51	pl (1.0-2.0)	5	pl=cp>opq=gl (40-80)		635	12	YC
JB06-51	pl (0.5-1.0)>cp (0.5)	8	pl=cp>opq=gl (40-120)		650	13	YD
JB07-51		?	pl=cp>ol=opq=gl (40-800)	doleritic	680	15	YD
JB08-51	pl (0.5)>cp (0.5)	3	pl=cp>ol=opq=gl (40-200)		715	16	YD
JB09-51	pl (0.5)>cp (1.0-2.0)	20	pl=cp>opq=gl (80-200)		700	14	YD
JB10-51	pl (>100)	?		GPB	545	7	YB

Appendix B: Bulk rock compositions

The "formation" in the table indicates Formations in the Western Ghats area and stratigraphic groups in the central and eastern area (chapter III).

The 1 sigma of calibration line for each element is as follows (Kaneko, 1995);

Major	(wt.%)	Trace	(ppm)
SiO_2	0.15	Sr	11
TiO_2	0.01	Rb	3
Al_2O_3	0.18	Ba	18
FeO*	0.03	Y	2
MgO	0.05	Zr	6
CaO	0.03	V	10
Na_2O	0.04	Cr	13
K_2O	0.01	Ni	3.3
P_2O_5	0.01	Nb	1.1
		Th	2.2

Table A2 Whole rock compositions of the Deccan Trap basalts analyzed by (a) XRF, (b) INAA. Abbreviation for each formation is same as Fig. 3.2.

Sample No.	flow No.	height (m)	forma-tion	SiO2 (wt.%)	TiO2	Al2O3	FeO*	MnO	MgO	CaO	Na2O	K2O	P2O5	Na2O+ K2O	Mg#	Rb (ppm)	Sr	Ba	Y	Zr	V	Cr	Ni	Cu	Zn	Ga	Nb	Sc	Th	Ba/Y (ratio)	Zr/Nb	Ba/Nb	Ba/Sr X10
AB01-21	1	604	Mah	49.19	3.41	12.39	16.66	0.23	5.43	9.55	2.47	0.39	0.29	2.86	40.6																			
AB02-21	2	610	Mah	49.34	3.06	13.37	14.39	0.23	6.32	10.36	2.40	0.32	0.22	2.72	47.9																	
AB03-61	3	640	Mah	49.09	3.69	12.04	15.77	0.33	6.07	9.86	2.45	0.43	0.27	2.88	44.7																	
AB04-21	4	671	Mah	48.56	3.70	13.46	14.75	0.21	5.88	10.36	2.42	0.46	0.21	2.87	45.5																	
AB04-22	4	702	Mah	48.75	3.16	13.59	15.16	0.21	5.80	10.19	2.41	0.46	0.27	2.87	44.5																	
AB04-23	4	702	Mah	49.69	3.53	14.06	12.61	0.25	5.51	11.17	2.42	0.49	0.29	2.91	47.8																	
AB04-24	4	702	Mah	48.48	3.75	13.15	15.05	0.22	6.10	10.41	2.15	0.44	0.26	2.60	45.9																	
AB04-25	4	702	Mah	48.62	3.79	13.42	15.28	0.22	5.20	10.39	2.23	0.60	0.27	2.83	41.6																	
AB05-21	5	725	Pan	49.56	1.95	15.85	12.90	0.18	5.86	11.03	2.32	0.25	0.10	2.57	48.8																	
KP-02-51	2	730	Mah	49.94	3.00	13.14	14.77	0.23	5.85	9.97	2.34	0.49	0.28	2.83	45.4	10.9	226	77	38	182	524	95	81	227	139	24	15	39	2.3	2.00	12.20	5.14	3.40
KP-03-51	3	835	Pan	50.28	1.85	13.88	13.46	0.19	6.54	11.25	2.09	0.29	0.17	2.38	50.5	3.3	150	48	32	115	407	92	75	191	110	20	8	43	1.3	1.52	15.11	6.33	3.20
KP-04-51	4	880	Pan	50.16	1.81	14.04	13.13	0.20	6.41	11.82	2.07	0.21	0.16	2.28	50.6	3.9	151	34	32	114	403	93	75	185	108	21	7	43	2.1	1.06	16.75	4.95	2.22
AG-02-51	2	123	Amb	49.13	2.58	14.20	14.20	0.19	6.00	11.10	2.18	0.19	0.22	2.38	47.0	7.1	219	5	34	146	486	84	91	175	124	24	10	37	1.0	0.15	14.93	0.51	0.23
AG-03-51	3	190	Amb	49.62	2.50	14.40	13.13	0.19	6.21	11.22	2.27	0.24	0.22	2.51	49.8	3.0	224	26	33	140	467	125	90	193	110	25	9	38	2.4	0.78	14.92	2.78	1.16
AG-04-51	4	200	Amb	49.58	2.51	14.30	13.38	0.19	5.93	11.48	2.21	0.21	0.21	2.43	48.2	7.6	229	13	33	139	468	112	84	151	110	23	10	35	2.4	0.40	14.44	1.37	0.57
AG-05-51	5	244	Amb	49.49	2.63	14.03	14.06	0.16	6.66	10.39	2.11	0.22	0.25	2.33	49.8	1.7	212	43	36	156	453	178	113	220	115	24	11	33	1.3	1.19	14.73	4.03	2.02
AG-05-52	5	244	Amb	49.48	2.70	14.00	13.97	0.21	6.17	10.43	2.33	0.44	0.26	2.77	48.1	9.1	212	67	37	167	465	178	110	228	118	23	11	36	1.8	1.80	15.52	6.24	3.17
AG-06-51	6	259	Amb	48.68	2.65	14.31	14.04	0.20	6.92	10.63	2.18	0.14	0.25	2.32	50.8	0.7	216	34	36	160	438	211	126	296	125	25	10	33	2.7	0.94	15.82	3.33	1.56
AG-07-51	7	290	Amb	49.22	2.43	13.83	13.44	0.18	7.37	10.73	2.17	0.41	0.22	2.58	53.5	10.1	202	77	34	143	441	398	183	209	121	22	9	34	2.0	2.28	16.05	8.66	3.82
AG-08-51	8	302	Amb	49.39	2.45	14.09	13.38	0.19	7.01	10.68	2.23	0.36	0.23	2.59	52.4	6.2	213	49	35	147	447	281	140	173	116	23	9	35	1.6	1.40	16.25	5.41	2.30
AG-09-51	9	335	Amb	49.65	2.51	13.62	14.13	0.21	6.32	10.59	2.31	0.41	0.24	2.72	48.4	10.6	199	45	38	159	486	109	84	225	124	24	10	38	2.4	1.17	16.49	4.63	2.24
AG-10-51	10	382	Amb	49.86	2.62	13.84	13.25	0.20	6.15	11.07	2.33	0.41	0.27	2.74	49.3	9.9	217	42	40	176	465	206	100	253	124	24	13	39	1.6	1.06	13.87	3.29	1.93
AG-11-51	11	427	Amb	50.22	2.36	13.94	12.81	0.21	6.29	11.37	2.25	0.34	0.21	2.59	50.7	8.1	210	44	32	144	428	195	98	176	110	24	11	40	1.9	1.38	12.70	3.86	2.08
AG-12-51	12	442	Amb	49.32	3.57	13.06	15.49	0.21	5.47	9.75	2.38	0.45	0.30	2.83	42.6	10.7	227	47	42	198	571	83	66	243	146	26	16	37	1.5	1.11	12.03	2.86	2.07
AG-12-52	12	457	Amb	49.35	3.89	12.33	16.43	0.24	4.99	9.52	2.39	0.53	0.33	2.92	38.9	17.0	216	76	44	213	593	80	62	231	160	25	18	37	2.8	1.75	11.78	4.22	3.53
AG-12-53	12	495	Amb	49.42	3.93	12.23	16.67	0.22	4.79	9.49	2.39	0.50	0.35	2.89	37.6	15.4	218	72	47	228	604	75	60	255	159	25	19	43	1.3	1.54	11.78	3.74	3.32
AG-13-51	13	504	Amb	49.19	3.18	14.63	13.70	0.19	5.70	10.28	2.44	0.37	0.31	2.82	46.6	4.8	287	70	35	173	459	112	89	191	136	26	18	34	1.6	2.02	9.39	3.81	2.44
AG-14-51	14	594	Mah	49.47	3.32	13.17	14.92	0.23	5.58	9.91	2.40	0.67	0.34	3.07	44.0	17.1	243	149	41	215	502	150	79	257	144	26	19	37	2.7	3.62	11.12	7.70	6.13
MA-001-51	1	40	Bus	50.18	1.93	14.20	13.30	0.19	6.27	11.30	2.27	0.21	0.17	2.48	49.7	0.4	219	69	30	117	398	99	74	193	107	22	8	39	2.4	2.31	14.40	8.51	3.15
MA-002-51	2	46	Bus	52.29	1.09	14.78	10.55	0.14	7.12	10.95	2.21	0.75	0.11	2.96	58.6	19.8	189	141	24	101	269	305	133	116	80	20	5	34	4.8	5.99	19.71	27.73	7.49
MA-A-51	A	149	Pol	49.53	3.04	12.90	15.02	0.20	6.05	9.84	2.47	0.66	0.30	3.13	45.8	14.2	264	127	41	194	462	112	75	197	126	23	13	31	2.6	3.09	15.25	10.00	4.82
MA-B-51	B	168	Pol	50.07	2.97	12.88	14.77	0.20	5.90	9.93	2.44	0.58	0.26	3.02	45.6	16.2	206	114	38	194	480	99	73	250	122	24	13	32	3.4	3.02	14.46	8.49	5.52
MA-F-51	F	272	Pol	51.55	1.99	14.21	11.63	0.18	6.60	10.94	2.31	0.40	0.20	2.71	54.3	20.0	208	120	31	143	359	286	112	187	100	21	10	32	0.3	3.83	14.40	12.07	5.76
MA-G-51	G	309	Pol	50.71	1.97	14.25	11.40	0.16	7.24	11.48	2.30	0.31	0.18	2.61	57.1	3.8	210	104	30	132	375	326	127	165	91	21	10	35	1.7	3.46	12.80	10.07	4.94
MA-H-51	H	336	Amb	50.15	2.01	14.21	12.99	0.22	6.05	11.42	2.39	0.38	0.18	2.78	49.4	6.8	202	71	31	119	356	109	70	140	94	21	9	33	2.4	2.27	12.97	7.70	3.51
MA-I-55	I	387	Amb	50.10	1.93	14.47	13.15	0.19	5.81	11.41	2.41	0.36	0.17	2.77	48.1	7.9	206	56	28	110	358	114	71	137	94	22	8	35	2.2	2.03	14.60	7.48	2.73
MA-K-55	K	428	Amb	49.58	2.17	14.02	12.90	0.18	6.80	11.52	2.31	0.31	0.19	2.63	52.5	4.5	210	44	30	135	396	128	97	202	99	21	9	36	2.5	1.44	14.63	4.74	2.08
MA-L-55	L	459	Amb	49.29	2.61	13.80	13.77	0.21	6.21	11.40	2.32	0.17	0.21	2.50	48.6	4.3	226	45	34	149	474	96	79	169	115	21	12	33	3.5	1.33	12.80	3.91	2.01
MA-N-55	N	529	Amb	49.00	2.64	13.30	14.81	0.21	6.18	11.10	2.37	0.16	0.24	2.54	46.7	0.8	215	33	35	155	482	80	88	233	123	23	11	38	2.1	0.93	14.09	2.96	1.52
MA-O-55	O	548	Amb	49.25	3.86	12.55	15.30	0.20	5.54	10.19	2.42	0.31	0.38	2.73	43.2	5.2	216	59	51	254	609	146	87	360	136	24	16	38	3.3	1.15	15.65	3.61	2.71
MA-P-51	P	568	Amb	50.61	2.71	13.06	13.60	0.20	6.35	10.93	2.04	0.21	0.28	2.25	49.5	0.4	175	21	36	152	460	164	83	168	111	22	10	34	0.9	0.57	14.59	1.97	1.17
MA-Q-55	Q	593	Amb	49.18	3.30	12.64	15.43	0.21	5.91	10.39	2.40	0.23	0.31	2.63	44.5	3.7	222	50	42	199	556	125	85	344	132	24	13	35	1.9	1.19	14.94	3.79	2.27
MA-R-56	R	625	Amb	49.29	3.13	13.23	14.62	0.21	5.92	10.67	2.42	0.21	0.29	2.64	45.9	4.1	227	52	42	186	509	141	91	230	125	24	13	33	1.6	1.23	14.07	3.92	2.28
MA-T-55	T	655	Amb	49.39	3.04	13.67	14.72	0.18	5.43	10.50	2.44	0.37	0.27	2.81	43.6	5.9	223	62	38	174	514	138	96	457	119	25	12	33	2.3	1.65	14.25	5.10	2.80
MA-U-55	U	694	Amb	49.18	2.48	13.69	13.95	0.21	6.59	11.28	2.23	0.17	0.22	2.41	49.8	3.2	202	48	33	141	430	105	83	159	114	23	10	36	3.2	1.43	13.52	4.58	2.36
MA-V-55	V	701	Amb	49.09	2.52	13.58	14.15	0.22	6.97	10.67	2.21	0.38	0.22	2.59	50.8	5.5	194	43	33	144	426	130	93	220	113	22	10	37	0.9	1.31	14.80	4.45	2.23

Table A2 (a) (---continued)

Sample No.	flow No.	height (m)	forma-tion	SiO2 (wt.%)	TiO2	Al2O3	FeO*	MnO	MgO	CaO	Na2O	K2O	P2O5	Na2O+ K2O	Mg#	Rb (ppm)	Sr	Ba	Y	Zr	V	Cr	Ni	Cu	Zn	Ga	Nb	Sc	Th	Ba/Y (ratio)	Zr/Nb	Ba/Nb	Ba/Sr X10
MA-W-21	W	734	Amb	48.16	2.83	13.91	14.83	0.20	6.78	10.95	2.00	0.13	0.22	2.13	48.9	0.4	196	22	34	155	464	122	94	239	134	25	11	37	1.9	0.63	14.35	1.99	1.10
MA-W-22	W	734	Amb	48.70	2.79	13.75	14.90	0.20	6.02	11.10	2.15	0.17	0.23	2.31	45.9	6.2	206	6	36	154	405	121	83	244	118	23	11	35	2.6	0.16	14.09	0.53	0.28
MA-W-23	W	734	Amb	48.93	2.77	13.60	14.30	0.21	6.42	11.18	2.23	0.13	0.23	2.36	48.5	1.7	208	25	34	152	396	124	90	209	112	24	11	33	0.8	0.75	14.37	2.38	1.21
MA-W-24	W	734	Amb	49.24	2.81	13.37	14.65	0.22	6.35	10.61	2.20	0.34	0.23	2.53	47.6	3.1	203	49	36	152	363	113	84	179	107	23	11	32	4.0	1.35	13.68	4.37	2.39
MA-W-25	W	734	Amb	48.90	2.77	13.38	14.62	0.21	6.69	10.67	2.19	0.33	0.24	2.52	49.0	3.7	195	48	34	148	373	120	82	171	106	21	10	32	1.8	1.41	14.80	4.75	2.44
MA-W-26	W	734	Amb	48.83	2.75	13.52	14.52	0.21	6.65	10.72	2.26	0.31	0.23	2.58	49.0	2.9	208	58	36	149	393	117	87	180	108	23	10	38	1.9	1.62	14.56	5.69	2.79
MA-W-27	W	734	Amb	48.96	2.78	13.31	14.56	0.20	6.54	10.86	2.26	0.29	0.24	2.56	48.5	3.5	204	61	36	155	437	120	85	218	112	23	11	32	2.1	1.69	14.46	5.67	2.98
MA-W-29	W	734	Amb	49.19	2.64	13.36	14.88	0.19	5.98	10.98	2.29	0.24	0.25	2.53	45.7	10.6	203	40	37	169	398	124	81	269	119	22	12	33	0.2	1.09	14.00	3.31	1.98
MA-W-31	W	734	Amb	48.84	2.79	13.33	14.66	0.22	6.57	10.89	2.22	0.24	0.23	2.46	48.5	4.7	199	40	34	148	423	129	86	188	110	22	11	33	1.8	1.18	14.05	3.81	2.01
MA-W-51	W	734	Amb	48.81	2.80	13.39	14.60	0.21	6.67	10.71	2.24	0.34	0.23	2.58	48.9	4.9	198	46	34	147	394	124	85	169	109	23	10	37	0.3	1.35	15.30	4.82	2.34
MA-X-51	X	773	Amb	49.00	2.56	13.74	13.85	0.19	7.13	10.84	2.18	0.30	0.21	2.48	51.9	1.0	200	52	31	135	415	208	111	225	106	22	10	34	1.7	1.65	13.61	5.24	2.59
MA-Y-51	Y	803	Amb	49.49	2.74	13.51	14.01	0.25	6.44	10.82	2.30	0.19	0.24	2.50	49.1	1.8	231	69	34	151	394	122	77	191	109	23	11	31	2.0	2.04	13.60	6.24	3.00
MA-Z2-51	Z2	883	Amb	49.23	3.79	12.14	16.03	0.20	5.90	9.56	2.38	0.45	0.31	2.83	43.6	7.0	203	67	43	214	515	97	71	347	135	25	17	31	2.5	1.55	12.79	4.01	3.30
MA-Z3-51	Z3	916	MK	48.85	4.53	12.01	16.37	0.20	4.95	9.46	2.51	0.67	0.45	3.18	38.8	14.8	248	129	44	250	551	56	70	275	166	25	27	33	1.5	2.93	9.29	4.79	5.19
MA-Z5-51	Z5	959	Mah	50.19	2.31	14.28	12.47	0.20	6.35	11.13	2.46	0.36	0.25	2.82	51.7	3.9	289	197	29	159	301	231	140	161	100	21	16	27	4.0	6.77	9.98	12.38	6.82
MA-Z6-55	Z6	987	Mah	50.73	2.31	14.03	12.18	0.18	6.46	10.99	2.46	0.42	0.23	2.88	52.7	13.7	290	169	28	157	314	260	139	153	106	21	16	29	2.7	6.09	9.96	10.68	5.82
MA-Z7-51	Z7	1016	Mah	49.79	3.53	12.76	15.01	0.21	5.25	9.97	2.54	0.58	0.36	3.12	42.3	11.7	245	192	43	225	485	96	59	274	140	25	22	35	1.8	4.43	10.23	8.74	7.84
MA-Z8-51	Z8	1058	Mah	49.49	3.66	12.93	14.92	0.23	5.22	10.35	2.50	0.35	0.36	2.84	42.3	10.8	248	114	43	234	463	89	61	283	134	23	22	34	4.6	2.64	10.54	5.15	4.61
MA-Z10-51	Z10	1091	Mah	49.87	3.33	13.05	14.15	0.20	5.72	10.41	2.50	0.46	0.31	2.95	45.9	8.7	225	122	40	200	488	149	80	243	130	24	17	36	2.7	3.01	11.76	7.15	5.40
MA-Z11-51	Z11	1130	Mah	49.79	2.65	14.10	13.17	0.20	5.76	11.32	2.39	0.37	0.25	2.76	47.9	6.1	224	120	34	167	400	149	81	225	113	21	14	34	2.2	3.55	12.13	8.67	5.33
MA-Z12-51	Z12	1197	Mah	49.54	2.62	14.73	12.74	0.18	5.97	11.27	2.39	0.31	0.25	2.70	49.6	6.6	226	80	34	157	382	197	88	215	103	22	12	34	1.5	2.39	12.83	6.55	3.53
BM-01-51	1	120	Bus	50.74	1.33	15.85	11.06	0.16	7.17	10.93	2.14	0.48	0.13	2.62	57.6	9.5	185	98	29	119	281	222	125	129	86	22	6	31	4.9	3.36	19.89	16.32	5.27
BM-02-51	2	135	Bus	51.64	1.15	14.89	10.81	0.17	7.36	11.51	1.77	0.59	0.11	2.36	58.8	19.6	168	126	25	86	284	297	97	136	81	20	5	40	3.1	5.04	18.28	26.80	7.51
BM-04-51	4	255	Pol	51.42	2.07	14.12	13.10	0.19	5.70	10.40	2.38	0.42	0.19	2.80	47.7	12.9	211	130	34	144	431	146	72	187	108	23	10	41	2.6	3.82	14.85	13.36	6.15
BM-05-51	5	300	Pol	49.57	2.76	13.40	14.92	0.19	6.08	10.12	2.21	0.51	0.25	2.71	46.1	10.2	218	73	37	176	459	126	89	231	125	26	11	34	1.6	2.00	16.23	6.77	3.36
BM-06-51	6	420	Pol	51.58	1.91	14.47	11.30	0.17	6.91	10.73	2.18	0.56	0.19	2.74	56.2	9.5	208	133	31	140	371	290	118	174	96	21	9	36	1.7	4.27	14.91	14.18	6.41
BM-07-51	7	490	Pol	51.17	2.36	14.39	11.38	0.16	6.52	10.98	2.37	0.46	0.22	2.83	54.6	7.2	221	102	34	154	417	280	113	180	103	24	10	36	2.9	2.97	14.78	9.81	4.62
BM-08-51	8	540	Amb	49.97	2.64	13.37	14.81	0.21	5.55	10.68	2.26	0.27	0.24	2.53	44.0	6.7	191	67	39	168	480	89	69	260	125	25	11	39	1.9	1.71	15.40	6.12	3.50
BM-09-51	9	565	Amb	49.92	2.03	14.32	12.46	0.20	6.63	11.97	2.09	0.21	0.18	2.30	52.7	2.8	204	46	29	125	422	123	96	185	102	22	8	39	1.6	1.58	15.30	5.56	2.23
BM-10-51	10	590	Amb	50.54	2.29	14.17	12.48	0.18	6.29	11.25	2.18	0.41	0.21	2.60	51.4	11.0	223	61	30	144	431	124	92	183	105	23	9	39	1.5	2.00	15.59	6.57	2.73
BM-11-51	11	660	Amb	49.36	2.60	13.78	14.06	0.24	5.98	11.34	2.20	0.22	0.21	2.42	47.2	7.9	217	11	33	149	493	93	85	168	121	25	11	36	2.1	0.33	13.58	1.01	0.51
BM-12-51	12	680	Amb	48.83	2.53	14.08	14.01	0.20	6.27	11.43	2.24	0.20	0.23	2.44	48.4	4.5	216	5	33	143	473	89	83	253	117	24	10	36	1.2	0.15	14.49	0.51	0.23
BM-13-51	13	710	Amb	49.90	2.62	13.95	13.23	0.19	5.91	11.34	2.29	0.34	0.24	2.62	48.4	9.5	218	9	35	155	491	207	103	210	115	24	10	36	0.7	0.27	14.86	0.90	0.43
BM-14-51	14	740	Amb	49.89	2.34	14.17	12.42	0.18	6.68	11.68	2.14	0.31	0.20	2.44	53.0	8.5	210	11	29	131	456	244	104	193	102	24	8	41	1.2	0.39	15.65	1.35	0.54
BM-15-51	15	780	Amb	49.65	2.71	13.95	14.21	0.22	6.10	10.26	2.26	0.40	0.25	2.66	47.4	6.3	213	62	38	160	479	90	81	253	124	26	10	36	1.2	1.65	15.60	6.02	2.90
BM-16-51	16	815	Amb	49.18	2.47	13.72	14.21	0.19	6.76	10.81	2.17	0.27	0.21	2.44	50.0	3.9	203	28	32	143	482	169	103	226	122	24	10	37	1.6	0.87	14.87	2.94	1.39
KK-02-51	2	695	Amb	49.81	2.32	14.27	12.37	0.18	6.83	11.65	2.08	0.28	0.20	2.36	53.6	4.5	212	28	31	132	441	239	108	196	101	23	9	39	1.0	0.91	14.25	3.03	1.33
KK-03A-51	3	740	Amb	49.22	2.38	13.91	13.78	0.19	6.84	11.17	2.11	0.21	0.21	2.32	51.0	1.5	205	28	32	136	469	172	114	212	119	23	9	38	1.2	0.86	15.23	3.12	1.36
KK-04-51	4	765	Amb	49.13	2.55	13.88	14.18	0.19	6.62	10.79	2.18	0.26	0.22	2.44	49.5	2.7	209	21	34	143	468	94	94	218	122	24	10	40	1.9	0.63	14.24	2.11	1.02
KK-05-51	5	785	Amb	48.62	2.72	13.78	14.48	0.21	6.53	11.08	2.17	0.18	0.24	2.35	48.6	1.6	214	29	36	153	498	144	92	170	125	25	11	40	1.9	0.80	14.51	2.70	1.33
KK-06-51	6	810	Amb	48.68	2.58	13.70	14.15	0.21	6.74	11.37	2.15	0.21	0.20	2.36	50.0	4.0	214	37	31	132	489	128	87	207	120	23	10	37	1.4	1.16	13.77	3.81	1.71
KK-06-52	6	810	Amb	49.19	2.46	13.82	13.87	0.19	6.65	11.18	2.16	0.25	0.22	2.41	50.1	2.8	210	28	33	138	460	133	92	213	119	24	10	36	2.1	0.87	13.45	2.75	1.34
KK-07-51	7	845	Amb	49.19	2.67	13.52	14.33	0.21	6.11	11.29	2.23	0.20	0.23	2.43	47.2	6.1	226	30	34	152	470	136	81	194	118	24	12	36	1.1	0.88	12.68	2.49	1.32
KK-08-51	8	865	Amb	48.39	2.68	13.85	14.31	0.26	6.41	11.44	2.23	0.21	0.23	2.44	48.4	3.7	223	34	34	151	464	140	85	239	122	25	12	40	1.0	1.01	12.42	2.83	1.55
KK-09-51	9	890	Amb	49.37	2.42	14.01	13.31	0.20	6.53	11.34	2.23	0.37	0.21	2.60	50.7	9.1	224	46	32	140	443	200	108	200	113	23	11	34	1.8	1.44	12.36	4.04	2.04
KK-10-51	10	900	Amb	49.00	2.44	14.09	13.57	0.20	6.83	11.36	2.07	0.23	0.21	2.30	51.3	3.4	216	38	30	135	426	191	111	206	109	23	11	33	1.7	1.26	12.39	3.44	1.74

Table A2 (a) (---continued)

Sample No.	flow No.	height (m)	forma-tion	SiO2 (wt.%)	TiO2	Al2O3	FeO*	MnO	MgO	CaO	Na2O	K2O	P2O5	Na2O+K2O	Mg#	Rb (ppm)	Sr	Ba	Y	Zr	V	Cr	Ni	Cu	Zn	Ga	Nb	Sc	Th	Ba/Y (ratio)	Zr/Nb	Ba/Nb	Ba/Sr X10
KK-11-51	11	910	Amb	48.84	2.93	13.34	15.10	0.21	5.83	11.05	2.25	0.20	0.25	2.46	44.7	3.9	226	28	36	165	498	77	85	234	130	24	13	39	2.0	0.79	12.79	2.19	1.25
KT-02-51	2	670	Amb	51.07	1.96	14.28	11.15	0.18	7.11	11.64	2.13	0.30	0.18	2.43	57.2	4.4	215	79	29	132	392	310	114	141	90	21	9	33	3.3	2.70	15.09	9.08	3.69
KT-03-51	3	700	Amb	50.61	2.65	12.70	15.38	0.23	5.23	10.10	2.41	0.43	0.25	2.84	41.6	8.4	205	83	39	174	514	64	52	326	133	26	11	38	0.8	2.13	15.95	7.58	4.02
KT-04-51	4	740	Amb	51.18	2.28	14.53	11.50	0.18	6.30	11.18	2.34	0.29	0.22	2.63	53.5	10.0	229	68	33	151	435	261	102	197	99	24	11	34	3.3	2.09	13.15	5.94	2.99
KT-05-51	5	750	Amb	49.88	2.06	13.99	12.57	0.18	6.82	12.00	2.11	0.21	0.19	2.32	53.2	2.0	208	27	29	123	435	178	94	174	103	23	7	40	1.5	0.95	16.74	3.74	1.32
KT-06-51	6	770	Amb	50.01	2.05	14.14	12.67	0.19	6.58	11.88	2.11	0.19	0.18	2.31	52.1	2.4	211	29	30	127	413	121	92	185	102	21	8	39	1.3	0.98	15.55	3.58	1.38
KT-07-51	7	795	Amb	49.51	2.32	13.86	13.43	0.19	6.53	11.64	2.16	0.15	0.21	2.31	50.5	1.0	215	31	31	132	462	124	93	210	111	24	10	40	1.6	1.00	13.68	3.21	1.44
KT-09-51	9	850	Amb	49.55	2.52	13.88	13.42	0.21	6.54	11.28	2.20	0.17	0.23	2.37	50.5	3.2	222	26	33	146	482	153	101	226	118	23	10	43	1.8	0.79	14.39	2.60	1.19
KT-10-51	10	880	Amb	49.67	2.98	13.79	13.47	0.19	5.99	11.22	2.22	0.18	0.28	2.40	48.3	4.9	224	20	40	191	542	167	97	279	120	25	13	37	1.2	0.50	14.93	1.57	0.89
KT-11-51	11	900	Amb	49.73	2.93	13.68	14.15	0.19	5.83	10.74	2.22	0.26	0.27	2.48	46.3	2.9	219	18	39	178	530	130	80	271	122	25	12	33	1.8	0.46	14.73	1.46	0.81
AK-01-51	1	90	Tha	51.46	1.82	13.53	12.20	0.17	7.43	10.51	2.12	0.58	0.17	2.70	56.1	16.3	193	97	31	135	315	369	159	159	96	21	7	30	3	3.12	18.32	13.18	5.06
AK-02-51	2	110	Tha	51.61	1.85	13.44	12.36	0.18	7.34	10.48	2.15	0.39	0.18	2.55	55.5	5.5	200	81	33	140	313	343	155	160	92	21	8	25	3	2.44	17.16	9.88	4.03
AK-03-51	3	130	Tha	51.35	1.86	13.54	12.33	0.18	7.43	10.67	2.16	0.28	0.18	2.44	55.8	5.6	202	80	32	142	334	346	158	185	93	22	9	24	3	2.48	16.70	9.43	3.97
BH-01	1	153	Tha	51.29	1.85	12.86	11.53	0.13	8.52	11.27	1.73	0.63	0.18	2.36	60.8	11.0	216	142	25	117	314	342	118	111	86	18	8	38	1.9	5.76	14.63	17.70	6.55
BH-03	3	200	Tha	49.60	1.92	13.24	12.56	0.16	8.25	11.58	1.88	0.62	0.18	2.50	57.9	13.2	232	91	25	113	348	445	142	129	87	16	8	31	0.7	3.73	14.49	11.71	3.93
BH-04	4	225	Tha	51.79	1.38	13.06	10.91	0.17	9.60	10.46	2.08	0.41	0.15	2.50	64.8	5.3	303	156	18	109	274	328	172	105	75	17	9	33	4.5	8.73	12.24	17.56	5.16
BH-05	5	270	Tha	53.41	1.50	14.07	10.77	0.16	7.26	9.66	2.33	0.66	0.16	2.99	58.6	13.5	341	173	21	122	304	191	107	121	78	16	8	39	1.8	8.30	14.51	20.55	5.07
BH-06	6	290	Tha	52.68	1.11	9.21	10.52	0.16	12.03	12.28	1.42	0.49	0.10	1.91	70.6	12.3	198	142	16	76	296	1481	298	95	67	14	6	34	2.8	8.89	13.40	24.96	7.18
BH-07	7	310	Tha	49.92	1.84	14.78	11.69	0.14	7.48	11.47	2.10	0.40	0.18	2.50	57.3	4.3	274	128	27	139	300	283	129	77	83	17	10	32	3.7	4.79	13.49	12.41	4.66
BH-08	8	316	Tha	50.46	2.30	13.27	13.03	0.18	7.44	10.12	2.27	0.71	0.22	2.98	54.5	20.2	257	155	30	147	339	329	181	179	99	22	11	35	3.7	5.24	13.77	14.44	6.00
BH-09	9	343	Bhi	50.86	2.21	15.64	11.76	0.15	5.38	10.34	2.48	0.96	0.23	3.44	49.0	32.0	311	142	29	152	352	159	78	178	90	21	12	33	1.2	4.86	12.99	12.13	4.56
BH-10	10	381	Bhi	50.22	2.25	15.55	11.90	0.16	5.85	10.99	2.31	0.55	0.22	2.87	50.7	23.5	263	70	29	149	384	195	99	190	92	20	11	33	3.3	2.36	13.55	6.32	2.64
BH-12	12	404	Kha	50.55	2.86	15.36	13.42	0.16	4.25	9.43	2.69	0.96	0.32	3.65	39.9	27.0	290	286	38	223	379	104	65	249	103	20	14	31	4.7	7.52	16.43	21.01	9.87
BH-13	13	442	Kha	47.92	1.58	17.00	13.31	0.17	5.91	11.15	2.44	0.36	0.16	2.80	48.2	4.4	222	182	30	106	264	78	147	168	105	22	5	34	1.7	6.13	19.92	34.25	8.19
BH-14	14	488	Kha	48.74	1.09	14.60	12.62	0.17	9.33	10.86	1.80	0.67	0.12	2.47	60.8	18.6	180	176	22	76	269	500	221	92	88	23	4	37	1.5	7.90	21.69	50.34	9.82
BH-15	15	508	Kha	50.87	2.39	14.11	15.21	0.17	4.12	9.38	2.66	0.84	0.25	3.50	36.2	19.9	274	225	35	173	399	59	56	210	123	22	10	40	3.8	6.53	16.65	21.66	8.21
BH-16-51	16	526	Kha	50.48	2.56	14.28	14.78	0.18	4.60	9.41	2.60	0.85	0.26	3.45	39.5	22.9	276	276	38	182	399	47	54	167	112	23	12	39	4.3	7.24	15.20	22.98	10.01
BH-16-52	16	526	Kha	50.68	2.75	13.81	14.87	0.19	4.64	9.26	2.62	0.89	0.28	3.51	39.6	23.8	266	286	40	198	437	48	49	151	116	21	13	35	3.7	7.11	14.98	21.67	10.74
IG-01	1	250	Jaw	52.02	1.79	13.11	11.42	0.19	7.69	10.65	2.19	0.81	0.13	3.00	58.5	15.0	194	187	26	128	273	456	96	54	82	20	8	29	4.2	7.16	15.24	22.26	9.62
IG-02	2	275	Jaw	51.55	1.70	12.50	11.11	0.15	9.00	11.50	1.80	0.55	0.14	2.35	62.9	14.3	191	174	27	125	268	426	92	56	82	20	8	33	3.2	6.53	16.25	22.65	9.13
IG-03	3	320	Jaw	51.22	1.71	14.47	11.28	0.16	7.10	11.56	1.78	0.57	0.16	2.34	56.9	15.0	145	150	27	139	311	263	50	43	73	20	8	34	4.9	5.52	18.22	19.76	10.39
IG-04	4	332	Jaw	50.80	3.29	12.72	15.35	0.23	4.78	9.00	2.55	1.00	0.29	3.55	39.5	22.0	256	252	39	223	490	59	41	182	122	25	15	31	4.2	6.54	14.75	16.66	9.82
IG-05	5	389	Jaw	49.86	2.93	12.76	15.47	0.22	5.41	9.86	2.53	0.68	0.27	3.21	42.3	11.9	282	263	35	208	446	83	57	131	112	25	15	31	3.9	7.46	14.12	17.86	9.30
IG-06	6	402	Jaw	50.76	3.48	14.25	14.23	0.19	3.90	8.75	2.75	1.37	0.33	4.12	36.5	54.8	237	362	48	312	413	67	40	197	122	27	21	25	7.8	7.52	14.69	17.09	15.27
IG-07	7	431	Iga	49.90	1.72	15.46	12.96	0.20	5.91	10.81	2.39	0.50	0.16	2.89	48.9	6.5	199	260	31	115	268	149	90	157	81	22	7	30	5.4	8.29	15.77	35.55	13.04
IG-08	8	465	Iga	49.56	2.52	14.65	13.18	0.18	5.82	10.34	2.69	0.81	0.25	3.50	48.1	18.4	256	269	35	189	354	217	98	162	89	24	12	26	3.4	7.59	15.71	22.40	10.49
IG-09	9	472	Iga	50.73	2.32	13.46	13.57	0.19	5.61	10.15	2.76	0.97	0.24	3.73	46.4	26.1	242	268	36	198	368	183	105	135	91	25	10	27	3.4	7.42	19.38	26.26	11.08
IG-10	10	480	Iga	51.60	2.09	14.55	12.36	0.15	5.45	9.67	2.87	1.05	0.22	3.92	48.0	26.7	245	246	32	189	342	106	71	66	81	23	9	25	4.0	7.71	20.71	27.02	10.04
IG-11	11	488	Iga	51.97	2.10	13.45	12.60	0.18	5.74	10.18	2.59	0.98	0.21	3.57	48.9	27.0	237	237	33	189	324	114	76	67	86	24	10	26	4.0	7.16	19.12	23.93	9.99
IG-12	12	497	Iga	51.30	2.20	14.62	12.30	0.19	5.47	9.89	2.80	1.01	0.22	3.81	48.2	28.0	238	230	32	187	337	111	65	70	89	23	9	27	3.4	7.28	22.04	27.05	9.66
IG-13	13	512	Iga	50.96	2.20	13.76	13.12	0.18	6.05	10.08	2.68	0.76	0.22	3.44	49.1	16.6	232	216	34	187	369	97	59	60	87	23	10	25	3.1	6.36	19.68	22.68	9.29
IG-14	14	526	Iga	51.15	2.12	14.09	12.68	0.18	5.85	10.22	2.73	0.76	0.21	3.49	49.2	14.5	240	207	30	173	332	93	65	50	81	24	9	25	3.9	6.80	19.20	22.96	8.62
IG-15	15	539	Tha	50.20	1.59	11.18	12.27	0.18	11.12	11.10	1.72	0.52	0.12	2.24	65.5	18.6	229	211	32	183	376	100	57	59	85	24	10	29	4.0	6.50	19.08	21.94	9.20
ST-1	1	295	ST I	51.08	2.74	13.43	13.46	0.22	4.59	10.00	3.32	0.62	0.55	3.94	41.7	14.2	268	89	42	119	382	107	68	232	110	18	12	30	2.3	2.14	9.67	7.22	3.32
ST-2	2	305	ST II	51.98	0.99	15.13	10.30	0.16	6.70	10.70	3.18	0.77	0.10	3.95	57.7	18.2	205	138	27	96	237	186	85	48	75	17	6	29	3.5	5.01	16.59	23.88	6.71
ST-6	3	362	ST II	50.03	2.72	13.68	13.01	0.15	5.84	10.78	3.27	0.28	0.25	3.55	48.5	1.3	266	43	41	188	438	191	94	203	110	24	14	17	3.0	1.05	13.66	3.15	1.63

Table A2 (a) (---continued)

Sample No.	flow No.	height (m)	forma-tion	SiO2 (wt.%)	TiO2	Al2O3	FeO*	MnO	MgO	CaO	Na2O	K2O	P2O5	Na2O+ K2O	Mg#	Rb (ppm)	Sr	Ba	Y	Zr	V	Cr	Ni	Cu	Zn	Ga	Nb	Sc	Th	Ba/Y (ratio)	Zr/Nb	Ba/Nb	Ba/Sr X10
ST-7	4	385	ST II	51.17	2.72	13.51	13.90	0.18	4.48	9.90	3.01	0.59	0.54	3.60	40.3	20.7	323	317	52	241	428	38	49	176	137	21	34	25	7.1	6.14	7.18	9.47	9.82
ST-9	5	430	ST III	50.85	2.14	14.42	12.40	0.18	6.07	10.84	2.27	0.64	0.18	2.91	50.7	19.2	289	73	32	137	380	80	90	235	112	22	9	26	1.2	2.31	15.10	8.05	2.53
ST-12	6	445	ST III	50.87	1.79	14.05	13.82	0.20	5.73	9.91	3.01	0.45	0.17	3.46	46.5	13.1	347	252	51	234	435	39	49	200	132	21	33	28	5.6	4.94	7.03	7.56	7.26
ST-14	7	475	ST III	48.29	2.92	12.66	16.45	0.20	5.47	9.49	3.48	0.74	0.28	4.22	41.1	18.5	109	23	53	213	579	84	67	407	155	21	21	37	4,1	0.43	10.33	1.10	2.08
ST-16	8	490	ST IV	49.61	2.43	14.33	12.43	0.17	6.69	11.22	2.56	0.35	0.21	2.91	53.0	2.7	232	83	37	157	343	276	117	203	95	22	12	13	1.8	2.25	12.76	6.76	3.59
ST-17	9	500	ST IV	50.22	2.27	14.43	11.94	0.17	6.32	10.68	3.17	0.59	0.21	3.76	52.6	14.4	212	76	36	155	363	264	109	235	98	23	11	24	2.2	2.11	13.64	6.68	3.58
ST-19	10	520	ST IV	48.15	2.28	13.72	13.95	0.17	6.57	12.01	2.70	0.25	0.19	2.95	49.7	6.7	189	5	35	157	416	81	86	216	121	24	10	27	2.7	0.14	15.17	0.48	0.26
ST-20	11	535	ST IV	50.03	2.24	13.65	13.65	0.18	6.27	11.23	2.26	0.30	0.19	2.56	49.1	1.8	215	26	35	152	383	79	83	217	111	23	10	29	1.5	0.74	15.23	2.60	1.20
ST-21	12	552	ST IV	49.87	2.31	13.82	13.47	0.17	6.12	11.26	2.55	0.25	0.19	2.80	48.8	0.4	211	29	35	154	395	74	85	229	114	21	11	29	0.9	0.83	13.88	2.62	1.38
ST-22	13	600	ST IV	49.95	2.25	13.33	13.87	0.16	5.78	9.53	3.94	0.99	0.20	4.93	46.6	40.1	232	73	33	153	344	69	77	217	121	22	11	18	2.5	2.20	14.27	6.83	3.16
ST-23	15	630	ST IV	48.51	2.44	13.89	14.14	0.18	6.45	11.84	2.13	0.22	0.20	2.35	48.9	0.4	205	17	39	167	418	83	85	222	121	23	11	22	1.7	0.45	15.17	1.58	0.85
ST-24	16	650	ST IV	47.42	2.40	14.39	14.32	0.19	6.19	12.62	2.14	0.12	0.20	2.26	47.5	0.4	207	5	37	163	438	78	86	238	119	25	12	26	3.4	0.13	13.64	0.42	0.24
ST-25	17	680	ST IV	49.54	2.27	13.47	13.78	0.18	6.16	11.38	2.72	0.31	0.19	3.03	48.4	0.4	210	28	35	151	393	80	81	223	113	23	10	31	2.8	0.79	14.51	2.68	1.33
ST-26	18	725	ST IV	49.73	2.46	13.95	13.78	0.20	5.89	11.25	2.17	0.28	0.29	2.45	47.3	0.4	212	5	37	155	410	79	86	232	117	22	11	28	1.7	0.13	14.01	0.45	0.24
ST-27	19	740	ST IV	48.55	2.36	14.02	14.20	0.20	6.25	11.89	2.09	0.25	0.19	2.34	48.0	8.2	237	5	36	151	430	86	87	213	117	22	11	30	3.5	0.14	13.67	0.45	0.21
ST-30	20	765	MK	52.26	2.80	13.50	13.33	0.21	4.49	8.81	3.00	1.04	0.56	4.04	41.4	28.6	258	217	52	247	425	36	49	189	141	21	34	21	7.6	4.14	7.17	6.30	8.39
ST-31	21	810	ST V	49.99	2.88	12.90	14.94	0.23	5.51	10.37	2.23	0.68	0.27	2.91	43.6	25.4	158	17	49	201	535	91	68	248	125	23	20	28	2.0	0.34	10.31	0.87	1.07
ST-32	22	860	ST V	49.87	2.12	14.93	12.36	0.16	5.93	11.54	2.34	0.56	0.19	2.90	50.2	10.8	252	58	33	143	335	74	80	124	87	22	9	30	2.1	1.75	15.42	6.29	2.31
ST-33	23	873	MK	52.19	0.81	15.06	9.74	0.15	7.40	11.59	2.34	0.65	0.08	2.99	61.4	10.2	413	123	25	71	201	256	89	116	71	18	5	32	1.6	4.94	13.35	23.27	2.97
ST-34	24	900	ST VI	50.94	2.41	13.81	12.97	0.18	6.09	10.93	2.28	0.17	0.21	2.45	49.6	0.6	278	162	39	156	432	107	77	218	93	22	18	40	2.6	4.15	8.55	8.89	5.83
ST-35	25	915	ST VI	48.57	2.32	13.91	13.53	0.20	6.08	11.37	3.39	0.33	0.30	3.72	48.5	0.4	271	170	40	158	519	117	79	213	108	21	19	41	2.9	4.22	8.14	8.74	6.29
ST-38	28	970	ST VI	51.03	1.86	14.21	13.42	0.19	5.80	10.71	2.30	0.31	0.18	2.61	47.5	2.4	159	109	40	116	420	104	63	222	100	19	11	46	1.9	2.71	10.65	9.93	6.84
ST-39	29	982	ST VII	52.22	1.10	15.57	10.36	0.15	6.97	11.28	1.81	0.44	0.10	2.25	58.5	4.4	388	250	31	91	265	200	88	97	77	19	7	40	4.0	8.17	13.66	37.50	6.43
ST-40	30	995	ST VII	52.55	1.08	15.48	10.06	0.16	7.04	11.63	1.69	0.21	0.10	1.90	59.5	1.0	281	160	29	93	279	215	93	129	80	16	6	41	4,2	5.61	15.61	26.74	5.70
ST-41	31	1008	ST VII	51.00	1.16	15.03	11.68	0.18	6.78	11.83	2.07	0.16	0.10	2.23	54.9	0.4	110	63	32	87	291	84	71	141	85	18	6	48	2.2	1.99	14.28	10.31	5.74
ST-42	32	1022	ST VII	52.61	0.91	15.28	10.08	0.14	7.22	11.34	1.65	0.70	0.08	2.35	60.0	19.3	212	123	25	76	235	205	85	110	75	16	5	39	2.5	4.94	16.37	26.42	5.79
ST-43	33	1032	ST VII	51.86	0.97	15.28	10.63	0.16	6.97	11.92	1.52	0.59	0.09	2.11	57.9	26.3	119	116	28	91	264	196	74	112	83	17	6	45	2.8	4.15	14.82	19.01	9.79
ST-44	34	1050	ST VII	52.52	0.86	15.33	9.66	0.14	7.25	11.65	1.98	0.54	0.08	2.52	61.1	11.7	137	172	26	81	228	237	87	122	75	18	5	43	3.6	6.55	16.06	34.30	12.57
ST-46	35	1063	ST VII	51.89	1.19	15.95	10.49	0.14	6.14	11.76	2.07	0.26	0.11	2.33	55.1	0.4	196	157	32	112	270	119	70	161	79	19	7	39	4.1	4.90	15.42	21.70	8.02
ST-47	36	1073	ST VIII	48.20	3.08	13.62	15.34	0.19	5.92	10.88	2.24	0.28	0.26	2.52	44.7	11.1	251	79	41	179	495	89	76	213	118	24	12	34	1.1	1.94	14.60	6.45	3.15
ST-48	37	1087	ST VIII	49.20	3.02	13.57	14.64	0.19	5.68	11.01	2.25	0.16	0.27	2.41	44.9	0.4	259	41	42	185	600	102	77	264	132	24	14	41	1.9	1.00	13.38	2.99	1.60
ST-49	38	1097	ST VIII	47.41	3.17	14.18	15.03	0.20	6.23	11.26	2.12	0.15	0.26	2.27	46.5	0.4	244	56	41	178	520	104	84	270	121	26	13	41	2.3	1.39	13.51	4.28	2.31
ST-50	39	1108	MK	60.26	0.97	13.09	9.31	0.13	4.73	9.36	1.78	0.27	0.11	2.05	51.6	7.6	175	121	28	102	257	87	59	120	77	17	7	32	4.4	4.28	15.37	18.27	6.91
ST-51	40	1112	ST IX	52.25	1.57	15.03	12.01	0.18	5.21	10.36	2.30	0.94	0.16	3.24	47.6	16.5	143	230	43	144	373	66	52	209	97	19	10	41	5.2	5.41	14.16	22.62	16.06
ST-52	41	1122	ST IX	51.59	1.59	15.15	12.15	0.17	5.24	10.58	2.53	0.84	0.16	3.37	47.5	16.4	159	219	39	148	407	71	55	191	101	21	11	42	5.5	5.54	13.93	20.64	13.73
AJ-01	1	550	AJ I	51.36	2.46	14.22	13.52	0.14	5.17	9.49	2.55	0.83	0.24	3.38	44.5	16.1	271	233	36	185	374	64	54	200	109	26	11	31	4.1	6.55	16.96	21.39	8.60
AJ-02-51	2	527	AJ I	50.94	2.54	13.71	14.44	0.18	5.20	9.67	2.53	0.54	0.25	3.07	43.0	20.6	250	234	37	201	425	100	70	202	119	25	11	30	4.4	6.26	17.61	20.55	9.38
AJ-02-52	2	527	AJ I	50.65	2.57	13.50	15.05	0.19	5.07	9.44	2.54	0.73	0.26	3.26	41.4	16.8	249	259	41	208	428	98	70	203	122	26	12	30	4.1	6.28	17.22	21.38	10.37
AJ-03-51	3	509	AJ I	52.12	2.71	13.01	14.59	0.17	4.88	8.63	2.44	1.13	0.31	3.58	41.2	37.1	278	315	40	226	398	80	58	153	107	25	14	34	2.8	7.84	16.63	23.13	11.31
AJ-03-52	3	509	AJ I	51.43	2.68	12.62	14.36	0.18	5.10	9.74	2.26	1.37	0.27	3.62	42.7	42.1	254	305	42	195	427	82	55	159	106	25	11	34	3.3	7.34	17.89	27.95	12.01
AJ-05	5	450	AJ I	51.95	2.66	12.82	15.22	0.17	4.39	8.80	2.49	1.19	0.31	3.69	37.7	33.3	264	366	42	224	418	90	53	177	112	24	13	33	4.8	8.72	17.07	27.96	13.90
AJ-07	7	400	AJ I	51.16	2.35	14.49	13.77	0.17	5.02	9.69	2.59	0.52	0.23	3.11	43.3	10.3	275	213	34	178	408	62	62	215	105	25	9	31	3.7	6.23	18.93	22.66	7.76
AJ-08	8	350	AJ I	50.42	2.95	14.34	13.94	0.17	5.08	9.75	2.60	0.44	0.32	3.04	43.3	12.2	274	233	39	238	374	97	88	265	107	27	16	26	5.3	5.92	14.96	14.64	8.51
BU-03-51	3	490	BU I	49.49	2.33	13.21	14.59	0.19	6.53	10.90	2.37	0.21	0.20	2.57	48.4	1.0	237	85	34	146	471	78	72	233	104	23	9	36	3.1	2.48	15.53	9.03	3.58
BU-04-51	4	507	BU I	49.78	2.37	13.16	14.47	0.20	6.12	10.87	2.47	0.35	0.22	2.82	47.0	8.4	215	100	38	160	466	69	78	194	114	22	10	33	2.4	2.60	15.47	9.67	4.64
BU-05-51	5	547	BU I	49.83	2.33	13.51	14.09	0.18	6.01	11.20	2.40	0.24	0.21	2.65	47.2	3.5	220	74	35	159	435	76	79	216	105	22	10	31	1.8	2.07	15.17	7.01	3.34

Table A2 (a) (---continued)

Sample No.	flow No.	height (m)	forma-tion	SiO2 (wt.%)	TiO2	Al2O3	FeO*	MnO	MgO	CaO	Na2O	K2O	P2O5	Na2O+ K2O	Mg#	Rb (ppm)	Sr	Ba	Y	Zr	V	Cr	Ni	Cu	Zn	Ga	Nb	Sc	Th	Ba/Y (ratio)	Zr/Nb	Ba/Nb	Ba/Sr X10
BU-06-51	6	556	BU I	49.64	2.24	13.32	14.26	0.20	6.41	11.05	2.36	0.32	0.20	2.68	48.5	2.1	213	83	35	146	440	101	84	210	110	23	10	40	2.4	2.38	15.15	8.60	3.90
BU-07-51	7	594	BU I	50.22	2.45	13.09	14.42	0.20	6.14	10.29	2.51	0.46	0.21	2.98	47.1	6.7	215	88	39	161	506	60	68	205	116	24	9	36	1.0	2.26	17.07	9.34	4.10
BU-08-51	8	634	BU I	50.51	2.79	13.27	13.89	0.17	5.91	9.89	2.62	0.68	0.27	3.30	47.1	17.9	227	116	42	193	563	183	88	265	117	24	13	33	2.8	2.76	14.37	8.66	5.13
LC-X1-51	1	450	BU I	51.17	2.62	13.35	14.43	0.20	5.27	9.96	2.35	0.39	0.26	2.74	43.4	14.5	262	116	37	184	478	78	53	206	123	25	12	37	3.6	3.15	15.41	9.77	4.44
LC-04-51	4	510	BU I	51.09	2.64	13.19	14.49	0.21	5.31	9.94	2.47	0.41	0.26	2.88	43.4	15.2	251	128	37	187	481	89	54	229	124	24	13	34	3.0	3.42	14.51	9.91	5.09
CK-01				49.47	2.34	13.32	14.56	0.19	6.37	10.96	2.24	0.34	0.21	2.58	47.8	4.3	210	99	36	152	359	67	73	188	100	16	10	39	3.7	2.75	15.95	10.43	4.72
P1-SF-89-2	1	380	P I	52.69	2.20	12.92	14.15	0.18	5.02	9.43	2.73	0.49	0.17	3.22	42.7	3.5	397	234	39	134	455	89	68	211	114	18	9	34	3.0	6.02	14.83	25.79	5.89
P2-P-89-1	2	400	P I	49.09	1.79	15.29	13.12	0.18	5.39	12.62	2.20	0.17	0.16	2.37	46.3	2.8	229	39	33	118	432	62	67	188	96	22	8	36	1.4	1.19	14.67	4.83	1.70
P3-SF-89-1	3	430	P I	50.59	2.86	15.08	12.88	0.15	5.31	10.15	2.47	0.27	0.23	2.74	46.4	0.4	246	73	44	182	630	94	85	282	124	26	13	42	2.8	1.64	14.44	5.80	2.97
P4-SF-89-1	4	450	P I	51.11	3.03	12.97	14.44	0.19	4.94	10.15	2.36	0.53	0.28	2.89	41.8	7.6	225	140	48	235	608	86	65	283	138	24	15	32	3.5	2.92	15.92	9.48	6.23
P5-Aa-89-1	5	475	P I	51.87	2.89	13.46	13.97	0.20	4.10	9.69	2.71	0.71	0.39	3.42	38.1	29.4	261	279	44	242	534	30	38	244	134	23	28	29	5.9	6.30	8.76	10.09	10.67
P6-SF-89-2	6	535	P II	51.66	2.00	13.94	13.37	0.17	5.30	11.44	1.74	0.21	0.17	1.95	45.4	2.3	789	260	34	112	421	49	59	187	116	20	9	33	1.4	7.73	12.38	28.88	3.30
P7-CP-89-1	7	570	P II	52.74	2.63	13.68	12.93	0.15	4.44	9.94	2.31	0.94	0.26	3.25	41.9	27.5	249	255	41	215	525	61	65	223	132	24	13	35	3.8	6.16	16.51	19.66	10.25
P8-Aa-89-1	8	590	P II	52.06	2.27	13.28	13.94	0.20	5.16	9.94	2.69	0.25	0.20	2.94	43.7	29.5	244	223	40	197	461	57	56	156	115	24	11	35	4.9	5.62	18.23	20.58	9.13
P9-CP-89-4	9	610	P II	51.52	2.36	14.08	13.41	0.16	5.03	9.82	2.39	1.01	0.22	3.40	44.0	0.5	336	149	40	156	499	89	65	221	110	21	10	33	3.1	3.77	15.80	15.10	4.44
P10-SF-89-3	10	640	P II	49.84	2.42	13.58	14.15	0.18	5.77	11.31	2.31	0.22	0.22	2.53	46.1	1.3	246	88	38	167	499	83	74	244	113	24	12	32	3.2	2.31	13.56	7.09	3.56
P11-Aa-89-3	11	720	P II	53.03	3.03	12.50	13.63	0.17	4.73	9.18	2.36	1.11	0.27	3.47	42.1	13.7	308	222	45	222	582	80	62	289	119	23	15	34	4.3	4.88	15.08	15.04	7.21
P12-Aa-89-2	12	750	MK	51.55	3.00	13.26	14.54	0.19	4.05	9.65	2.60	0.78	0.39	3.38	36.9	33.1	257	270	45	246	534	32	38	247	136	23	27	28	6.0	5.99	9.13	10.03	10.50
P13-Aa-89-1	13	770	P III	51.71	2.78	12.86	14.25	0.16	5.49	10.09	2.17	0.26	0.24	2.43	44.7	1.2	211	66	40	191	495	75	72	268	130	22	13	35	3.5	1.64	14.45	4.97	3.11
P14-Aa-89-2	14	790	P III	49.32	3.03	13.34	15.15	0.18	5.43	10.72	2.33	0.24	0.26	2.57	42.9	5.0	229	71	43	205	570	57	63	311	135	24	14	37	3.9	1.66	14.82	5.13	3.09
P15-Aa-89-2	15	820	P III	49.80	2.47	13.50	14.04	0.19	6.08	11.27	2.18	0.26	0.21	2.44	47.6	3.7	215	67	37	164	503	77	78	187	121	22	11	40	3.0	1.84	14.66	6.01	3.12
P16-SF-89-1	16	830	P III	50.99	2.29	13.41	13.84	0.15	5.94	10.94	2.00	0.26	0.19	2.26	47.4	0.4	199	85	36	152	457	100	79	225	119	22	11	39	2.3	2.35	13.94	7.78	4.26
P17-Aa-89-1	17	860	P III	49.22	2.38	13.74	14.25	0.19	6.29	11.05	2.25	0.43	0.21	2.68	48.1	4.7	199	79	37	158	485	78	86	212	118	23	10	40	1.6	2.12	15.31	7.66	3.97
P18-Aa-89-1	18	930	P III	50.07	2.53	13.79	14.17	0.20	5.52	10.33	2.37	0.80	0.23	3.17	45.0	23.0	194	99	39	177	537	81	75	223	126	24	11	34	2.0	2.54	15.55	8.70	5.10
P19-Aa-89-1	19	1000	P VI	49.57	2.03	13.74	12.43	0.17	7.79	11.98	1.98	0.15	0.16	2.13	56.8	1.5	200	45	31	122	458	451	200	194	101	21	8	39	1.1	1.44	16.27	6.00	2.25
P20-Aa-89-1	20	1020	P VI	48.55	2.23	15.07	12.71	0.15	7.00	11.66	2.24	0.20	0.18	2.44	53.6	0.4	214	61	33	137	494	103	93	197	107	24	9	39	0.8	1.85	15.58	6.97	2.86
P21-Aa-89-2	21	1040	MK	51.71	1.38	15.37	11.76	0.16	5.52	11.25	2.38	0.32	0.14	2.70	49.6	12.5	137	156	37	120	352	112	61	189	98	20	8	43	3.3	4.22	14.68	18.99	11.33
P22-Aa-89-2	22	1100	PV	49.34	2.58	13.94	13.59	0.18	6.46	11.24	2.27	0.20	0.21	2.47	49.9	2.6	240	77	36	156	472	126	96	236	107	24	12	31	1.4	2.13	13.54	6.65	3.20
CH-01	1	455	CH I	50.94	3.39	13.06	14.55	0.19	4.93	9.38	2.41	0.76	0.39	3.17	41.5	11.4	293	265	47	272	500	100	63	276	132	17	17	34	4.4	5.66	16.47	16.07	9.06
CH-02	2	472	CH I	50.80	3.21	12.98	14.75	0.19	4.99	9.68	2.54	0.53	0.33	3.07	41.5	34.5	292	251	44	237	475	129	66	270	122	30	14	31	5.3	5.74	17.27	18.34	8.62
CH-03	3	500	CH I	51.94	2.62	13.50	13.63	0.18	5.02	9.52	2.46	0.87	0.26	3.33	43.6	23.5	332	179	37	184	418	71	50	233	95	21	12	32	2.8	4.91	14.83	14.46	5.40
CH-04	4	525	CH I	51.54	2.23	14.41	12.58	0.18	5.71	9.31	3.32	0.52	0.20	3.84	48.8	15.3	354	200	32	152	394	118	70	198	102	21	10	30	5.0	6.26	14.86	19.65	5.66
CH-05	5	533	MK	49.67	2.12	14.08	12.77	0.18	6.73	11.96	2.02	0.30	0.17	2.32	52.5	7.0	208	40	28	113	392	257	97	181	89	24	7	34	2.4	1.40	16.17	5.67	1.91
CH-06-51	6	542	CH II	50.98	3.16	13.21	14.46	0.18	5.05	9.48	1.96	1.18	0.34	3.14	42.3	19.7	242	206	46	248	486	132	69	271	126	29	16	34	4.1	4.52	15.50	12.86	8.50
CH-06-52	6	542	CH II	50.39	3.16	13.11	15.11	0.19	5.05	9.77	2.13	0.75	0.34	2.88	41.2	22.1	299	197	44	242	473	133	70	263	127	28	16	35	6.4	4.53	15.59	12.74	6.59
CH-07	7	567	CH II	51.16	3.06	12.68	14.82	0.20	5.19	9.61	2.35	0.63	0.30	2.98	42.3	11.1	212	138	46	225	504	84	60	291	128	26	14	32	3.7	2.96	15.81	9.68	6.47
CH-08	8	584	CH II	50.26	3.23	13.35	15.10	0.19	5.04	9.94	2.22	0.35	0.32	2.57	41.2	4.1	404	188	45	228	513	145	72	264	130	29	15	34	2.4	4.18	15.60	12.85	4.64
CH-09	9	595	CH II	51.98	3.03	12.76	14.03	0.18	4.91	9.27	1.68	1.85	0.32	3.53	42.3	23.9	305	286	41	229	466	142	65	240	116	26	14	32	2.7	7.00	16.15	20.12	9.37
CH-10	10	605	CH II	50.88	2.82	13.25	14.37	0.19	5.67	10.25	1.97	0.32	0.28	2.29	45.3	8.8	299	176	37	195	428	70	67	222	114	27	12	33	3.1	4.82	16.07	14.53	5.87
CH-11	11	600	CH II	50.50	2.19	14.64	13.67	0.15	5.58	10.75	1.75	0.57	0.20	2.32	46.1	16.3	194	83	33	145	356	121	66	181	110	25	9	37	3.5	2.53	15.63	8.97	4.29
CH-12	12	608	MK	51.81	3.56	12.43	15.27	0.21	4.07	9.20	2.53	0.54	0.39	3.07	35.9	23.7	240	199	54	291	528	40	36	281	153	28	19	37	5.3	3.67	15.33	10.47	8.28
CH-13-52	13	632	CH III	50.21	2.71	12.96	15.70	0.20	5.06	10.22	2.35	0.33	0.26	2.68	40.3	13.4	222	94	41	189	473	51	58	250	130	26	13	37	4.4	2.31	14.42	7.18	4.24
CH-13-53	13	632	CH III	50.47	2.83	13.03	15.21	0.20	5.06	10.27	2.31	0.36	0.27	2.67	41.1	12.6	228	97	41	189	459	47	53	264	119	26	12	32	4.9	2.36	15.64	7.98	4.24
CH-14	14	670	CH III	50.37	2.76	12.84	15.65	0.21	5.25	10.14	2.20	0.31	0.26	2.51	41.3	10.9	221	96	39	190	481	52	56	252	129	27	13	32	4.4	2.44	14.27	7.20	4.34
CH-15	15	693	CH III	50.18	3.09	12.42	16.16	0.21	4.85	10.10	2.38	0.32	0.30	2.70	38.6	13.5	222	100	46	216	471	35	50	292	134	25	16	38	4.0	2.20	13.85	6.44	4.52
CH-16	16	707	CH III	50.15	3.20	12.39	16.14	0.22	4.96	10.08	2.28	0.28	0.29	2.56	39.2	11.0	228	94	45	212	489	36	48	292	129	28	14	34	4.7	2.06	14.83	6.54	4.10

Table A2 (a) (---continued)

Sample No.	flow No.	height (m)	forma-tion	SiO2 (wt.%)	TiO2	Al2O3	FeO*	MnO	MgO	CaO	Na2O	K2O	P2O5	Na2O+K2O	Mg#	Rb (ppm)	Sr	Ba	Y	Zr	V	Cr	Ni	Cu	Zn	Ga	Nb	Sc	Th	Ba/Y (ratio)	Zr/Nb	Ba/Nb	Ba/Sr X10
CH-17	17	713	CH III	49.97	2.44	13.04	14.69	0.20	5.88	10.99	2.22	0.34	0.23	2.56	45.6	11.2	206	93	35	158	454	103	69	231	118	22	13	38	2.3	2.65	12.46	7.32	4.51
CH-18	18	762	CH III	50.26	2.51	13.25	14.86	0.18	5.69	10.20	2.24	0.58	0.22	2.82	44.5	14.1	194	106	38	160	387	78	69	199	107	25	11	39	3.1	2.79	14.81	9.81	5.45
CH-19	19	782	CH III	50.47	2.47	13.34	14.27	0.20	5.84	10.77	2.18	0.24	0.22	2.42	46.2	3.0	248	73	37	158	463	83	67	218	110	25	11	37	4.2	1.96	14.73	6.79	2.93
CH-20-51	20	800	CH III	49.98	2.42	13.37	14.83	0.21	5.86	10.32	2.29	0.50	0.23	2.79	45.3	10.3	197	110	37	161	448	83	68	234	109	26	10	33	2.0	2.95	16.78	11.46	5.59
CH-20-52	20	800	CH III	50.04	2.42	13.35	14.62	0.21	5.94	10.39	2.29	0.53	0.22	2.82	46.0	12.1	191	115	35	158	440	84	67	202	108	25	9	32	2.4	3.25	16.76	12.22	6.01
CH-21	21	823	CH III	51.42	2.44	13.05	14.37	0.20	5.71	10.21	2.15	0.24	0.21	2.39	45.5	5.5	199	42	34	146	412	55	57	231	104	17	9	16	3.0	1.26	15.99	4.64	2.13
CH-22	22	835	CH III	50.63	2.40	13.98	12.89	0.17	6.22	10.83	2.22	0.43	0.22	2.65	50.3	6.3	217	113	34	150	349	112	84	189	85	17	11	21	4.2	3.37	14.04	10.55	5.21
CH-23	23	866	CH III	48.86	2.37	13.63	14.79	0.20	6.61	10.97	2.13	0.23	0.21	2.36	48.4	8.3	190	33	31	129	417	150	107	216	111	4	8	4	1.4	1.06	15.86	4.12	1.75
CH-24	24	869	CH III	50.65	2.43	13.79	13.06	0.19	6.00	11.13	2.16	0.34	0.25	2.50	49.1	13.9	217	99	35	162	403	112	81	220	98	18	12	25	3.6	2.84	13.29	8.07	4.53
CH-25-51	25	878	CH III	51.04	2.41	13.65	13.17	0.16	5.91	10.36	2.37	0.67	0.25	3.04	48.5	18.1	205	119	34	167	449	113	82	210	100	17	12	5	5.1	3.48	13.56	9.68	5.81
CH-25-52	25	880	CH III	50.44	2.29	14.03	12.86	0.19	6.26	11.15	2.26	0.31	0.22	2.57	50.5	8.3	225	102	34	150	420	123	89	219	96	20	11	25	3.2	3.05	14.31	9.74	4.54
CH-27	27	887	CH III	48.41	2.56	13.61	14.52	0.20	6.94	11.29	2.12	0.14	0.22	2.26	50.1	1.5	209	36	31	139	427	202	116	220	107	16	9	18	2.1	1.15	14.96	3.88	1.73
CH-28	28	899	CH IV	52.01	1.35	14.74	11.91	0.18	5.87	11.19	2.26	0.35	0.14	2.61	50.8	18.0	137	146	34	109	324	133	60	168	84	16	7	10	3.4	4.30	15.75	21.13	10.67
CH-30-51	30	919	CH IV	51.78	1.32	14.45	11.78	0.18	6.44	11.47	2.11	0.34	0.13	2.45	53.4	11.2	132	138	33	105	323	163	64	166	86	15	7	4	2.1	4.14	15.63	20.57	10.48
CH-30-52	30	919	CH IV	52.19	1.39	14.79	12.41	0.18	5.29	10.92	2.32	0.36	0.15	2.68	47.2	20.2	132	126	35	113	322	102	52	167	94	17	7	3	4.7	3.64	15.89	17.76	9.56
CH-31-51	31	960	CH IV	51.69	1.39	14.64	12.97	0.17	5.75	10.50	2.06	0.67	0.14	2.73	48.2	13.8	186	146	35	113	314	91	54	164	88	15	7	11	1.5	4.20	16.56	21.47	7.87
CH-32-51	32	980	CH V	49.38	2.55	13.53	14.09	0.19	6.52	11.03	2.24	0.24	0.23	2.48	49.2	1.6	220	87	34	144	430	135	97	209	108	17	11	43	2.4	2.56	13.70	8.27	3.94
CH-32-52	32	980	CH V	49.19	2.53	13.61	14.25	0.19	6.47	11.25	2.06	0.23	0.22	2.29	48.8	8.2	217	55	32	145	408	143	96	241	108	16	11	39	2.9	1.70	13.40	5.05	2.51
CH-33	33	1013	CH V	49.27	2.33	13.79	13.65	0.18	6.73	11.47	2.18	0.19	0.20	2.37	50.8	0.9	219	57	30	129	409	154	100	208	102	18	10	38	1.9	1.92	12.81	5.66	2.61
CH-34	34	1035	CH V	49.43	2.80	13.61	13.73	0.17	6.50	10.92	2.33	0.27	0.24	2.60	49.8	2.4	238	59	34	157	436	103	96	220	112	17	13	27	0.9	1.72	11.96	4.47	2.45
CH-36	36	1090	CH V	49.13	2.46	13.52	14.73	0.19	6.26	11.01	2.19	0.28	0.22	2.47	47.1	10.5	217	84	34	144	413	137	104	221	113	16	11	16	2.6	2.50	13.22	7.74	3.89
MG-02-51	2	260	MG I	50.64	2.37	14.05	12.90	0.16	5.97	10.67	2.35	0.67	0.22	3.02	49.3	19.2	266	133	34	161	413	149	106	242	100	24	12	28	2.8	3.90	13.87	11.43	4.98
MG-03-51	3	340	MG I	50.86	2.46	13.74	14.46	0.18	5.02	9.77	2.61	0.64	0.25	3.25	42.1	11.6	289	223	36	189	462	63	64	220	115	25	11	28	3.5	6.17	17.08	20.17	7.73
MG-04-51	4	370	MG I	51.48	2.31	14.20	12.85	0.17	5.34	10.29	2.57	0.55	0.22	3.12	46.6	12.4	266	211	35	176	425	78	74	191	108	24	11	26	5.4	5.94	16.67	20.00	7.91
MG-05-51	5	445	MG I	50.20	2.68	12.97	15.13	0.20	5.34	10.26	2.52	0.41	0.28	2.93	42.5	15.5	226	109	44	211	490	102	79	277	124	24	14	32	3.3	2.48	14.65	7.57	4.82
MG-06-51	6	480	MG II	48.63	2.38	13.54	14.79	0.20	6.41	11.49	2.18	0.17	0.21	2.34	47.6	1.9	209	21	35	139	510	126	107	243	121	23	10	35	0.6	0.59	13.82	2.06	0.99
MG-07-51	7	510	MG II	48.94	2.72	13.36	15.26	0.20	5.89	10.60	2.41	0.37	0.25	2.78	44.7	7.6	229	63	38	164	540	83	81	280	131	23	13	34	0.6	1.67	12.89	4.97	2.76
KV-01-51	1	330	KV I	49.05	2.71	13.14	15.37	0.21	5.82	10.62	2.49	0.32	0.28	2.81	44.3	6.5	224	60	42	189	544	81	81	318	133	24	14	32	2.8	1.44	13.94	4.40	2.67
KV-02-51	2	345	KV I	48.66	2.92	13.54	14.36	0.19	6.64	10.97	2.30	0.18	0.25	2.48	49.2	0.8	242	40	38	176	513	209	134	265	126	24	15	31	1.6	1.05	11.41	2.61	1.66
KV-04-51	4	375	KV I	48.54	2.65	13.71	14.75	0.19	6.41	10.77	2.42	0.32	0.24	2.74	47.7	5.9	248	53	35	167	498	103	105	239	125	25	14	29	2.4	1.51	11.87	3.74	2.13
KV-04-52	4	375	KV I	48.93	2.63	13.92	14.00	0.18	6.49	10.92	2.42	0.29	0.23	2.71	49.3	1.5	252	68	33	155	459	98	108	225	115	23	13	25	1.6	2.03	11.71	5.12	2.69
KV-04-53	4	375	KV I	48.58	2.65	13.85	14.28	0.19	6.70	10.77	2.42	0.34	0.23	2.76	49.6	4.6	248	63	34	158	456	100	109	225	118	24	13	33	1.1	1.85	11.96	4.76	2.53
AN-01				50.86	1.23	13.88	13.63	0.21	6.38	11.24	2.20	0.25	0.12	2.45	49.6	7.2	110	77	36	90	365	45	63	208	101	18	7	43	3.4	2.13	13.29	11.37	7.01
AN-02				49.57	2.34	13.90	12.94	0.18	6.93	11.65	2.16	0.14	0.19	2.30	52.9	0.3	221	44	29	136	393	200	103	204	103	23	10	35	1.6	1.50	13.37	4.33	2.00
TL-01				49.92	2.12	14.03	12.37	0.19	7.10	11.44	1.91	0.71	0.19	2.62	54.6	21.6	247	134	26	124	337	240	127	174	90	16	10	38	4.2	5.18	12.30	13.24	5.42
TL-52				49.40	3.22	12.66	17.37	0.24	4.34	9.12	2.58	0.71	0.34	3.29	34.4	37.4	270	213	42	238	470	75	47	236	137	18	17	40	4.6	5.09	13.69	12.25	7.91
NY-03-51	3	330	NY I	47.89	2.71	13.58	15.63	0.20	6.26	10.78	2.41	0.30	0.24	2.71	45.7	3.8	244	68	35	161	509	122	106	270	125	25	13	32	1.1	1.95	12.37	5.22	2.78
NY-02-51	2	315	NY I	48.67	2.83	13.20	16.17	0.21	5.62	10.30	2.26	0.49	0.25	2.75	42.1	12.3	206	83	40	172	582	84	82	295	146	23	14	41	1.4	2.04	12.35	5.92	4.01
NY-01-51	1	290	NY I	49.25	2.47	13.86	13.95	0.19	6.51	11.00	2.29	0.24	0.23	2.53	49.5	4.0	228	52	35	155	489	135	108	239	123	22	12	32	1.5	1.46	13.00	4.34	2.27
NP-01-51				50.31	2.81	13.56	14.31	0.19	5.28	10.50	2.44	0.35	0.24	2.79	43.6	1.7	230	137	37	184	450	47	60	245	111	25	12	30	2.4	3.66	14.98	11.13	5.95
NP-02-51				50.79	2.49	13.59	13.58	0.18	5.74	10.60	2.46	0.34	0.21	2.80	47.0	1.4	218	131	37	156	491	65	63	249	123	24	10	35	2.3	3.55	16.26	13.64	6.00
NP11-51				50.10	2.29	13.16	14.75	0.23	5.85	10.76	2.43	0.25	0.20	2.68	45.4	6.9	209	79	36	149	464	66	59	222	107	0	9	31	1.7	2.23	17.51	9.34	3.81
NC01-51	1	400	NC I	50.75	2.54	13.11	15.05	0.21	4.83	10.33	2.48	0.43	0.27	2.91	40.2	14.3	210	120	41	192	444	50	58	240	123	25	12	30	2.3	2.90	15.49	9.64	5.70
NC02-51-01	8	650	YD	51.39	3.16	12.89	15.08	0.20	4.20	9.37	2.76	0.58	0.38	3.34	36.9	36.4	213	177	50	280	488	63	50	275	138	25	18	31	3.3	3.54	15.99	10.10	8.32
NC02-51-02	8	650	YD	52.15	3.27	12.95	14.69	0.19	4.36	9.12	1.79	1.09	0.39	2.88	38.4	38.6	221	305	50	283	507	65	48	275	141	25	18	35	5.1	6.12	15.57	16.76	13.81
NC03-51	7	630	YD	50.23	2.42	13.06	15.15	0.21	5.42	10.45	2.42	0.38	0.25	2.80	42.9	6.3	198	111	40	184	464	102	71	250	118	23	12	32	3.7	2.75	15.57	9.37	5.57

Table A2 (a) (---continued)

Sample No.	flow No.	height (m)	forma-tion	SiO2 (wt.%)	TiO2	Al2O3	FeO*	MnO	MgO	CaO	Na2O	K2O	P2O5	Na2O+K2O	Mg#	Rb (ppm)	Sr	Ba	Y	Zr	V	Cr	Ni	Cu	Zn	Ga	Nb	Sc	Th	Ba/Y (ratio)	Zr/Nb	Ba/Nb	Ba/Sr X10
NC04-51	7	630	YD	50.19	2.48	13.34	14.88	0.21	5.26	10.61	2.43	0.34	0.26	2.77	42.6	9.1	217	100	39	193	446	44	62	239	119	23	13	32	2.0	2.59	14.88	7.71	4.61
NC05-51	6	580	YC	50.74	2.81	12.78	14.91	0.20	4.84	10.14	2.49	0.78	0.30	3.27	40.5	23.0	203	156	44	218	450	71	63	210	117	26	14	28	4.6	3.53	15.80	11.27	7.65
NC06-51	4	540	YC	50.88	2.56	14.33	13.23	0.19	5.09	10.68	2.45	0.34	0.25	2.79	44.7	8.2	293	209	34	183	398	64	63	204	103	25	11	26	2.5	6.21	16.07	18.36	7.14
NC06-52	4	540	YC	50.76	2.74	12.93	14.92	0.20	5.05	9.78	2.50	0.82	0.32	3.32	41.5	23.8	206	172	46	230	432	64	55	273	119	26	15	32	4.7	3.74	15.31	11.44	8.35
NJ01-51	10	585	YC	50.43	2.52	13.04	15.09	0.22	5.19	10.26	2.48	0.50	0.28	2.98	41.9	16.9	215	113	41	208	431	41	55	256	120	24	14	33	3.1	2.74	15.37	8.33	5.24
NJ02-51	4	440	YA	51.29	3.18	12.66	14.91	0.21	4.61	9.35	2.55	0.85	0.38	3.40	39.3	16.2	217	249	51	280	483	60	47	279	131	24	17	30	5.9	4.93	16.11	14.30	11.48
NJ04-51	3	410	YA	50.05	1.91	12.74	12.40	0.22	8.25	12.23	1.90	0.12	0.18	2.02	58.2	2.3	173	51	30	125	400	511	172	191	87	19	8	41	2.1	1.68	15.44	6.30	2.94
NJ04-52	3	410	YA	51.42	2.04	13.35	12.10	0.22	6.98	11.64	1.95	0.12	0.19	2.07	54.7	1.8	184	59	31	128	435	273	111	200	86	22	8	38	1.5	1.91	15.84	7.22	3.18
NJ05-51	2	395	NJ I	51.99	2.23	13.37	13.29	0.22	5.40	9.77	3.16	0.35	0.21	3.51	46.0	2.8	643	533	34	139	445	67	49	224	103	18	8	32	2.5	15.85	16.72	64.17	8.28
NJ06-51	5	460	YA	48.66	2.84	13.67	14.18	0.23	6.30	11.34	2.31	0.24	0.24	2.55	48.2	3.0	247	86	33	154	350	121	93	202	94	26	12	30	3.4	2.58	12.69	7.10	3.48
NJ07-51	6	475	YB	50.27	1.91	13.89	12.68	0.20	6.64	11.78	2.26	0.18	0.18	2.44	52.3	3.2	205	110	30	126	380	166	89	181	100	21	9	36	2.5	3.62	13.67	11.97	5.38
NJ09-51	14	630	YD	48.56	2.26	14.32	13.91	0.25	6.77	10.96	2.62	0.12	0.23	2.74	50.5	1.8	211	61	38	157	466	140	77	201	112	25	11	42	1.9	1.59	14.54	5.63	2.89
NJ10-51	15	640	YD	49.55	2.90	13.09	15.31	0.22	5.68	10.42	2.24	0.27	0.31	2.51	43.8	2.5	209	148	42	202	520	127	85	294	125	24	15	37	4.0	3.50	13.47	9.86	7.07
NJ11-51	13	600	YD	50.71	2.06	14.28	12.80	0.22	5.69	11.51	2.37	0.16	0.19	2.53	48.2	1.1	236	88	32	132	345	154	81	118	84	21	9	40	2.5	2.75	14.47	9.63	3.71
NJ12-51	12	585	YC	50.29	2.10	14.18	13.22	0.21	5.92	11.42	2.28	0.18	0.21	2.46	48.4	2.1	208	93	34	146	417	169	76	224	106	23	12	36	3.0	2.74	12.50	7.91	4.45
NJ13-51	11	575	YC	53.47	2.16	12.77	14.05	0.18	4.95	9.84	2.16	0.19	0.22	2.35	42.5	1.4	231	166	35	153	381	72	54	263	95	21	11	37	3.6	4.78	13.92	15.05	7.17
NJ14-51	9	535	YC	50.29	1.86	13.92	13.05	0.21	6.56	11.58	2.16	0.19	0.19	2.35	51.3	2.6	205	72	30	125	385	168	95	179	104	23	9	38	3.3	2.43	13.32	7.69	3.53
NJ15-51	8	525	YC	48.93	1.98	14.39	13.11	0.20	6.62	12.34	2.13	0.11	0.19	2.24	51.4	0.8	212	55	31	126	401	160	96	184	105	23	10	43	2.0	1.78	13.15	5.74	2.60
NJ17-51	7	500	YB	49.56	3.19	13.19	14.36	0.21	5.72	10.70	2.45	0.26	0.35	2.71	45.5	6.8	229	120	41	217	527	219	108	269	124	27	19	31	4.1	2.93	11.37	6.28	5.23
NJ18-51	5	460	YA	49.17	2.63	13.98	13.43	0.19	6.61	11.52	2.14	0.09	0.24	2.23	50.8	0.7	233	24	34	166	415	145	103	234	102	25	13	33	2.6	0.70	12.76	1.82	1.02
NJ19-51	4	440	YA	48.80	2.74	13.47	14.57	0.20	6.29	10.93	2.36	0.39	0.25	2.75	47.5	8.3	229	81	34	161	430	136	93	251	106	26	14	35	1.5	2.39	11.90	5.97	3.52
NJ21-51	7	500	YB	49.40	3.26	13.11	14.68	0.20	5.77	10.57	2.41	0.24	0.36	2.65	45.2	5.1	236	113	44	227	525	196	103	292	125	27	20	30	2.5	2.59	11.25	5.57	4.77
JB01-51	3	450	YA	51.06	2.88	13.51	14.46	0.21	4.58	10.12	2.50	0.36	0.31	2.86	39.9	15.0	218	141	45	220	458	92	61	265	123	26	15	33	3.6	3.16	14.79	9.47	6.48
JB02-51	5	470	YA	51.26	2.91	12.89	14.74	0.21	4.84	9.94	2.49	0.41	0.32	2.90	40.8	15.7	208	142	45	229	469	102	61	276	129	25	16	36	2.5	3.13	14.67	9.11	6.82
JB02-52	5	545	YA	53.52	2.89	13.08	12.94	0.18	5.09	9.45	2.16	0.38	0.30	2.54	45.2	6.1	446	1222	43	213	483	82	48	276	119	22	14	35	4.7	28.49	15.11	86.68	27.42
JB04-51	9	580	YC	50.98	2.19	14.59	11.78	0.23	6.43	10.88	2.53	0.18	0.22	2.71	53.4	0.4	188	54	34	139	483	173	80	227	107	23	10	39	0.4	1.61	13.40	5.22	2.89
JB05-51	12	635	YC	51.03	3.42	13.42	15.98	0.20	2.94	8.85	2.65	0.61	0.91	3.26	27.8	18.1	290	250	89	577	356	11	31	568	176	34	38	27	9.1	2.82	15.26	6.62	8.64
JB06-51	13	650	YD	50.10	2.20	13.52	14.75	0.22	5.67	10.74	2.37	0.21	0.24	2.58	44.6	5.4	194	104	36	160	455	92	65	223	113	22	11	39	2.3	2.92	14.26	9.24	5.33
JB07-51	15	680	YD	50.36	2.17	13.68	14.43	0.21	5.55	10.78	2.30	0.30	0.23	2.60	44.6	9.0	187	94	36	158	449	106	74	239	111	21	12	35	1.7	2.60	13.02	7.80	5.06
JB08-51	16	715	YD	50.42	2.50	13.06	14.80	0.22	5.51	10.48	2.40	0.32	0.28	2.72	43.8	8.7	209	120	38	179	455	66	65	249	126	23	12	34	4.2	3.14	14.94	10.01	5.76
JB09-51	14	700	YD	50.52	2.17	13.41	14.15	0.22	5.93	10.90	2.25	0.22	0.23	2.47	46.8	6.9	181	96	37	158	440	114	73	245	116	23	12	42	4.9	2.61	13.36	8.12	5.28
JB10-51	7	545	YB	56.27	2.40	14.65	10.77	0.16	4.16	8.79	2.42	0.12	0.27	2.54	44.8	0.8	375	276	30	154	367	134	74	220	87	21	14	25	3.2	9.27	11.37	20.47	7.38
BI01-51	1	180		51.95	3.36	13.57	13.01	0.19	4.17	8.83	2.76	1.72	0.45	4.48	40.2	49.2	313	358	44	323	420	72	59	253	114	26	37	31	9.2	8.18	8.78	9.74	11.47
BI01-52	1	180		51.99	3.51	13.44	12.86	0.20	4.09	8.91	2.78	1.77	0.45	4.55	40.0	51.7	313	369	47	330	420	42	47	255	117	27	36	29	9.7	7.91	9.14	10.22	11.78
BI01-53	1	180		52.29	3.64	13.71	12.23	0.18	4.11	9.16	2.87	1.37	0.44	4.24	41.3	51.4	347	396	47	336	403	48	48	248	112	28	37	27	9.8	8.41	9.03	10.63	11.40
BI02-51	2	192		49.93	3.13	13.41	14.58	0.22	4.66	9.72	2.70	1.26	0.39	3.96	40.1	29.5	310	301	42	263	436	40	44	218	118	24	29	33	6.4	7.25	9.00	10.31	9.70
BI04-51	3	200		50.52	2.63	14.05	12.07	0.19	6.08	10.93	2.57	0.66	0.30	3.23	51.4	26.1	320	251	37	216	374	154	100	160	97	24	24	30	4.7	6.83	8.90	10.31	7.83
BI05-51	4	220		49.66	3.25	13.34	13.97	0.22	5.28	10.89	2.49	0.55	0.34	3.04	44.2	10.4	327	227	40	240	456	56	61	232	113	26	26	32	6.4	5.74	9.10	8.59	6.95
BI06-51	13	595		51.80	2.08	14.17	13.25	0.17	5.02	10.00	2.58	0.70	0.23	3.28	44.3	20.7	247	201	34	181	378	63	57	170	106	25	10	33	5.3	5.95	17.91	19.85	8.11
BI07-51	12	550		51.85	2.52	13.07	14.18	0.20	5.06	9.53	2.53	0.79	0.28	3.32	42.8	17.0	248	285	42	211	434	68	52	193	117	24	13	36	3.9	6.82	16.72	22.63	11.52
BI08-51	11	510		50.84	3.10	13.60	13.92	0.18	4.87	9.59	2.70	0.82	0.39	3.52	42.3	21.2	248	278	47	272	451	84	67	309	123	27	17	30	5.0	5.93	15.70	16.08	11.22
BI09-57	10	458		50.36	2.45	13.58	14.40	0.20	5.31	10.55	2.43	0.48	0.25	2.91	43.6	21.4	231	169	35	178	457	92	65	212	117	23	14	33	4.7	4.88	12.81	12.12	7.29
BI09-58	10	458		50.52	2.38	13.81	13.79	0.21	5.38	10.77	2.43	0.46	0.24	2.89	45.0	18.1	230	156	34	173	433	90	72	238	120	24	14	37	1.0	4.59	12.52	11.30	6.77
BI09-59	10	458		50.24	2.41	13.67	14.20	0.23	5.42	10.76	2.33	0.50	0.25	2.83	44.5	7.8	232	170	35	173	457	94	71	237	113	24	14	36	3.2	4.87	12.59	12.43	7.35
BI10-51	9	448		50.78	1.33	14.99	12.35	0.25	6.18	11.79	1.99	0.24	0.11	2.23	51.2	8.4	156	103	29	93	344	72	64	163	85	21	8	37	3.5	3.63	11.71	13.09	6.63
BI11-51	8	424		50.35	2.24	13.61	14.35	0.21	5.20	10.48	2.46	0.81	0.29	3.27	43.2	12.2	242	266	37	173	433	59	49	233	107	21	24	38	5.6	7.12	7.20	11.05	11.01

Table A2 (a) (---continued)

Sample No.	flow No.	height (m)	forma-tion	SiO2 (wt.%)	TiO2	Al2O3	FeO*	MnO	MgO	CaO	Na2O	K2O	P2O5	Na2O+ K2O	Mg#	Rb (ppm)	Sr	Ba	Y	Zr	V	Cr	Ni	Cu	Zn	Ga	Nb	Sc	Th	Ba/Y (ratio)	Zr/Nb	Ba/Nb	Ba/Sr X10
BI12-51	7	376		50.16	2.22	13.89	12.28	0.18	6.47	11.91	2.19	0.50	0.20	2.69	52.5	13.4	264	117	29	141	348	184	105	183	92	22	14	36	2.5	4.09	10.04	8.34	4.42
BI12-52	7	376		50.31	2.26	13.98	12.25	0.17	6.46	11.63	2.21	0.52	0.20	2.73	52.5	13.7	264	123	29	146	338	173	101	204	97	23	14	39	3.6	4.21	10.78	9.11	4.67
BI13-51	6	292		50.24	2.76	13.67	13.52	0.21	5.52	10.77	2.60	0.44	0.27	3.04	46.1	17.9	278	144	36	203	436	82	74	250	110	24	21	34	2.6	3.97	9.64	6.86	5.18
BI13-52	6	292		50.14	2.52	14.22	13.15	0.19	5.66	10.93	2.54	0.40	0.26	2.94	47.4	12.0	287	145	34	185	411	93	84	232	105	23	19	34	2.7	4.29	9.81	7.65	5.04
BI13-53	6	292		50.15	2.59	14.02	13.08	0.19	5.83	11.04	2.48	0.38	0.25	2.86	48.3	10.8	291	142	34	184	401	95	81	215	100	25	18	34	3.9	4.13	10.26	7.91	4.86
BI13-54	6	292		50.46	2.60	14.12	12.96	0.20	5.51	10.93	2.55	0.42	0.26	2.97	47.1	11.1	287	141	35	190	412	91	77	237	108	23	19	39	3.4	4.01	9.82	7.31	4.92
BI13-55	6	292		50.33	2.61	14.23	12.91	0.21	5.46	10.96	2.64	0.39	0.27	3.03	47.0	13.8	287	128	34	190	415	85	77	233	108	25	20	36	2.3	3.82	9.33	6.29	4.47
BI14-51	5	240		50.19	2.93	14.23	12.94	0.23	4.74	10.88	2.56	0.96	0.33	3.52	43.4	20.4	322	232	38	220	384	44	64	212	97	27	24	30	5.1	6.10	9.03	9.50	7.19

Table A2 (b) (---continued)

Sample No.	MA-W-25		KK-06-51		AG-10-51		CH-27		CH-32-52		P15-Aa-89-2		BU05-51	
		error		error		error		error		error		error		error
La (ppm)	10.48	0.10	8.83	0.11	11.73	0.11	9.38	0.10	11.40	0.11	13.36	0.12	13.85	0.13
Ce	24.57	0.16	20.79	0.16	27.85	0.17	22.06	0.15	26.68	0.16	29.34	0.17	30.78	0.18
Nd	18.71	0.46	15.60	0.43	20.55	0.49	16.27	0.43	18.67	0.45	19.98	0.49	21.07	0.50
Sm	5.35	0.01	4.54	0.01	5.74	0.01	4.73	0.01	5.02	0.01	5.26	0.01	5.53	0.01
Eu	2.04	0.02	1.73	0.02	2.06	0.02	1.79	0.02	1.88	0.02	1.89	0.02	1.99	0.02
Tb	1.05	0.04	0.90	0.04	1.07	0.04	0.93	0.04	0.93	0.03	0.99	0.04	1.03	0.04
Yb	3.29	0.12	2.85	0.11	3.33	0.11	2.94	0.11	3.06	0.12	3.04	0.11	3.41	0.13
Lu	0.48	0.02	0.40	0.01	0.49	0.02	0.42	0.01	0.43	0.01	0.47	0.02	0.51	0.02
Sc (ppm)	39.18	0.05	38.08	0.05	35.79	0.05	35.86	0.05	37.16	0.05	38.56	0.05	41.11	0.05
Hf	3.81	0.05	3.12	0.05	4.00	0.05	3.30	0.05	3.58	0.05	3.76	0.05	3.94	0.05
Ta	0.95	0.06	0.77	0.05	1.07	0.06	0.90	0.06	1.10	0.06	0.95	0.06	0.91	0.06
Th	1.08	0.03	0.83	0.03	1.13	0.03	0.88	0.02	1.16	0.02	1.77	0.03	1.86	0.03
U	0.12	0.01	0.15	0.01	0.22	0.02	0.13	0.01	0.16	0.01	0.36	0.02	0.33	0.01
Co	56.11	0.28	55.35	0.28	49.75	0.26	53.10	0.27	53.21	0.26	53.53	0.27	57.76	0.28
Sr	188	14	197	16	209	15	185	15	201	13	217	16	233	16
Ba	72	15	65	16	81	15	33	15	55	13	66	16	60	14
Zr	131	18	124	19	131	19	102	15	109	15	137	19	144	20
Cr	109.44	0.44	95.12	0.45	157.05	0.27	172.07	0.50	117.60	0.44	61.86	0.41	68.08	0.44
FeO (wt.%)	14.58	0.05	14.10	0.05	12.68	0.04	13.15	0.04	13.71	0.04	14.14	0.05	14.56	0.05
Na2O	2.26	0.01	2.25	0.01	2.33	0.01	2.07	0.01	2.14	0.01	2.25	0.01	2.50	0.01
K2O	0.33	0.043	0.13	0.025	0.44	0.044	0.09	0.025	0.14	0.026	0.15	0.028	0.19	0.045

Appendix C: Compositions of olivine phenocrysts

Olivine phenocrysts in four basalts of Deccan Traps were analyzed with JXA-8800R EPMA of the Earthquake Research Institute, University of Tokyo. Representative analyses are listed in Table A3. Although three samples, AK-12-52, AK-12-53 and NK-03-51, are MgO-rich basalts (> 10 wt.%), Fo contents of olivine phenocrysts are lower than Fo_{80} (Fig. A1). NY-02-51 sample is the uncontaminated basalts.

Table A3 (a) Representative chemical compositions of olivine phenocrysts in Deccan Traps basalts. (b) Chemical compositions of melt inclusion in olivine phenocrysts in NY-02-51 sample. (c) Olivine-liquid Fe-Mg exchange distribution coefficient, $K_D = (Fe/Mg)^{olivine}/(Fe/Mg)^{liquid}$, for NY-02-51 sample reported in Fig. A5 (a) and (b).

AK-12-52	SiO2	FeO*	MgO	CaO	Total	Fo
ol1	38.59	22.52	39.45	0.21	100.77	75.7
ol2	38.37	21.84	39.74	0.18	100.12	76.4
ol3	38.57	21.36	39.60	0.23	99.75	76.8
ol4	38.49	20.48	40.59	0.20	99.76	77.9
ol5	38.76	20.59	40.08	0.21	99.64	77.6
ol6	38.76	20.46	40.89	0.22	100.33	78.1
ol7	39.21	19.90	40.86	0.25	100.22	78.5
ol8	38.84	21.70	39.63	0.23	100.40	76.5
ol9	38.62	21.88	39.45	0.20	100.16	76.3
ol10	39.02	20.11	40.51	0.25	99.89	78.2
ol11	38.53	20.60	40.44	0.24	99.80	77.8
ol12	38.80	21.48	39.99	0.24	100.51	76.8
ol13	38.63	21.81	40.27	0.18	100.89	76.7
ol14	38.86	20.29	40.94	0.22	100.30	78.2
ol15	38.59	19.78	41.30	0.27	99.94	78.8
ol16	38.61	21.88	39.82	0.24	100.55	76.4
ol17	38.72	20.32	41.26	0.23	100.53	78.4
ol18	38.63	20.26	41.11	0.26	100.25	78.3
ol19	55.01	14.13	26.73	3.66	99.52	77.1
ol20	38.33	20.78	40.27	0.22	99.59	77.5
ol21	38.39	19.44	40.93	0.23	98.99	79.0
ol22	38.56	20.04	41.31	0.24	100.15	78.6
ol23	38.86	19.70	41.09	0.22	99.87	78.8
ol24	38.87	20.13	41.59	0.26	100.86	78.6
ol25	38.94	19.92	41.30	0.22	100.37	78.7
ol26	38.66	20.08	40.97	0.28	99.99	78.4

AK-12-53	SiO2	FeO*	MgO	CaO	Total	Fo
ol1	38.13	20.88	40.11	0.22	99.34	77.4
ol2	38.50	21.31	39.73	0.20	99.73	76.9
ol3	38.67	20.55	39.91	0.25	99.38	77.6
ol4	38.40	20.23	40.35	0.21	99.19	78.0
ol5	38.54	20.94	40.55	0.25	100.27	77.5
ol6	38.15	21.40	40.28	0.25	100.07	77.0
ol7	38.31	20.83	39.81	0.25	99.21	77.3
ol8	38.38	21.90	39.59	0.24	100.11	76.3
ol9	38.52	21.73	39.54	0.24	100.03	76.4
ol10	37.89	22.12	39.47	0.16	99.64	76.1
ol11	39.53	21.06	39.88	0.17	100.64	77.1
ol12	38.82	21.43	39.96	0.20	100.40	76.9
ol13	38.09	21.91	38.96	0.22	99.18	76.0
ol14	38.97	21.57	40.41	0.24	101.19	77.0
ol15	38.85	21.44	40.38	0.28	100.94	77.0
ol16	38.67	20.34	39.93	0.26	99.19	77.8

Table A3 (--- continued)

NK-03-51	SiO2	FeO*	MgO	CaO	Total	Fo
ol1	38.89	19.86	41.05	0.27	100.07	78.6
ol2	38.99	18.72	41.50	0.27	99.48	79.8
ol3	38.98	20.26	41.76	0.26	101.27	78.6
ol4	39.26	19.29	41.56	0.26	100.38	79.3
ol5	38.06	19.51	40.07	0.27	97.90	78.5
ol6	38.78	19.87	41.17	0.29	100.11	78.7
ol7	39.13	19.51	40.61	0.25	99.50	78.8
ol8	38.80	20.08	41.06	0.30	100.24	78.5
ol9	39.13	19.28	41.10	0.24	99.76	79.2
ol10	38.96	19.34	40.84	0.28	99.41	79.0
ol11	38.86	21.62	39.84	0.27	100.60	76.7
ol12	38.58	20.03	41.07	0.28	99.95	78.5
ol13	39.66	20.26	42.30	0.29	102.51	78.8
ol14	37.67	20.04	38.73	0.25	96.69	77.5
ol15	38.65	20.59	41.28	0.22	100.74	78.1
ol16	38.18	19.66	40.79	0.30	98.94	78.7

NY02-51	SiO2	FeO*	MgO	CaO	Total	Fo
ol0	37.71	27.84	33.49	0.34	99.38	68.2
ol1	37.75	29.15	34.56	0.31	101.77	67.9
ol2	37.66	29.25	34.69	0.28	101.87	67.9
ol3	37.42	28.57	34.32	0.34	100.65	68.2
ol4	37.36	29.66	34.39	0.31	101.72	67.4
ol5	37.86	29.62	34.26	0.34	102.08	67.3
ol6	37.78	28.49	34.45	0.40	101.11	68.3
ol7	37.79	29.27	34.29	0.36	101.71	67.6

(b)

NY02-51	SiO2	TiO2	Al2O3	FeO*	MgO	CaO	Na2O	Total	Mg#
ol1.IC15	50.67	3.07	12.61	16.19	4.57	10.53	1.32	99.15	33.48
ol2.IC17	50.40	3.04	12.37	15.99	5.07	11.26	1.77	100.10	36.10
ol2.IC18	49.89	3.03	12.33	16.01	5.05	11.09	1.45	99.22	36.00
ol3.IC19	49.76	3.13	12.67	16.47	5.26	10.04	1.59	99.14	36.27
ol3.IC20	48.91	3.06	12.61	15.82	5.10	10.29	1.33	97.37	36.46
ol4.IC21	50.01	3.19	12.67	16.19	5.13	9.79	1.38	98.60	36.11
ol4.IC22	50.98	3.22	12.93	15.66	4.83	10.22	1.21	99.43	35.45
ol6.IC25	49.48	3.07	12.51	15.85	4.68	11.12	1.37	98.32	34.51
ol6.IC26	49.61	3.10	12.53	16.11	4.69	11.21	1.60	99.10	34.18

Table A3 (--- continued)

(c)

NY02-51	ol		glass			KD
	FeO*	MgO	FeO*	FeO	MgO	Fe-Mg
ol1.IC15	29.15	34.56	16.19	13.76	4.57	0.28
ol2.IC17	29.25	34.69	15.99	13.59	5.07	0.31
ol2.IC18	29.25	34.69	16.01	13.61	5.05	0.31
ol3.IC19	28.57	34.32	16.47	14.00	5.26	0.31
ol3.IC20	28.57	34.32	15.82	13.45	5.10	0.32
ol4.IC21	29.66	34.39	16.19	13.76	5.13	0.32
ol4.IC22	29.66	34.39	15.66	13.31	4.83	0.31
ol6.IC25	28.49	34.45	15.85	13.47	4.68	0.29
ol6.IC26	28.49	34.45	16.11	13.70	4.69	0.28

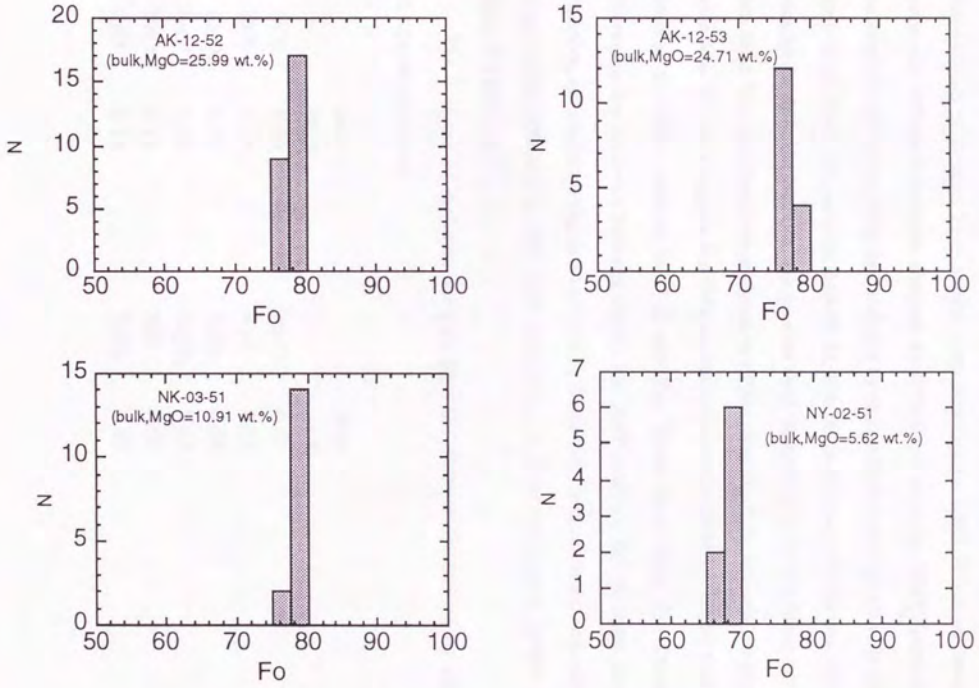

Fig. A1 Histogram of Fo contents of olivine phenocrysts in the Deccan Trap basalts.

Appendix D: Compositional difference between XRF and EPMA analyses

Experimental products were analyzed by electron microprobe, while whole rock compositions of Deccan Trap basalts were obtained by XRF. When we recognize systematic difference between analyses by EPMA and those by XRF, discussion on fractional crystallization using data analyzed by two methods makes problem. In order to check the problem, two samples (MA-W-25, BH-14) from Deccan Traps were analyzed twice by the different methods. The powder used for XRF analysis was fused and made glass bead. The glass bead was analyzed by EPMA. Results of the analysis are shown in Table A4a. We can recognize that SiO_2 contents obtained by EPMA is higher than those obtained by XRF, whereas FeO* is opposite. These facts show that systematic differences are observed between EPMA and XRF analyses for the same samples. Therefore, before comparing data analyzed by the two different methods, major element compositions obtained by XRF were normalized to those obtained by EPMA using values in Table A4b.

The 1 sigma of replicate analyses for each element determined by electron microprobe as follows:

	error wt.%		error wt.%
SiO_2	0.29	Na_2O	0.09
TiO_2	0.19	K_2O	0.03
Al_2O_3	0.17	P_2O_5	0.04
FeO*	0.40	Cr_2O_3	0.03
MnO	0.12	NiO	0.01
CaO	0.14	V_2O_3	0.03

Table A4 (a) Results of analyses by different methods (EPMA and XRF analyses). Fused whole rocks were analyzed by EPMA. (b) Parameter used for correction by which EPMA data were converted into XRF data.

(a)

Sample No.	MA-W-25	MA-W-25	BH-14	BH-14
Analyser	XRF	EPMA	XRF	EPMA
SiO2 (wt.%)	49.12	49.94	48.88	49.42
TiO2	2.78	2.68	1.09	1.21
Al2O3	13.44	13.72	14.64	14.53
FeO*	14.68	14.05	12.66	11.52
MgO	6.72	6.62	9.36	9.31
CaO	10.72	10.53	10.90	11.28
Na2O	2.20	2.22	1.80	2.10
K2O	0.33	0.23	0.67	0.64

(b)

Sample No.	MA-W-25	BH-14	average
SiO2 (wt.%)	0.984	0.989	0.986
TiO2	1.037	0.903	0.970
Al2O3	0.980	1.008	0.994
FeO*	1.045	1.099	1.072
MgO	1.015	1.005	1.010
CaO	1.018	0.966	0.992
Na2O	0.991	0.860	0.925
K2O	1.441	1.049	1.245

Appendix E: Fractional crystallization models

The method of the calculation is reported by Grove *et al.* (1992). Three pieces of information are required to calculate the fractional crystallization path of a basalt: (1) a prediction of the phase appearance sequence as the magma cools, (2) the composition of the crystallizing phases, and (3) the proportions of the crystallizing phase. Algebraic relations obtained from experimentally produced phase boundaries on the Oliv-Cpx-Plag projection plane in the Oliv-Plag-Cpx-Qtz pseudo-quaternary, and constraints from mineral/melt exchange reactions derived from experimentally produced mineral-melt pairs, both described in this appendix, are used to calculate a crystallization path.

(1) Prediction of the phase appearance sequence as the magma cools.

Step (1) requires prediction of the pertinent phase boundaries for a given lava composition. For Deccan Trap basalts, the pertinent phase boundaries are the OPM (olivine-plagioclase-melt), OAM (olivine-augite-melt), and OPAM (olivine-plagioclase-augite-melt) boundaries. Grove *et al.* (1992) estimated the OPM, OAM and OPAM boundaries for MORB in the Oliv-Plag-Cpx-Qtz pseudo-quaternary based on melting experiments (Fig. A2). They have found that the OPAM boundary "line" project as a "point" in the Oliv-Cpx-Plag pseudoternary (Fig. A2). Moreover, they have reported that the OPM (OAM) boundary in this projection is a line that extends down toward the Oliv-Plag (Oliv-Cpx) sideline of the pseudo-ternary (Fig. A2).

In this thesis, the OPM, OAM and OPAM boundaries in the Oliv-Cpx-Plag pseudoternary are determined based on the melting experiments of Deccan Trap basalts (Fig. A2). These boundaries are similar to the one atmosphere boundaries determined by Grove *et al.* (1992). Although data are scattered, I found that the OPAM boundary "line" project as a "point" in the Oliv-Cpx-Plag pseudoternary, and the OPM (OAM) boundary in this projection is a line that extends down toward the Oliv-Plag (Oliv-Cpx) sideline of the pseudo-ternary. Thus, the phase boundaries in the Oliv-Cpx-Plag pseudoternary provide enough information to constrain the relative roles of olivine, plagioclase and augite fractionation.

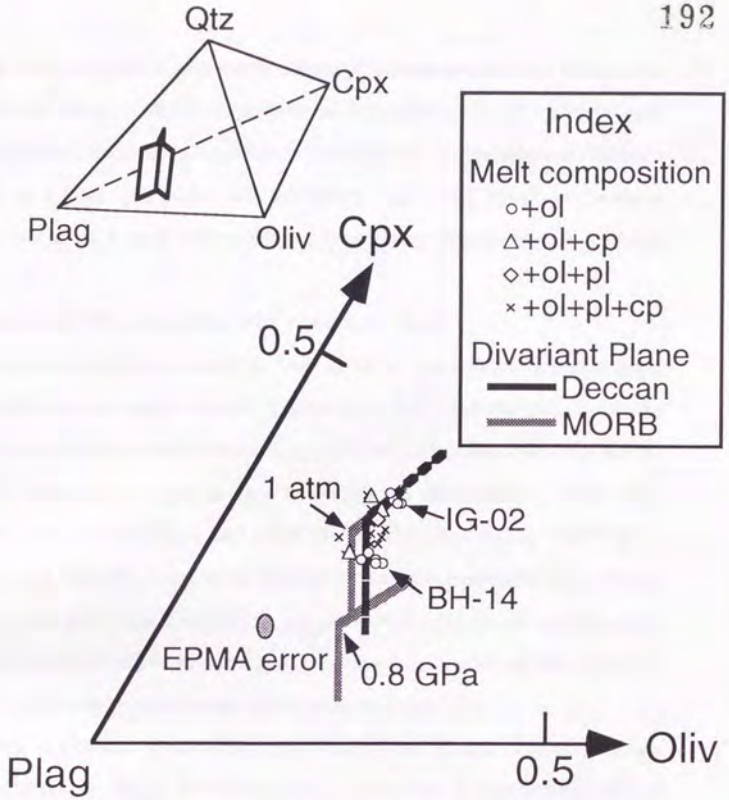

Fig. A2 Center: Pseudoternary projections showing experimentally produced liquids at 1 atm for three starting materials (IG-02, BH-14 and MA-W-25) collected from Deccan Traps. Projection onto the pseudoternary Oliv-Plag-Cpx from Qtz shows that the oliv+plag+augite+melt (OPAM) boundary line collapses to a point, and the oliv+plag+melt (OPM), oliv+augite+melt (OAM) and plag+augite+melt (PAM) boundary planes collapse to lines. OPM and OAM boundaries of MORB at 1 atm and 0.8 GPa are also drawn. EPMA error: 2 sigma error for replicate EPMA analyses. Inset: The pseudoquaternary tetrahedron Oliv-Plag-Cpx-Qtz viewed in 3-D perspective shows the OPAM boundary (central line) and the OPM, OAM and PAM boundaries (planes that intersect to form the central line). These planes separate the primary phase volumes of oliv, plag and augite. oliv (Oliv): olivine, plag (Plag): plagioclase, Cpx: augite, Qtz: Quarts.

With mass proportions and compositions of phases crystallizing along these boundaries, the change in liquid composition can be calculated. Furthermore for each liquid, information on its coexisting phases is provided from the exchange relationships for Fe-Mg in olivine and augite with coexisting liquid, and for Ca-Na between plagioclase and liquid. A method for estimating augite compositional variation is present below.

(2) Estimating the compositions of the crystallizing phases.

For the uncontaminated basalts in Deccan Traps, the crystallizing phases are olivine, plagioclase and augite. Olivine is removed as stoichiometric $(Mg, Fe)_2SiO_4$. Plagioclase is removed as stoichiometric $(Ca_{1-x}, Na_x)Al_{2-x}Si_{2+x}O_8$. TiO_2, Al_2O_3, CaO and Na_2O composition in augite is fixed to the average composition of the melting experiments at one atmosphere and QFM (Table 4.2). $NaAlSi_2O_6$, $CaTiAl_2O_6$, $CaAlAlSiO_6$ and $Ca_2Si_2O_6$ components in augite are calculated using the TiO_2, Al_2O_3, CaO and Na_2O, and these components are fixed in the fractional crystallization calculation. $(Mg, Fe)_2Si_2O_6$ components in augite is also calculated using FeO plus MgO composition of the melting experiments at one atmosphere and QFM.

The Mg and Fe ratio of olivine and augite and Ca and Na ratio of plagioclase are calculated based on K_D's. Fe-Mg exchange distribution coefficients ($K_D = (Fe/Mg)^{mineral}/(Fe/Mg)^{melt}$) used for olivine and augite are 0.27 and 0.23 (QFM condition), respectively (Table A5). Ca-Na exchange distribution coefficient ($K_D = (Ca/Na)^{plagioclase}/(Ca/Na)^{melt}$ for plagioclase is 0.97 (Table A5).

(3) Estimating the proportions of the crystallizing phases.

First, the phase boundaries are estimated in the Oliv-Cpx-Plag pseudoternaries, as described above. Phase proportions are then estimated using an iterative approach. In the case of the OPM boundary, the evolving melt compositions should track along the estimated the OPM boundary 'line' towards the OPAM 'point'. If the trend defined by the evolving liquids does not match the estimated boundary, the proportions of olivine and plagioclase are adjusted, and the calculation is repeated. In the case of the OPAM boundary, the evolving melt compositions should project near coincidentally in the Oliv-

Table A5 Mineral-liquid Fe-Mg or Ca-Na exchange distribution coefficient, $K_D = (Fe/Mg)^{mineral}/(Fe/Mg)^{liquid}$ or $(Ca/Na)^{plagioclase}/(Ca/Na)^{liquid}$ for each run product reported in Table 4.2. Only calculated results prefixed with sharps were adopted for the calculations of K_D. All quenched liquids and crystals of the experiments prefixed with sharps were homogeneous (1 sigma of the standard deviations of SiO_2 are lower than 2.0 wt.%).

Run no.	T (°C)	fO2	KD(ol-gl)		KD(cp-gl)		KD(pl-gl)	
MA-W-25			Fe-Mg	error	Fe-Mg	error	Ca-Na	error
#32-1	1155	QFM	#0.285	0.011	0.274	0.024	#0.830	0.053
#36-1	1134	QFM	#0.284	0.014			#0.743	0.051
#25-1	1124	QFM	#0.269	0.023	0.255	0.028	#0.912	0.036
#37-1	1119	QFM	0.280	0.013	0.197	0.024	0.799	0.055
#35-1	1114	QFM	0.279	0.013	0.201	0.020	0.764	0.051
MA-W-25			Fe-Mg	error	Fe-Mg	error	Ca-Na	error
#2-1	1154	NNO	0.346	0.012			0.907	0.03
#33-1	1144	NNO			0.226	0.020	1.104	0.052
#18-1	1134	NNO			0.322	0.014	0.835	0.050
#28-1	1123	NNO			0.273	0.024	0.922	0.089
BH-14			Fe-Mg	error	Fe-Mg	error	Ca-Na	error
#38-1	1214	QFM	#0.281	0.009				
#31-1	1190	QFM	0.266					
#34-1	1175	QFM	#0.257	0.013	#0.221	0.020	#0.960	0.066
#26-2	1163	QFM	#0.263	0.011	#0.250	0.017	#0.890	0.065
#24-2	1144	QFM	#0.277	0.011	#0.225	0.018	#1.096	0.073
#25-2	1124	QFM	#0.276	0.012	0.252	0.017	#1.296	0.080
#35-2	1114	QFM	0.287	0.024	0.219	0.018	0.987	0.054
IG-02			Fe-Mg	error	Fe-Mg	error	Ca-Na	error
#38-2	1214	QFM	#0.269	0.016				
#31-2	1190	QFM	#0.278	0.015	#0.238	0.029		
#34-2	1175	QFM	#0.276	0.011	#0.234	0.022		
#32-2	1155	QFM	#0.273	0.012	#0.231	0.029	#0.920	0.079
#36-2	1134	QFM	#0.279	0.018	#0.231	0.017	#1.087	0.091
#37-2	1119	QFM	0.238	0.019	0.175	0.014	1.178	0.054
average			0.27	0.008	0.23	0.006	0.97	0.166

Cpx-Plag projection, on the top of the estimated OPAM boundary. Thus, proportions of olivine, plagioclase and augite are varied accordingly until this behavior is achieved.

In summary, the fractional crystallization calculation is performed in the following manner.

1. Estimate the positions of the OPAM, OPM and OAM boundaries using the melting experiments.

2. Composition of the uncontaminated basalt is plotted on Oliv-Cpx-Plag pseudoternary projected from Qtz apex (Tormey *et al.*, 1987) and the projected composition of the basalt is compared with the position of the boundaries. If the basalt lies in the Oliv phase volume on the Oliv-Plag-Cpx pseudoternary, olivine of the equilibrium composition is the only phase removed. If the basalt lies on the OPM (OAM) boundary, olivine plus plagioclase (augite) of equilibrium compositions are removed (in appropriate proportions, iterated to as described above). If the basalt lies on the OPAM boundary, the compositions of all three phases are calculated using the appropriate K_D's and all three phases are subtracted (in appropriate proportions, iterated to as described above).

3. In calculation, a 1 wt.% of total solid(s) is(are) removed. The melt composition is renormalized to 100 %. The new fractionated melt composition is again used to estimate the positions of the saturation boundaries in the Oliv-Plag-Cpx pseudoternary. The predicted position of the saturation boundaries is compared with the new melt composition. If the liquid is found to lie on a saturation boundary, the crystallization assemblage is changed to the appropriate assemblage (olivine plus augite, olivine plus plagioclase plus augite etc.). The compositions of the phases are calculated using K_D's and these compositions are again subtracted from the liquid in the appropriate proportions.

Appendix F: Adiabatic upwelling

The adiabatic upwelling have been proposed to estimate P-T path of the composite plume (McKenzie, 1984). The entropy is defined to be constant.

$$dS = \left(\frac{\partial S}{\partial X}\right)_{P,T} dX + \left(\frac{\partial S}{\partial T}\right)_{X,P} dT + \left(\frac{\partial S}{\partial P}\right)_{X,T} dP = 0 \qquad \text{(G1)}$$

McKenzie (1984) has converted equation (G1) to

$$\frac{dX}{dP} = \frac{-\frac{C_p}{T}\left(\frac{\partial T}{\partial P}\right)_X + \frac{\alpha_s}{\rho_s} + \left(\frac{\alpha_l}{\rho_l} - \frac{\alpha_s}{\rho_s}\right)X}{\Delta S + \frac{C_p}{T}\left(\frac{\partial T}{\partial X}\right)_P} \qquad \text{(G2)}$$

where, C_p is specific heat of magma and solid at constant pressure, α_f is the thermal expansion coefficient of magma, α_s is the thermal expansion coefficient of solid, ρ_l is the density of magma, ρ_s is the density of solid and ΔS is the entropy change on melting. The values of C_p, α_l, α_s, ρ_l and ρ_s proposed by McKenzie (1984) were used in the calculations. ΔS was predicted to 440 J/kg/K (Fukuyama, 1986).

The relationship among pressure (P), temperature (T) and degree of melting (X) for basaltic block or layer and ambient lherzolite part in the composite plume were estimated using data of the melting experiments. I estimated the value of T given by equation (4.3) for the ambient lherzolite part of the composite plume, and the value of T given by

$$T=1013+85.80P+384.3X-48.35PX \qquad \text{(G3)}$$

for basaltic block or layer in the composite plume. Equation (G3) was estimated from the melting experiments of MORB (this study).

Equation (G2) was integrated numerically, using the fourth order Runge-Kutta scheme. At each P, X, the T was obtained from equation (4.3) for melting of the ambient lherzolite part or equation (G4) for melting of basaltic block or layer in the composite plume.

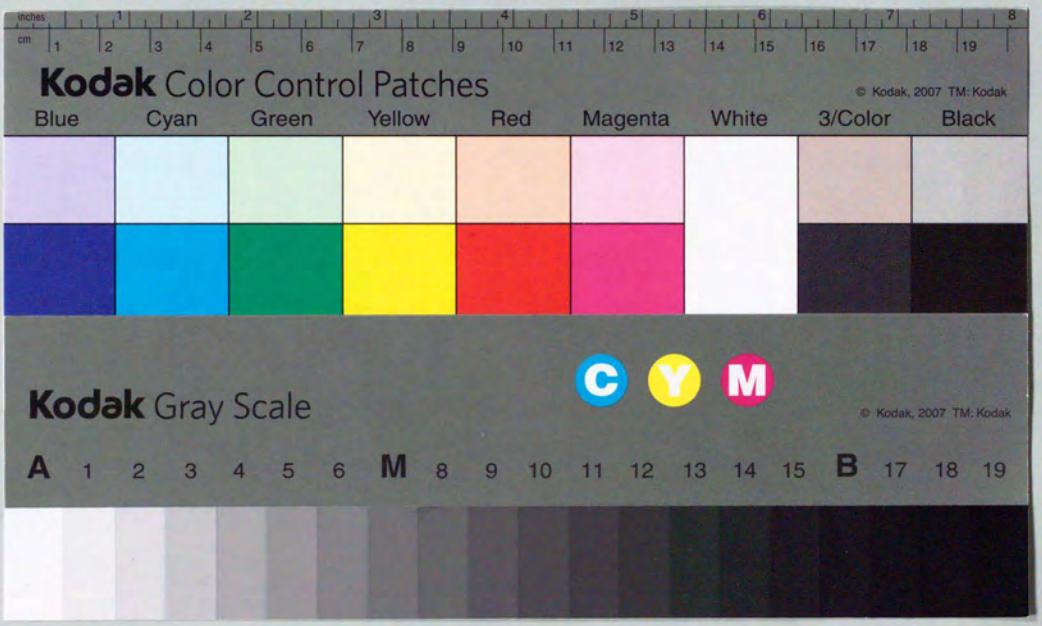
inches
cm
Kodak Color Control Patches
© Kodak, 2007 TM: Kodak
Blue
Cyan
Green
Yellow
Red
Magenta
White
3/Color
Black
Kodak Gray Scale
C
Y
M
© Kodak, 2007 TM: Kodak
A 1 2 3 4 5 6 M 8 9 10 11 12 13 14 15 B 17 18 19